London South Bank University

Optimisation of a neuromuscular electrical stimulation paradigm for targeted strengthening of an intrinsic foot muscle

Andrei Leonardo Pérez Olivera

https://orcid.org/0000-0002-0443-1831

A thesis submitted in partial fulfilment of the requirements of London South Bank University for the degree of Doctor of Philosophy

November 2021

Abstract

The intrinsic foot muscles stabilise and stiffen the foot during posture and locomotion. Since they are placed under continued load, these muscles merit training to meet the weight-bearing demands of everyday activities. Their strengthening is however a largely neglected area and furthermore, the occurrence of common foot-related pathologies is associated with their dysfunction. Indeed, atrophy and dysfunction of the strongest intrinsic foot muscle, abductor hallucis (AbH), is symptomatic to pes planus and Hallux Valgus. AbH's oblique mechanical action along with an inability for its voluntary activation in many individuals limits the strengthening capacity of existing training modalities. Due to the superficial location of AbH, neuromuscular electrical stimulation (NMES) offers a solution to this problem; however, its efficacy for muscle strength gains relies on high stimulation-intensity protocols, which are uncomfortable and limit participant adherence. Therefore, the purpose of this thesis was to develop an optimised NMES paradigm that is tolerable and efficacious for a targeted strengthening intervention of AbH.

The studies reported in this thesis were undertaken with the overarching aim to systematically establish a tolerable and low stimulation-intensity NMES paradigm to train AbH. With this motivation in mind, four sequential experimental studies were designed to identify the optimal mode of NMES application (muscle vs nerve) and stimulation pulse duration (Chapter 3), pulse frequency and train duration (Chapter 4), training stimulus intensity (Chapter 5), and duty-cycle (Chapter 6), respectively. A major finding from the work undertaken in this thesis was the prevalent inability to voluntary activate AbH that exists in healthy participants. Since this inability also limits the measurement of voluntary force generation following an intervention, this thesis also developed a methodological approach that overcomes this limitation. Collectively, the studies in this thesis demonstrated that NMES successfully evokes contractions from AbH irrespective of ability for its voluntary activation and can therefore be used as a training modality.

The optimised NMES paradigm presented in this thesis targets the motor point of AbH using 22s-trains of 1ms pulses at 20-100-20Hz with an intensity of 200% motor threshold and a 1:4 duty-cycle. This wide-pulse, high-frequency, low-intensity paradigm promotes adherence and has the potential to depolarise sensory axons due to their lower rheobase, and evoke contractions with a contribution of the central nervous system. When delivered using long trains and an alternating frequency pattern, it can take advantage of post-tetanic potentiation to produce force, which is then preserved across trains using a duty-cycle with long rest periods.

This thesis intended to bind the aforementioned experimental chapters together with a final chapter investigating the effectiveness of the developed NMES paradigm in strengthening AbH following long-term exposure. However, the implementation of this study was not possible in light of the COVID-19 pandemic and is therefore not reported in this thesis. Nevertheless, future work in this area can benefit from the extensive methodological work undertaken in this thesis and implement a longitudinal study to better understand the clinical implications for targeted AbH strengthening via NMES.

TABLE OF CONTENTS

List of abbreviations

AbH: Abductor hallucis

NMES: Neuromuscular electrical stimulation

MN: Motoneuron

MU: Motor unit

EMG: Electromyography

M_{wave}: Compound muscle action potential

M_{max130}: Maximal compound muscle action potential at supramaximal intensity

MVC: Maximal voluntary contraction

1MPJ: First metatarsophalangeal joint

MT: Motor threshold

SD: Standard deviation

SEM: Standard error of the mean

SEm: Standard error of the measurement

PTP: Post-tetanic potentiation

PRE: Baseline measurement

POST: Post measurement

PNS: Peripheral nerve stimulation

Acknowledgements

This thesis would not exist without the constant help and advice of very important people during these years. Paraphrasing Sir Isaac Newton, they are the *giants* who have put their shoulders for me to stand on and allow me to see further.

Firstly, I would like to express my sincere gratitude to my supervisors, *Dr Darren James* and *Prof Katya Mileva*, for the time invested in supporting me and for their invaluable advice at every step of my PhD studies. It was a pleasure and an honour to have you both as my mentors, I have learned so much from the two of you.

Darren- Thank you for your patience, support and guidance throughout all these years. I am really grateful to you for motivating me to continue my studies at this level and for providing me with every opportunity to thrive and achieve so much during this journey. I really value all the feedback you have provided me about my work as well as your encouraging words before every event where I have disseminated it. Thank you for being willing to share your knowledge and expertise with me and for always being there to help me overcome the many challenges that doing a PhD entails.

Katya- Thank you for the patience, always thoughtful advice, and your willingness to share your knowledge and experience with me in this process. Thank you for, together with Darren, captivating my attention and interest in neuromechanics, from inspiring lectures to reading recommendations, ever since I was an undergrad. I really appreciate your continued guidance and support throughout these years, which made this journey a lot smoother. I am also really thankful for providing always a different perspective on my work with your feedback and for helping me become more skilful and competent.

I would also like to extend my gratitude to *Prof Kiros Karamanidis* for sharing with me his experience and passion for research during my PhD. *Kiros*- I am deeply grateful for the insightful discussions we had about my project and for your always constructive feedback

and suggestions. Thank you also for contributing to my development as a researcher and for thinking of me when opportunities to expand my knowledge arose.

I would also like to offer my thanks to *Mr Matthew Solan* for his contribution and advice on the potential real-world application of the work undertaken in this project.

I gratefully acknowledge the *British Orthopaedic Foot and Ankle Society* and *The Physiological Society* for the internship opportunities that empowered me with the competence and insight of this research area that allowed me to initiate my doctoral training.

My special thanks to the *Sport and Exercise Research Centre* at *LSBU* for the financial support provided for my PhD project. I am also very thankful to *Bill*, *Ashlee* and *Jorge* for their technical support, which was integral to conducting my studies.

Many thanks to all of the participants that have volunteered to take part in my studies for making the time and effort to visit the lab and make this project possible.

I would also like to thank my examiners *Dr Farris* and *Dr Epro* for their experience, time and effort put into evaluating my thesis and Viva Voce, and many thanks to *Prof Rietveld* for her time and chairing support.

Many thanks to the past and present members of the *PhD office* for always providing the advice and group support that was needed during my doctoral training. Thank you all for the interesting conversations during our coffee and lunch breaks. Special thanks to *Liam* and the J212 lab group: *Matthias, Julian, Micha*, *Yiannis* and *Gas*. For your fellowship and for sharing your time and experience with me, which made my doctoral training so much more enjoyable, I say to you: Thank you! Danke! Ευχαριστώ! and Aitäh!

Finally, I would like to thank my family and friends in Bolivia, Spain and the UK for their persistent love and for always believing in me. *Mami*, gracias por ser esa gigante valerosa de la que me he podido apoyar cuando más lo he necesitado y también esa

que me ha alzado para poder darme todas las oportunidades que me han traído a donde estoy hoy. Te dedico esta tesis como forma de agradecerte todos los sacrificios que has hecho por mí. Te quiero mucho y espero siempre poder compartir contigo todos mis logros. *Pilar*, hermanita, gracias por todo lo que has hecho para apoyarme ahora y siempre. Eres la luz que aparece cuando me he sentido a oscuras, a veces diciendo "raamen". Te quiero mucho y quiero que sepas que estoy muy orgulloso de ti. *Papá*, gracias por confiar en mí y por inspirarme a siempre ser mejor. *Yaya*, gracias por tu afecto y siempre cuidarme y enseñarme cuanto pudiste. *Keith*, I thank you for always giving me your unwavering support and helping me get here by sharing your experience and wisdom. *Mamá Leonor*, gracias por ser esa raíz tan fuerte de la que ha crecido esta familia. Gracias por tus consejos y ser nuestro ejemplo de esfuerzo y resiliencia. Te quiero mucho. *Papá Víctor*, muchas gracias por todos tus consejos y el apoyo que siempre me has dado. Han sido una gran fuente de alegría y calma para mi durante mis estudios. Gracias también por hacer todo lo posible por comunicarme con mi mamá Leonor. Te quiero mucho. Gracias a todos mis *tíos/as y primos/as* por brindarme siempre su cariño. Gracias también a mi *papá Martín* y *yayo Ángel* que, aunque ya no estén aquí y no me haya podido despedir de ellos por la distancia que nos separaba, sé que me cuidan desde allí arriba y los llevo siempre en la memoria.

Declaration

I declare that the research presented within this thesis is the original work of the author unless stated. This work has been submitted solely for the degree of Doctor of Philosophy to London South Bank University.

Andrei L. Pérez Olivera

30th November 2021

List of publications

Olivera, A. L. P., Solan, M. C., Karamanidis, K., Mileva, K. N., & James, D. C. (2021). A voluntary activation deficit in m. abductor hallucis exists in asymptomatic feet. Journal of Biomechanics, 110863.

Olivera, A. L. P., Alzapiedi, D. F., Solan, M. C., Karamanidis, K., Mileva, K. N., & James, D. C. (2020). Direct muscle electrical stimulation as a method for the in vivo assessment of force production in m. abductor hallucis. Journal of biomechanics, 100, 109606.

Conference proceedings

Olivera A.L.P., Karamanidis K., Mileva K.N., James D.C. Strengthening abductor hallucis is problematic: an investigation of the problem and a solution via neuromuscular electrical stimulation. KNIMS - Competence Network for Immobilization-Related Muscle Disorders Third Annual Conference, Cologne, Germany, March 2021.

Olivera A.L.P., Mileva K.N., James D.C. Strengthening an intrinsic foot muscle via neuromuscular electrical stimulation. PhD Colloquium Berlin Humboldt-University and London South Bank University, London, United Kingdom, December 2020.

Olivera A.L.P., Mileva K.N., James D.C. Neuromuscular electrical stimulation training of an intrinsic foot muscle: what stimulus intensity should be used? 18th Staffordshire Conference on Clinical Biomechanics, Staffordshire, United Kingdom, May 2020.

Olivera A.L.P., James D.C., Mileva K.N., Karamanidis K. Investigating the force generating capacity of *m.* abductor hallucis. XXIV Annual Congress of the European College of Sport Science, Prague, Czech Republic, July 2019.

Olivera A.L.P., James D.C., Mileva K.N. Reproducibility of the neuromechanical responses evoked in muscle abductor hallucis by medial plantar nerve stimulation. The British Association of Sport and Exercise Sciences (BASES) Student Conference, Dundee, United Kingdom, April 2019.

Olivera A.L.P., James D.C., Mileva K..N. Reproducibility of the neuromechanical responses evoked in muscle abductor hallucis by medial plantar nerve stimulation. London South Bank University's Annual Mini Doctoral Conference, London, United Kingdom, April 2019.

Olivera A.L.P., James D.C., Mileva K.N. Strengthening an intrinsic foot muscle via neuromuscular electrical stimulation. London South Bank University's Annual Mini Doctoral Conference, London, United Kingdom, February 2018.

Thesis overview

The intrinsic foot muscles originate and insert below the ankle joint and work collectively to provide stability to the foot during static posture, and stiffness to the forefoot for forward progression during locomotion. Akin to other muscles in the body that are placed under continued load, the intrinsic muscles merit training to meet the weight-bearing demands that are placed on them during everyday static and dynamic activities. The strengthening of these muscles is however a largely neglected area and furthermore, the occurrence of common lower-limb pathologies is associated with their dysfunction. More specifically, an atrophied and dysfunctional abductor hallucis (AbH) is symptomatic to pes planus and Hallux Valgus foot pathologies, which are in turn associated with overuse injury occurrence in the young and an increased likelihood of falling in the elderly populations, respectively. AbH is the strongest intrinsic foot muscle and abducts and flexes the Hallux in an oblique line of action. It stabilises the medial longitudinal arch in posture and stiffens the first metatarsophalangeal joint (1MPJ) for forward progression. Atrophy and dysfunction in AbH may be prevented and/or attenuated through training. Having said that, AbH's complex mechanical action along with an inability for its voluntary activation that is present in both pathological and healthy populations limit the benefits for this muscle from existing training modalities. Given the superficial location of AbH, neuromuscular electrical stimulation (NMES) offers a solution to this problem; however, in contrast to voluntary training, motor unit recruitment and discharge patterns for force production via NMES are non-selective and spatially fixed. Consequently, its efficacy for muscle strength gains relies on high stimulation-intensity protocols, which are uncomfortable and limit participant/patient adherence. Therefore, the purpose of this thesis was to develop an optimised NMES paradigm that is tolerable and efficacious for a targeted strengthening intervention of AbH.

The underpinning motivation for the work conducted herein was to promote the tolerability to, and clinical utility of, NMES delivery to AbH, by implementing a low

stimulation-intensity approach. With this motivation in mind, four sequential experimental studies were designed to identify the optimal mode of NMES application (muscle vs nerve) and stimulation pulse duration, pulse frequency and train duration, training stimulus intensity, and duty-cycle, respectively. The respective outcomes from each study were evaluated using methods including peripheral nerve stimulation, electromyography and force dynamometry. NMES current intensity was set as a percentage of AbH's motor threshold (MT) and delivered via surface electrodes positioned at the pre-identified motor point (motor endplates area) of AbH (cathode) and the 1MPJ (anode). The stimulation protocol for each investigation was delivered while participants were seated with their foot fixed in plantarflexion (35°) and Hallux suspended in dorsal flexion (10°) from a force transducer integrated within a custom-made seating apparatus.

The first experimental study, reported in Chapter 3 (*n*=13), was designed to identify the optimal mode of delivery (muscle vs nerve) and stimulation parameters to elicit AbH MT (frequency and pulse duration). The current intensity-duration relationship was used to optimise the MT determination procedure. The individual rheobase, which represents the minimal current intensity for depolarisation of a given tissue, and the chronaxie, which represents the pulse duration for depolarisation using an intensity value of twice the rheobase, were determined. AbH MTs for muscle and nerve stimulation were identified with 5-pulse trains delivered at frequencies of 10, 20 and 100Hz. Individual intensity-duration curves (mode x frequency) were constructed for pulse durations of 0.05, 0.1, 0.2, 0.5, 1 and 2ms and linearly transformed into charge-duration plots (Weiss linear transformation) to calculate the rheobase (mA) and chronaxie (ms) values. A two-way repeated measures ANOVA (mode x frequency) was performed to analyse the main effects on rheobase and significant differences were followed up with post-hoc pairwise comparisons to identify the stimulation frequency that evoked the lowest rheobase. Chronaxie at this rheobase was then computed by rearranging the Weiss linear

regression function ($y = b + mx$), where y = 0, b = charge, m = rheobase and x = chronaxie. The results revealed that, in comparison to nerve, muscle stimulation required significantly lower intensity to reach rheobase ($p<0.01$; $\eta^2=0.45$). A significant main effect of frequency was found ($p<0.001$; $\eta^2=0.63$) and post-hoc pairwise comparisons of the frequencies tested on muscle revealed that 100Hz required the lowest intensity to obtain rheobase (1.39mA) compared to 10Hz (vs 1.58mA; $p<0.01$) and 20Hz (vs 1.52mA; $p<0.05$). The average chronaxie (pulse duration) resulting from 5-pulse trains at 100Hz on muscle was 1.15ms. Individual chronaxies were then compared to simulated participant responses corresponding to a 1ms pulse-width (frequently used in the literature) and there was no significant difference ($p>0.05$). Thus, the findings from this study have revealed that direct-muscle electrical stimulation requires a lower stimulus intensity than nerve stimulation; and in this first step of designing an NMES paradigm for AbH training, its MT should be determined (for subsequent NMES intensity selection) using a train of 5 x 1ms wide pulses delivered at high frequency (100Hz).

The second study (Chapter 4; *n*=15) was designed to identify the most effective NMES pulse frequency and train duration to maximise the evoked AbH force and minimise muscle fatigue. Peripheral fatigue in AbH was assessed by time-amplitude parameters of the compound muscle action potential (M_{wave}) and corresponding twitch force evoked in response to three single supramaximal (130% of maximal M_{wave}) pulses delivered to the medial plantar nerve. Three paired supramaximal pulses at 10Hz and 100Hz were also delivered to compute a fatigue index ($F_{paired10/100Hz}$) to assess for low frequency fatigue. Force production was assessed from the second pulse of the paired stimuli at 100Hz ($T2_{100Hz}$). These assessments were made before (PRE) and immediately after (POST) stimulating AbH with a set of 5 NMES trains delivered in three frequency patterns (20Hz, 100Hz and alternating (20-100-20Hz)) with each train lasting 6s, 10s or 22s within each frequency pattern. A three-factor (frequency x train duration x time) repeated measures ANOVA was performed to analyse for main effects of time (PRE and POST)

on all parameters measured. Then, a two-way repeated measures ANOVA for main and interaction effects of train duration (6s, 10s, and 22s) and time (PRE vs POST) was performed for each pulse frequency and significant effects were followed up with post-hoc pairwise comparisons. No peripheral or low-frequency fatigue was found in any of the frequency and train duration combinations tested. However, $T2_{100Hz}$ was significantly increased in the alternating frequency pattern delivered in trains lasting 22s (6.9±2.0N vs 7.8±2.4N; p=0.01). This increased force production is indicative of post-tetanic potentiation occurrence achieved following the alternation of frequencies coupled with the higher number of pulses delivered within the train. This frequency pattern and train duration combination is incorporated into the NMES paradigm, which thus far constitutes 22s-trains of 1ms pulses delivered at alternating frequencies (20-100-20Hz) to AbH's motor point.

The purpose of the third study (Chapter 5; *n*=13) was to ascertain a minimum NMES training stimulus intensity for expected strength gains whilst maintaining its tolerability. Previous research has shown that an NMES intensity corresponding to at least 20% MVC is the minimum required threshold to be confident of muscle strengthening. Due to the complex mechanical action of AbH, an MVC is not always achievable in people and therefore standardising stimulus intensity relative to AbH MT is an acceptable alternative. However, the equivalence of this approach to the relative magnitude of MVC has yet to be investigated. In this study, the individual voluntary activation ratio (VAR) in AbH was first assessed via the twitch interpolation technique and used to group participants as *able* (VAR≥0.9; *n*=3) or *unable* (VAR<0.9; *n*=10) to fully activate this muscle. Then, the maximal force produced during contractions evoked by direct-muscle NMES (7s trains of 1ms pulses at 20Hz with progressively increased intensity from 150% to 300% MT) from the *able* participants (VAR=0.93; range: 0.91-0.95) was expressed relative to their MVC force. It was shown that an intensity of at least 200% MT was required to evoke an average force of 11.2 (7.0-18.5)N, which exceeds 20 (21-45)% MVC. Stimulation at this

intensity was perceived as tolerable (mean 3.3; range 2-5) when evaluated on a 10-point visual analogue scale. Despite not being able to activate AbH to its full capacity, the maximum absolute forces produced during the graded NMES protocol were comparable between the groups implying that the peripheral contractility of AbH is intact irrespective of the ability of individuals to voluntary activate AbH to its full capacity. These findings inform a recommendation for a minimum NMES training stimulus intensity and demonstrate that direct-muscle NMES overcomes the prevailing inability for voluntary AbH activation. Thus far, NMES applied to the motor point of AbH, using 22s-trains of 1ms pulses delivered in an alternating frequency pattern (20-100-20Hz) and at an intensity of 200% MT represent the optimised paradigm.

The final experimental chapter (Chapter 6; *n*=8) investigated the effect of NMES duty-cycle on evoked force and muscle fatigue. The time-amplitude parameters describing the excitability (M_{max130}) and contractility (twitch force) of AbH were assessed as indicators for peripheral fatigue; and similar to Chapter 4, the $F_{paired10/100Hz}$ was calculated to assess the low frequency fatigue component. These measures were acquired before (PRE) and following (POST) the application of 5 x 22s trains delivered to AbH using duty-cycles of 1:1 (22s rest), 1:2 (44s) and 1:4 (88s). In addition, the force time integral (FTI; N•s) of the 1st and 5th stimulation trains were calculated to evaluate the decay in the evoked force. A two-factor (duty-cycle x time) repeated measures ANOVA was performed to analyse main and interaction effects and significant findings were followed up with post-hoc pairwise comparisons. Non-parametric Wilcoxon sign-rank tests were performed to compare time effects in M_{max130} terminal phase area, peak twitch force and $F_{paired10/100Hz}$. A significant time effect was found in the evoked force ($p<0.001$; $\eta^2=0.92$), where FTI was significantly reduced in the 5th stimulation train when compared to the 1st train, independently of the duty-cycle used. Post-hoc comparisons revealed that the reduction was significantly greater using a 1:1 duty cycle (-66.8±10.9%) when compared to a 1:4 (vs -35.0±17.3%; $p\leq0.001$), but not a 1:2 (vs -39.8±13.6%; $p>0.05$) duty-cycle.

No peripheral or low-frequency fatigue was found following any of the duty-cycles tested. Thus, the 1:4 duty-cycle, in comparison to using 1:1, enhanced the excitation-contraction coupling dynamics in AbH possibly because it incorporates sufficient time for recovery of the metabolic changes that occur during repetitive contractions, and therefore should be recommended. The findings from this study complete a strengthening paradigm in which NMES is delivered to the motor point of AbH; the paradigm consists of 22s-trains of 1ms pulses delivered at 20-100-20Hz with an intensity equivalent of 200% MT and a 1:4 duty cycle.

This thesis identified a high prevalence of an inability in healthy people to voluntary activate AbH fully. It was further demonstrated that NMES can overcome this inability by evoking force from AbH comparable to individuals who are able to fully activate the muscle. NMES therefore should be used as a strengthening modality not only for the pathological but also asymptomatic feet. The overarching feature of the optimised NMES paradigm developed in this thesis is that it has been built on the use of wide duration pulses (1ms), which keeps the intensity low; yet to a sufficient level where muscle strengthening can be anticipated (200% MT). In doing so, it overcomes the discomfort associated with high-intensity protocols, thus promoting its tolerability and adherence. Combined with an alternating frequency pattern and long train durations, this paradigm promotes higher and longer-lasting force production because the force evoked by stimulation at 100Hz is sustained for longer when interspersed with pulses delivered at 20Hz as opposed to shorter constant frequency trains. The increased capacity of this stimulation pattern to evoke force, as assessed by $T2_{100Hz}$, is likely underpinned by post-tetanic potentiation. The force produced during these NMES trains can be further preserved by implementing a 1:4 duty-cycle with long rest intervals that permit the replenishment of metabolites required for contraction. Cumulatively, the findings from this series of studies present an optimised and tolerable NMES paradigm for a targeted strengthening intervention of AbH.

1.0 Literature review

This chapter reviews current knowledge on the use of neuromuscular electrical stimulation (NMES) as a potential modality to train an intrinsic foot muscle. I first provide a general overview of how the neuromuscular system works to produce and regulate force, as well as its capacity to adapt in response to training stimulus. Next, I introduce the relevance of abductor hallucis (AbH) muscle for the function of the foot, human posture and locomotion. I highlight the need to strengthen this muscle and how NMES overcomes the difficulties to achieve this. Finally, I provide an overview of the different parameters that are integrated within an NMES paradigm and how these require consideration in order to target AbH.

1.1 Muscle adaptations to training

1.1.1 Muscle Activation

Spinal motoneurons (MNs) that innervate a given muscle emanate from clusters or pools located in the ventral horn of the spine to control the descending inputs from the central nervous system that are later transduced into force. MNs, their axons, as well as the muscle fibres they innervate, are excitable tissues and their behaviour is thus governed by the electrical properties for excitation of their respective membranes. For example, in a simple cable model and following Ohm's law, the voltage threshold for the MN's membrane depolarisation is directly proportional to the synaptic current and inversely proportional to the total input resistivity (sum of the resistivity of dendrites and soma membrane). The lipidic bilayer of the membrane sets its resting potential based on the gradient between the intracellular and extracellular ionic concentrations of sodium ($[Na^+]$), potassium ($[K^+]$) and chloride ($[Cl^-]$), where $[Na^+]$ and $[Cl^-]$ is greater outside the membrane, and $[K^+]$ is greater in the intracellular space. Correspondingly, the membrane resting potential conventionally equates to -70mV (i.e., more negative on the inside than

the outside) for ionic equilibrium, and its voltage threshold is determined mainly by the sensitivity of its Na^+ channels. The total resistivity largely depends on the size of the MN (number and extent of dendritic branches) and density of ionic channels (K^+, Na^+, Cl^-), where smaller MNs will be recruited prior to larger MNs because the former require the least synaptic current to bring about a change in the membrane potential to reach voltage threshold (Heckman & Enoka, 2012).

MN excitability depends on the rheobase of its membrane, which represents the minimum synaptic current required to reach the threshold for depolarisation. When the synaptic current exceeds the threshold, the MN transduces the input into a repetitive discharge of action potentials in a linear frequency-current intensity relationship (Fig. 1.1A), which varies depending on the synaptic (metabotropic) input. The slope of the function it describes represents the input-output gain of the MN (Fig. 1.1B), where the steeper the slope due to subthreshold depolarisation (lowered voltage threshold), action potential threshold hyperpolarisation, afterhyperpolarisation reduction (due to decreased input resistivity) and persistent inward currents amplification, the greater the gain. Both (Fig. 1.1), the voltage threshold and input-output gain collectively define the MN excitability (Heckman & Enoka, 2012). Furthermore, the bistability behaviour of persistent inward currents allows for the firing of action potentials during long periods of time in the presence of lower synaptic input or amplifies the net current for repetitive discharge of action potentials. The activation of these currents will eventually contribute to the output of MNs, and the eventual force generated by motor units (MUs) (Heckman & Enoka, 2012).

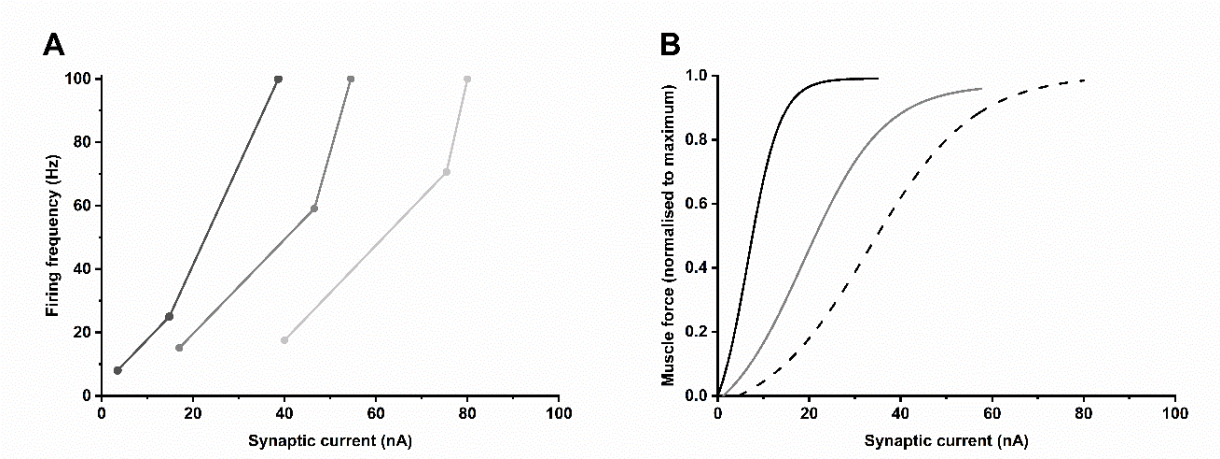

Figure 1.1. A: Firing frequency-current intensity relationship for a type S (i.e. slow; black), FR (i.e. fast fatigue resistant; dark grey) and FF (i.e. fast fatigable; light grey) motor units (MUs) from a motoneuron (MN) model. The first symbol for each MN type represents the frequency and current at threshold, whereas the second represents the frequency and current at the transition from the primary to the secondary range of increasing discharging rate, which is represented by the two linear regions between symbols, respectively. **B:** Representation of the input (current)-output (force) gain of a pool of MUs at three distinct levels of neuromodulation: high (black), medium (grey) and low (dashed). A shift from left to right would be indicative of increased persistent inward currents, depolarised rest potentials and decreased potentials thresholds. These theoretical approximations were reconstructed based on data taken from Heckman & Binder, (1991) for A and presented in Heckman & Enoka, (2012) for B.

The motor output and consequent force production are regulated by the combination of MU recruitment and discharging rate for a given synaptic input current. During submaximal force production, the primary source is MU recruitment until it reaches its upper limit, where firing rate becomes the prominent generator of higher levels of force (Cutsem et al., 1997). The recruitment threshold of MUs is muscle specific, for example, for the muscle adductor pollicis is ~30% of maximal voluntary contraction (MVC)

(Duchateau & Enoka, 2011), whilst for the flexor hallucis brevis can be up to 98% MVC force (Aeles, et al, 2020). The firing frequency during sustained voluntary contractions ranges between 5-40Hz (Cutsem et al., 1997; Conwit et al., 1999), though they have been shown to reach above 200Hz during rapid ballistic contractions (Del Vecchio et al., 2019). Muscles that require sustained contractions at relatively low force will produce lower firing frequencies (e.g. 3-11Hz) early in the contraction (e.g. AbH), as opposed to those that require contracting rapidly for shorter periods of time, which will in contrast rely on higher frequencies (e.g. 5-23Hz) to modulate early production of force (e.g. flexor hallucis brevis) (Aeles et al., 2020). The action potential fired by the excited MNs depolarises the sarcolemma of all its muscle fibres that are innervated by it in an all-or-none fashion, which results in the release of calcium ions (Ca^{2+}) from the sarcoplasmic reticulum and a concomitant increase in transient myoplasmic calcium concentration ([Ca^{2+}]) to bind to troponin C for cross-bridge interaction, which brings about a muscle contraction (excitation-contraction coupling). The contraction that results from a single action potential produces a twitch force response, which is then repeated in line with the firing rate of MUs (Heckman & Enoka, 2012).

The increase in muscle force occurs as a result of the synchronous and repetitive excitation of the sarcolemma that increases the release of Ca^{2+} from the sarcoplasmic reticulum, which is then available for cross-bridge interaction. Release of Ca^{2+} increases force production until a saturation level is reached, at which no further increase in force occurs (Place et al., 2010). The force relationship to the firing frequency is approximately sigmoidal due to an upper limit in the capacity of the contractile machinery to cycle repeatedly to produce force. This relationship plateaus at high frequencies (e.g. ≥50Hz) (Edwards et al., 1977; Macefield et al., 1996; Binder-Macleod et al., 1998), which is underpinned by a saturated Ca^{2+}-uptake from the myoplasm that results in maximal rate of cross-bridge interaction during muscle contraction (Gregory et al., 2007; Mettler & Griffin, 2010). For summation of twitch forces into a tetanic contraction, a range of ~20-

50Hz is considered within the physiological range for muscle contractions. If the interval between action potentials is lower than this range, full relaxation (i.e. re-uptake of Ca^{2+} by the sarcoplasmic reticulum) of the muscle from the first potential(s) ensues and no summation in force occurs following subsequent potentials (Binder-Macleod & McDermond, 1992; MacIntosh & Willis, 2000). This will result in an unfused tetanic state of contraction.

1.1.2 Muscle mechanics

The mechanical interaction of the contractile machinery and passive-elastic framework of the muscle-tendon unit, to generate active and passive force respectively, permit the transduction of force into movement. At the sarcomere level, the cross-bridge interaction, where the thick (myosin) and thin (actin) protein complexes slide cyclically for muscle contraction, is considered responsible to produce active force (Huxley, 1957). To achieve this contraction or at passive states, the filamentous protein titin spans from the M-band to Z-band to provide structural stability and provision of passive-elastic force to the sarcomere (Herzog, 2018). At the muscle-tendon unit's level, the interaction between contractile and passive elements has been schematised in the Hill's three-component behavioural model. In this model, the contractile component represents the muscle's capacity to contract and produce force, whilst the series and parallel elastic components represent the elasticity and stiffness, respectively, of all elastic elements of the muscle-tendon unit that transfer the force generated (Hill, 1938). The structures associated with the latter components are the tendon, aponeurosis and extracellular matrix of connective tissue that surrounds the contractile machinery within muscle fibres (Gillies & Lieber, 2011). Thus, tendons ultimately transduce the force generated by the muscle to the bones to produce a moment about a joint.

In addition to the level of activation during the excitation process and the muscle architecture, the active force produced is also related to the muscle's length and velocity of contraction. Specifically, the force-length and force-velocity relationships are the mechanical properties that influence the muscle's capacity to generate force.

1.1.2.1 Force-length relationship

Theoretically, at the sarcomere level, maximum force is achieved when the maximum number of myosin and actin filaments are overlapped to form cross-bridges, and this overlap varies as a function of changes in the sarcomere's length (Gans, 1982; Rassier et al., 1999). The force-length relationship, which is based on in vitro single muscle fibre experiments, describes a parabolic curve with the resting length of the sarcomere being considered the original length. As the length of the sarcomere increases, so does the force production to mark the ascending limb of the curve where cross-bridge formation is progressively maximised. At the optimal length, and plateau of the curve, the force produced is constant and the changes in length are minimal providing maximum capacity for cross-bridge formation. If the sarcomere is lengthened further from this point, the force produced decreases as the filaments are placed further apart (Gans, 1982; Rassier et al., 1999; Maganaris, 2001). Nevertheless, when the sarcomere is lengthened further its optimal range for force production, the passive force increases exponentially due to the contribution of titin and other passive-elastic elements (Herzog, 2018). When considering the entire muscle, its operating range along this theoretical curve is based on its function to meet the demands placed on them.

In vivo empiric identification of the optimal muscle-tendon length and operating range of a muscle or group of muscles on the theoretical sarcomeric force-length relationship is inferred by the curve describing the joint moment–angle relationship (Maganaris, 2001; Karamanidis & Arampatzis, 2005; De Monte & Arampatzis, 2009). As tendons insert into

the bone at a distance to the joint, the moment generated during muscle contraction causes the rotation of the bone about the joint to bring about movement. The perpendicular distance between the axis of rotation at the joint and the muscle-tendon unit's insertion represents the internal moment arm. Given the difficulty to measure this internal moment arm, the joint moment–angle relationship considers instead the external moment arm, which is defined as the perpendicular distance between a joint and the line of force production. The torque produced ($T=I \bullet \alpha$, where I represents rotational inertia and α represents angular acceleration) reflects the sum of all the muscle moments acting about a joint and therefore the term 'joint moment' is commonly adopted. The magnitude of a joint moment is equal to the product of the force produced by the muscle-tendon unit and the external moment arm. Since the length of the muscle changes when the joint is positioned at different angles, the joint moment–angle relationship can be constructed as forces of different magnitudes will be produced at different joint angles. The joint moment–angle relationship has therefore served to identify the optimal operating range of muscle groups such as the plantarflexors (Maganaris, 2001; De Monte & Arampatzis, 2009), dorsiflexors (Maganaris, 2001) and knee extensors (Karamanidis & Arampatzis, 2005). For example, the tibialis anterior and soleus muscles operate on the ascending and plateau region of this curve (Maganaris, 2001), whereas the knee extensors operate around the curve's plateau region (Karamanidis & Arampatzis, 2005).

1.1.2.2 Force-velocity relationship

The force-velocity relationship describes the muscle-tendon unit's capacity to produce force as a function of its velocity. Specifically, higher forces are produced at lower velocities and vice versa (Hill, 1938). In a similar fashion to the force-length relationship, the force-velocity has also been postulated to follow a theoretical basis of sarcomeric sliding filaments and kinetics of cross-bridge formation (Huxley, 1957). This would suggest that force production is reduced as fewer cross-bridges are formed at a high

velocity, or lower velocities allow the forming of a greater number of cross-bridges for force production. When considering the muscle's behaviours during dynamic contraction, the force (or torque)-(angular) velocity follows a double-hyperbolic curve (sigmoidal pattern) that accounts for the concentric (shortening) and eccentric (lengthening) components of the performed movement (Reeves & Narici, 2003; Alcazar et al., 2019). This shape of the force-velocity curve may provide mechanical stability to the sarcomeric filament at high forces, in turn, it allows the muscle to remain nearly isometric within a larger range for force production. This means that muscles are able to withstand being overloaded whilst having a relative change in their length and thus be protected from injury (Alcazar et al., 2019). Given this capacity of muscles to tolerate high loads during eccentric contractions, eccentric resistance training is often considered a superior training mode to concentric loading for achieving hypertrophy. However, this is equivocal as both types of training have led to similar hypertrophic results (Franchi et al., 2017). The difference between the training modes appears to reside in the distinct mechanisms and adaptations that underlie the strengthening achieved, which appear to be contraction type-specific (Franchi et al., 2017).

1.1.3 Adaptations to training and their assessment

Training of muscle refers to the production of force via muscle contraction at regular time intervals and with the intention to evoke gains in strength, power, motor performance, and/or muscle hypertrophy. The neuromuscular system adapts in response to long-term exposure to training in order to meet the force production demands efficiently. Neurological adaptations of the neural input that drives muscle activation and the morphological adaptations of the target muscle can both contribute to the resultant increase in force-generation capacity. Nevertheless, the strength gains achieved due to

neurological adaptations precede those due to muscle hypertrophy, and will therefore be the focus of this thesis.

Training first induces adaptive changes at the brain (Tadeu Serra et al., 2019) and spinal level (Gazula et al., 2004) that lead to a greater neural drive to the muscle and the ability to maximise its activation and produce force. Muscle activation is enhanced by training-induced plasticity in the neuronal network presented as enhanced facilitation of synaptic processes and reduced inhibition at the primary motor cortex level and/or the spinal synaptic and descending pathways from the MN pool (Weier et al., 2012; Mason et al., 2020; Siddique et al., 2020).

Animal studies have noted that activity-dependent brain-derived neurotrophic factor is expressed in select areas of the brain (hippocampus and motor cortex; Tadeu Serra et al., 2019) and spinal cord (Gomez-Pinilla, 2002; Joseph et al., 2012) after training. This neurotrophic factor is considered an important precursor of neuroplasticity due to its role in neuroprotection (e.g. preservation of dendrites integrity after an insult to the system) and as an activator of protein synthesis signalling pathways for neuronal growth (Park & Poo, 2013; Tadeu Serra et al., 2019). At the spinal level, expression of brain-derived neurotrophic factor in MNs after training has been found (Gomez-Pinilla, 2002; Joseph et al., 2012) to potentially participate in inducing growth of the dendritic arbour (Gazula et al., 2004; Gardiner et al., 2006), or changes in other areas of the MN (e.g. soma, the initial segment of axon, axon; Gardiner et al., 2006). An increase in MN dendritic branches in response to training therefore affects MN excitability (Gazula et al., 2004; Gardiner, 2006), given the correlation between membrane resistivity and the size of the MN (Gardiner et al., 2006; Krutki et al., 2017). For example, increased firing rate, a steeper slope of the frequency-current relationship, increased input resistance and reduced rheobase were found in the MNs of rats following 5 weeks of resistance training (Krutki et al., 2017). However, training-induced changes in the MN morphology may be minimal (Gardiner et al., 2006), or have a more prominent role in neuroprotection (Gazula

et al., 2004). In humans, direct assessment of MN morphology or excitability is methodologically impossible, but electromyography (EMG) allows an indirect and minimally invasive assessment via MU behaviour.

EMG is a widely used tool to record the summation of all the MU action potentials generated during a contraction. In combination with electrical stimulation, surface EMG can be used to discern adaptations occurring at the muscle or spinal level. Stimulating the peripheral nerve supplying a given muscle (or muscle group) results in the synchronised and time-locked depolarisation of MN axons, which evokes a compound muscle action potential (or M_{wave}) from all the innervated muscle fibres. Increasing the stimulation intensity to a supramaximal level ensures the activation of all MUs from the MN pool (Maffiuletti & Martin, 2001; Palmieri et al., 2004). The latency of the evoked M_{wave} depends on the distance from the stimulation site to the muscle (medial plantar nerve to AbH is ~7ms; James et al., 2018), and reflects the propagation integrity along the MN and/or muscle sarcolemma (Kouzaki et al., 2016; James et al., 2018). The amplitude and area of the M_{wave} are indicators of the electrogenic Na^+-K^+ transport across the sarcolemma and T tubules and indirectly reflect the number of MUs recruited and their level of synchronisation (Clausen, 2003). The M_{wave} area is the product of the amplitude and duration of the potential, and the latter changes as a function of the muscle fibres' conduction velocity, where a slower conduction results in the broadening of the duration of the potential (Bigland-Ritchie et al., 1979; Merletti et al., 1990; Galea, 2001). Together, these parameters can be used to assess training adaptations in the peripheral excitability of a muscle.

Indeed, changes in peripheral excitability have been previously found after training. Specifically, 7 weeks of elbow flexion MVCs resulted in an ~85% increase of the supramaximal M_{wave} amplitude evoked from the biceps brachii (Colson et al., 2009). A comparable increment of ~49% was also found following 7 weeks of NMES training of the same target muscle at a high intensity (60-70% MVC) (Colson et al., 2000). These

findings indicate that training, via voluntary or NMES-evoked contractions, results in more efficient membrane ionic and electrogenic processes, and thus increased peripheral excitability of the target muscle that ultimately contributes to the strength gains observed.

Low-intensity NMES training has also elicited peripheral excitability adaptations. Indeed, a 20% increase of the supramaximal M_{wave} amplitude was observed in the soleus after a 2-week NMES intervention delivered at low intensity (20% MVC) (Bouguetoch et al., 2021). Again, this would indicate that the peripheral excitability of this muscle was increased and already evident following the short-term exposure to NMES. An increase in the latency and area of the supramaximal M_{wave} has been found in AbH following a training session with NMES, indicative of reduced conductivity and excitability due to peripheral fatigue (James et al., 2018). These findings provide evidence that adaptations occurring at the peripheral level in response to training can be assessed in the intrinsic foot musculature via the evoked M_{wave} and its shape.

As for adaptations in the spinal excitability, the amplitude of the Hoffmann or H-reflex is traditionally evaluated to provide an indication of the MN pool responsiveness at the spinal level following training (Knikou, 2008; McNeil et al., 2013; Siddique et al., 2020). For example, the H -reflex amplitude recorded at the soleus was found to increase by 17% and 15%, measured respectively during 20% and 60% MVC, following three weeks of maximal plantarflexion resistance training (Holtermann et al., 2007). The H-reflex is often evoked at submaximal stimulation intensities and has a longer latency than the M_{wave} (Palmieri et al., 2004; Knikou, 2008; McNeil et al., 2013). Though the H-reflex can be obtained from the soleus at rest given its strong central modulation, a submaximal (often weak) voluntary contraction facilitates the discharge of the reflex and is recommended (Knikou, 2008; Burke, 2016). In the AbH muscle, the H-reflex is technically difficult to obtain even during voluntary contractions (Burke, 2016) and has been found absent in up to 25% of healthy older individuals (Versino et al., 2007). In

those from whom H-reflex can be obtained, it showed amplitudes of ~6mV and a latency of ~38ms when the stimulation is applied to the tibial nerve at the popliteal fossa (Ellrich et al., 1998; Versino et al., 2007), as recording it when stimulating at the medial plantar nerve is difficult (Versino et al., 2007). The number of studies recording the H-reflex from the intrinsic foot muscles is scarce and following training interventions have not been reported. Therefore, in contrast to evoking the M_{wave}, using the H-reflex for this muscle and quantifying spinal excitability adaptations is constrained.

Peripheral muscle contractility and its adaptations in response to training interventions can be assessed from the twitch contraction subsequent to the evoked M_{wave}. This force response is recorded via dynamometry and provides an indication of the integrity of the excitation-contraction coupling, cross-bridge formation and relaxation processes (Fitts, 1994; Rampichini et al., 2014). Specifically, its peak force reflects the number of strongly bound cross-bridges formed to produce the contraction (Fitts, 1994), and its half relaxation time represents the processes of Ca^{2+} re-uptake from the myoplasm and cross-bridge detachment (Hill et al., 2001). An increased peak twitch force has been reported for knee extensors (17%) after an 8-week maximal resistance training intervention (Rich & Cafarelli, 2000) and in the soleus (21%) after 2 weeks of low intensity (20% MVC) NMES training (Bouguetoch et al., 2021). Furthermore, acute adaptations in the half-relaxation time of AbH twitch force have been reported following ~30min of low intensity NMES (James et al., 2018), which shows a reduced excitation-contraction coupling and contractility of the muscle due to an impaired capacity for Ca^{2+} re-uptake (Hill et al., 2001). Therefore, assessing the evoked M_{wave} and the corresponding twitch force provides an indication of at least peripheral excitability and contractility training-induced adaptations.

The performance of an MVC is a standardised method for measuring strength adaptations after training. The maximum force (or its rotational equivalent: torque) measured during its performance represents the muscle's capacity for force generation,

and changes in this capacity are attributable to morphological as well as neurological training-induced adaptations (Duchateau et al., 2006). In other words, increased excitability of the entire central nervous system to initiate the neural drive for activation of all MUs, as well as enhanced contractility of the muscle fibres, contribute to an augmented production of force in response to training (Scaglioni et al., 2002; Duchateau et al., 2006; Duchateau et al., 2021). However, performing the MVC of individual muscles can be difficult (Arinci Incel et al., 2003). This is particularly true for the intrinsic foot muscles, which most often have been assessed as a group and in combination with the extrinsic foot musculature (Soysa et al., 2012; Goldmann & Brüggemann, 2012; Yamauchi & Koyama, 2019ab). Attempts to isolate the force generated by a single muscle, e.g. AbH (Kelly et al., 2013) and flexor hallucis brevis (Aeles et al., 2020), have required extensive familiarisation and constant inspection of synergists activation via surface EMG to minimise their contribution (Aeles et al., 2020).

The neurological adaptations contributing to the increased muscle ability for force production following training can be quantified by the interpolated twitch technique for assessing the voluntary activation during an MVC (Merton, 1954). During an MVC, a small percentage of the target muscle's MN pool may not be sufficiently excited by the volitional command (Merton, 1954; Allen et al., 1995; Herbert & Gandevia, 1999). In order to ensure that all MUs are activated, a pair of electrical pulses (100Hz) can be delivered to the peripheral nerve or the corresponding end-plate nerve terminals of the muscle (motor point area) during the MVC (Belanger & McComas, 1981; Herbert & Gandevia, 1999; Oskouei et al., 2003; Shield & Zhou, 2004). As a result, an evoked twitch force is superimposed over the MVC force. A second set of paired stimuli delivered during rest represents the evoked twitch force when all MUs are activated by the stimulation alone (Shield & Zhou, 2004). Based on the amplitude of the interpolated twitch force, represented as a fraction of the resting twitch force, voluntary activation can

be quantified (Merton, 1954; Allen et al., 1995; Herbert & Gandevia, 1999; Shield & Zhou, 2004).

In summary, neurological adaptations are underpinned by changes occurring in the excitability of the central nervous system and MUs. The impact of an enhanced central drive and peripheral excitability to generate a muscle contraction and produce force can be indirectly assessed with the use of EMG. The combination of this technique with peripheral nerve stimulation provides a standardised method to assess the peripheral and spinal excitability through the electrically evoked action potentials, the M_{wave} and H-reflex, respectively. When the M_{wave} is evoked at supramaximal intensity, the propagation efficiency along all MUs within a muscle, and the integrity of the ionic transport along the sarcolemma, can be assessed following a training intervention by measuring its latency, amplitude and area. For its part, the subsequent twitch force can be used to assess the peripheral contractility as it provides an indication of the excitation-contraction coupling. The MVC is regarded as a gold standard assessment of global training-induced adaptations, which includes both neurological and morphological adaptations. The MVC in combination with the interpolated twitch technique has been implemented to assess the voluntary activation, and discern the neurological capacity to drive muscle for contraction. However, the production of MVC force is not straightforward for all muscles specifically those with small size such as the intrinsic foot muscles.

1.2 The intrinsic foot muscles

The foot is a complex and versatile structure comprised of 28 bones, which along with its 107 ligaments, provide the framework to form 35 joints. The bones can be grouped into the tarsals, metatarsals, and phalanges (Fig. 1.2A). The joints formed can be considered in combination and grouped into the subtalar, transverse tarsal (calcaneocuboid and talonavicular joints), tarsometatarsal (cuneo- and cuboid-

metatarsal joints), metatarsophalangeal, and interphalangeal joints (Fig. 1.2B) (Joseph, 1954; Leardini et al., 2001; Lakin et al., 2001; Nester et al., 2002 Frimenko et al., 2012), which allow triaxial motion (Nester et al., 2014) with the exception of the interphalangeal joint, which allows only sagittal plane motion (Joseph, 1954). This multijointed and multiplanar structure, and the arches it forms with the plantar fascia, are controlled by the collective work of the foot muscles (McKeon et al., 2015).

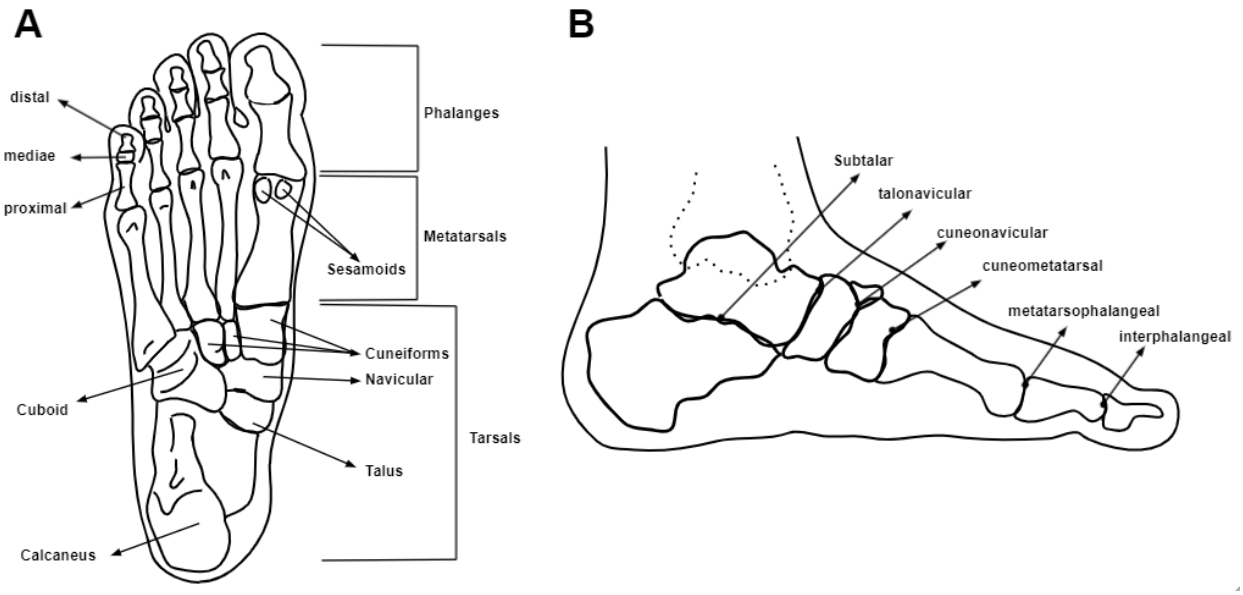

Figure 1.2. Representation of the bones of the foot (**A**; transverse plane, plantar view) and its joints (**B**; sagittal plane, medial view). Note that the calcaneocuboid and cuboid-metatarsal joints are not shown in B. The illustrations presented in this figure were redrawn based on the work of Muscolino (2016).

The muscles that control the foot complex can be grouped into intrinsic and extrinsic muscles. The intrinsic foot muscles originate and insert within the foot to actively stabilise and stiffen its multiple joints during static posture and locomotion demands (Kelly et al., 2012; 2014, 2015; Farris et al., 2019). They are grouped into four layers based on their

superficiality (Fig. 1.3): the AbH, flexor digitorum brevis and abductor digiti minimi are within the first and most superficial layer; the second layer is made of the quadratus plantae and lumbricals; the third layer is composed of the flexor digiti minimi, adductor hallucis and flexor hallucis brevis; and the fourth and deepest layer is made of the plantar interossei, dorsal interossei and extensor digitorum brevis. The first and second layers run along the medial and lateral longitudinal arches, whilst the third and fourth do so in alignment with the anterior and posterior transverse arches of the foot (McKeon et al., 2015). For their part, the extrinsic foot muscles originate above the ankle joint and act as global movers that work together with the intrinsic musculature to generate foot motion (McKeon et al., 2015). The specific contribution of the intrinsic foot muscles allows to control the deformation of the arches when the external load on the foot is increased (Kelly et al., 2012), thus providing stability during posture, and stiff metatarsophalangeal joints to push forward during locomotion (Kelly et al., 2015; Farris et al., 2019). When the intrinsic foot muscles are unable to provide stability because they are fatigued (Headlee et al., 2008) or their nerve supply has been interrupted (Fiolkowski et al., 2003), the functional integrity of the foot is impaired due to a consequent collapsed foot arch. In contrast, increased activation of these muscles prevents the deformation of the arch when the foot is under load (Kelly et al., 2012; 2014). However, interventions targeting these muscles to preserve their function are largely ignored (McKeon et al., 2015), which perhaps explains why their dysfunction is symptomatic to common foot pathologies (Stewart et al., 2013; Angin et al., 2014) and associated with lower limb over-use injuries (Zhang et al., 2019).

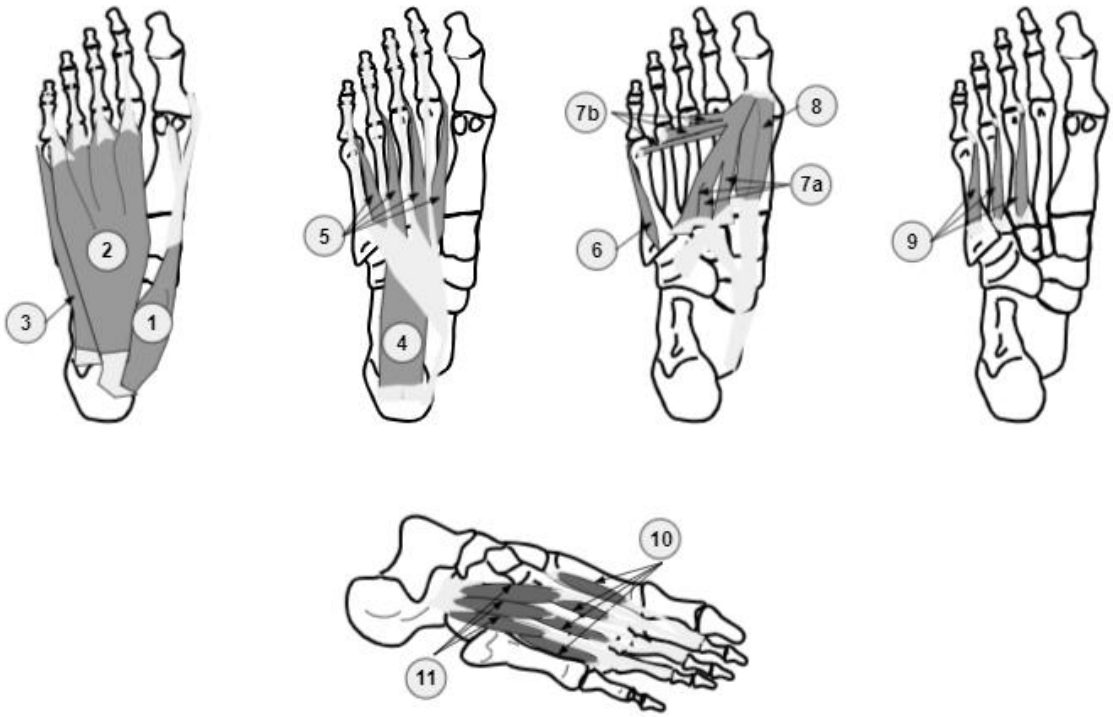

Figure 1.3. Representation of the intrinsic foot muscles redrawn based on the work from McKeon et al., (2015). Based on their superficiality, the intrinsic foot muscles are grouped into four layers: the first and most superficial layer includes the AbH (1), flexor digitorum brevis (2) and abductor digiti minimi (3); the second layer is made of the quadratus plantae (4; with insertion into the flexor digitorum tendon) and lumbricals (5); the third layer is composed of the flexor digiti minimi (6), adductor hallucis oblique (7a) and transverse (7b) heads, and flexor hallucis brevis (8); and the fourth and deepest layer is made of the plantar interossei (9), dorsal interossei (10) and extensor digitorum brevis (11).

Given its size, function and location, the AbH is perhaps the most relevant intrinsic foot muscle. AbH has a larger size compared to other intrinsic foot muscles (Kura et al., 1997) and importantly, the muscle-tendon unit courses the medial aspect of the foot from the calcaneus to Hallux and therefore dynamically supports the medial longitudinal arch for posture (Kelly et al., 2012; 2014), and stiffens the forefoot (Farris et al., 2019) during locomotion.

1.2.1 Abductor Hallucis (AbH)

1.2.1.1 AbH morphology

AbH originates from three locations: the medial tubercle of the calcaneus, the flexor retinaculum and a few fibres from the plantar aponeurosis (Wong, 2007; Agawany & Meguid, 2010). Its tendon runs across and inferiorly to the first metatarsophalangeal joint (1MPJ) inserting at the proximal phalanx of the Hallux, though in some individuals the tendon splits to also insert at the joint and the medial sesamoid bone (Brenner, 1999). The origin and insertion location of the AbH tendon enables the simultaneous abduction and flexion of the Hallux in an oblique line of action. This is important to stabilise the metatarsophalangeal joint as it has the greatest range of motion of the foot joints permitting up to 60° dorsiflexion during the push-off phase of gait (Bojsen-Møller & Lamoreux, 1979), where it undergoes an estimated 86% body weight load (Jacob, 2001).

Located within the superficial layer of the intrinsic foot muscles (Fig. 1.3), AbH is supplied by the medial plantar artery and innervated by a branch of the medial plantar nerve (Fig. 1.4B). The corresponding motor-nerve ending zones are concentrated within an area (motor point area) that is located posterior and inferior to the navicular tuberosity (Choi et al., 2017). Correspondingly, the navicular tuberosity represents a reliable reference for the identification of the most excitable area for stimulation of this muscle (James et al., 2013; 2018).

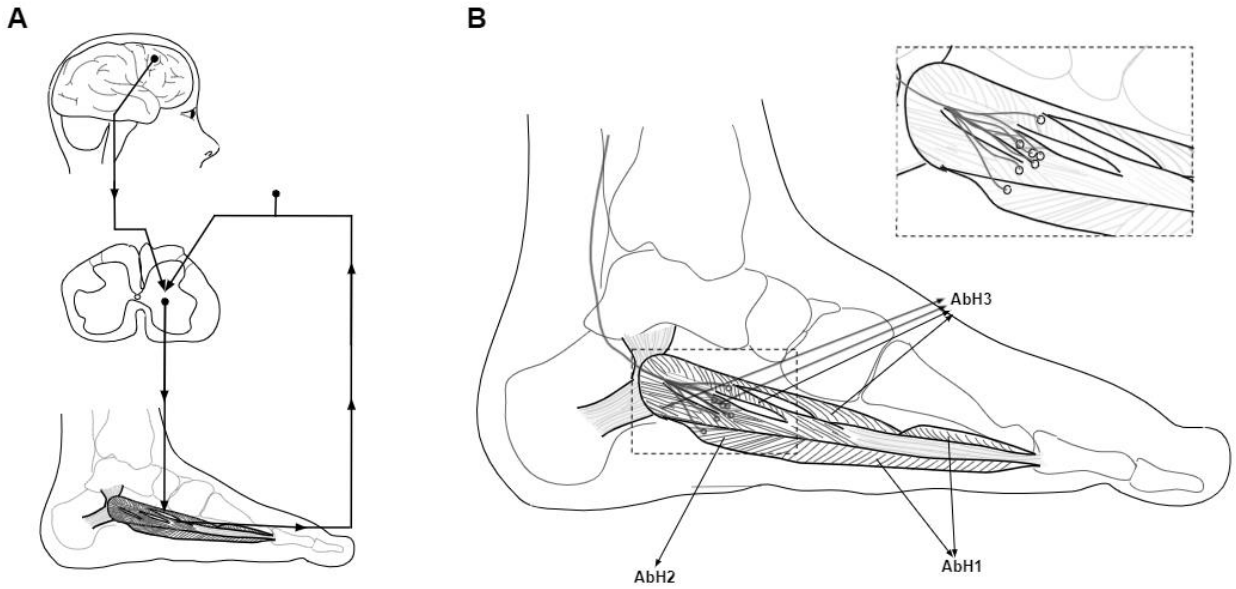

Figure 1.4. A: Schematic representation of the connection of AbH to the central nervous system via efferent and afferent pathways. **B:** Representation of the AbH morphology with its complex fibre segmentation into AbH1 (unipennate and/or bipennate and/or multipennate), AbH2 (parallel and/or unipennate and/or bipennate) and AbH3 (multipennate) based on the work from Kura et al., (1997) and Tosovic et al., (2012). A representation of the potential location of the motor-nerve ending zones (motor point area) of the medial plantar nerve is also shown (white circles) based on the work of Choi et al., (2017).

AbH has the greatest volume (~15cm^3) and the largest physiological cross-sectional area (6.7cm^2) of all the intrinsic foot muscles (Kura et al., 1997), making it perhaps the strongest muscle within the foot. On average, it has a fibre length of ~2.3cm, and a muscle length ranging between 11.6cm and 14.3cm (Kura et al., 1997; Tosovic et al., 2012). This equates to a low fibre-to-muscle length ratio (i.e. 0.2) (Kura et al., 1997; Tosovic et al., 2012), implying that AbH is a pennate muscle with its short muscle fibres at one or more angles to the line of force production. As a result, AbH has a morphological preference for maximising force production at the expense of contractile velocity (Kura et al., 1997). Indeed, having shorter fibres alongside each other results in

a greater pennation angle (~19° in AbH; Tosovic et al., 2012) and physiological cross-sectional area, which increases its force generating capacity (Lieber and Bodine-Fowler, 1993; Narici et al., 2016). This is further supported by its low number (~48) of MUs (Minetto et al., 2009; Johns & Fuglevand, 2011; Kelly et al., 2013), which are primarily of slow twitch type and have a relatively low firing frequency (i.e. 14Hz) (Širca et al., 1990; Kelly et al., 2013). Together, these muscle characteristics and morphological arrangement render AbH capable to produce relatively high forces for sustained periods of time when recruited to control the posture of the foot.

AbH has a complex morphology (Fig.1.4B). Specifically, four distinct segments have been reported in this muscle, with each presenting a different architectural configuration: parallel, unipennate, bipennate and/or multipennate, rendering the muscle with an average of ~19° of pennation angle (Tosovic et al., 2012). This multi-segmented morphology is represented by the often-observed trapezoidal shape of AbH (Kura et al., 1997; Agawany & Meguid, 2010; Tosovic et al., 2012). The multipennate segment is the most proximal and strongest (5.2cm^2 of physiological cross-sectional area and lowest fibre-to-muscle length ratio), and largely represents the muscle's overall force generating capacity (Tosovic et al., 2012). It may be mainly responsible for Hallux abduction while the other sections are perhaps more involved in producing stabilising forces for the foot arches (Tosovic et al., 2012).

Having morphologically different sections within the same muscle may also lead to a non-uniform activation of its MUs for flexion and/or abduction of the Hallux (Tosovic et al., 2012) in order to directionally tune the force produced by its fibres. For example, Paton & Brown (1994) and Falla & Farina (2008) noted that different segments of the pectoralis major and trapezius muscle, respectively, were selectively activated to match the force production required for a given task. This may be explained by the different MU behaviour (recruitment and firing rate) available to control force, which has also been found to be muscle segment-dependent (Falla & Farina, 2008). Accordingly, the different

segments of AbH may perhaps be activated selectively or in synchronisation in order to efficiently meet the force generation demands in the line of action required for a given motor task (abduction, flexion, or a combination of both) (Fig.1.4), however, this has not been investigated.

1.2.1.2 AbH function

AbH has been shown to have an important role in human posture and locomotion. During posture, this muscle provides support to the medial longitudinal arch of the foot (Wong, 2007; Kelly et al., 2012; 2014, 2015; Kirby, 2017). For example, Kelly et al. (2012) demonstrated that the EMG activity of AbH increased in order to meet the change in postural demand from double to single limb support. In doing so, AbH is capable of controlling the deformation of the medial longitudinal arch as the load placed on the foot increases (Kelly et al., 2012, 2014). Indeed, in a subsequent study, Kelly et al. (2014) showed that the activation of AbH increased as the external load was progressively applied to the foot while participants were seated in order to deform the arch. They then went on to show that if sustained electrical stimulation was applied to the muscle whilst under load, the deformation of the arch, both in length and height, was significantly reduced due to the foot posture changes achieved by the evoked contraction. To further support the crucial role of AbH during static weight bearing stance, a collapsed medial longitudinal arch is found when this muscle has been fatigued (Headlee et al., 2008) or its supplying nerve blocked (Fiolkowski et al., 2003).

During locomotion, AbH has an active role in exerting counteracting forces in order to stiffen the 1MPJ (Farris et al., 2019) as it provides a rigid forefoot to control the forward motion of the body (Miyazaki & Yamamoto, 1993; Rolian et al., 2009). Indeed, an increasing EMG activity of AbH was found from foot contact to toe-off during walking and running at different velocities (Kelly et al., 2015). Similarly, reduced moments about the

metatarsophalangeal joint during walking and running were found when the supplying nerve was blocked (Farris et al., 2019). This implies that the impaired function of the AbH resulted in a reduced stiffness of the joint and prevented the generation of moments for normal push-off. As a consequence, proximal joints such as the hip were required to increase the work produced in order to compensate for the reduced capacity of this muscle (Farris et al., 2019).

Dysfunction in AbH is symptomatic in a number of lower-limb related pathologies. Particularly, a smaller morphology of this muscle has been found in individuals with pes planus (Angin et al., 2014; Zhang et al., 2019), lesser toe deformities (e.g. claw/hammer toes; Mickle et al., 2018), chronic plantar heel pain (Franettovich-Smith et al., 2019) and Hallux Valgus (Stewart et al., 2013; Aiyer et al., 2015). Hallux Valgus is a progressive forefoot deformity that results in the lateral deviation of the Hallux and a prominence that develops on the dorsomedial aspect of the first metatarsophalangeal joint; this is a highly prevalent condition which affects 23% of adult (18-65 years old) and 36% of elderly (>65 years old) populations (Stewart et al., 2013). In people with Hallux Valgus, the AbH is atrophied and the reduction in its size increases by as much as ~20% with the severity of the deformation (Stewart et al., 2013) and ageing (Aiyer et al., 2015). The resulting deformed bony prominence at the medial aspect of the joint leads to the displacement of the insertion of the muscle leading to its inability to abduct the Hallux (Arinci İncel et al., 2003; Stewart et al., 2013). Attempts to mitigate the effects of Hallux Valgus on the integrity of AbH have been made with, for example, the implementation of gross foot manoeuvres in combination with orthoses wearing (Kim et al., 2015). Nevertheless, these attempts are still limited in being able to target AbH in isolation and the muscle's complex morphology.

1.2.1.3 Approaches for strengthening AbH

A number of foot exercises exist to strengthen AbH. Specifically, the short foot exercise has been put forward to train AbH (Newsham, 2010; Lynn et al., 2012; Mulligan & Cook, 2013; McKeon et al., 2015). It is performed by maintaining the forefoot and heel on the floor while simultaneously attempting to shorten the distance between the head of the 1MPJ and heel, without flexing the toes. Similarly, the toes-spread-out has been advocated as a way to target the intrinsic musculature and the AbH in particular (Heo et al., 2011; Kim et al., 2013; Kim et al., 2015; Goo et al., 2016; Mortka et al., 2020). It is performed while the foot is on the floor and by first extending the toes, and subsequently abducting the fifth digit followed by the abduction of the Hallux (Kim et al., 2013). Other strengthening exercises for AbH are the toe-flexion manoeuvres against a resistance (Headlee et al., 2008; Goldmann & Brüggemann, 2012; Ridge et al., 2017; Yamauchi & Koyama, 2019ab), or the toe curls (Jung et al., 2011; Lynn et al., 2012; Chung et al., 2016), which are performed by scrunching with the toes a towel placed underneath the foot.

In healthy populations, the toes-spread out and the short foot exercises elicit greater AbH activation compared to the toe-curls and toe-flexion exercises. Using EMG, Jung et al. (2011) showed that the short foot exercise activated AbH to ~45% and ~73% MVC during sitting and single-leg standing, respectively, whereas the toe curls exercise activated the muscle only by ~10% and ~18% in each position. Also, increased EMG activity was found in AbH during gait following four weeks of either toes-spread-out exercises alone or in combination with gluteus maximums training. Specifically, a higher activation by ~41% and ~46% MVC were measured at toe-off, respectively (Goo et al., 2016). In people with mild Hallux Valgus, the AbH EMG activity during toes-spread-out exercise was almost twice as higher than during short foot exercise (~90% vs ~44% MVC, respectively) (Kim et al., 2013). In a subsequent study, Kim et al. (2015) compared, also in people with Hallux Valgus, the impact of wearing orthoses alone against wearing them

in combination with the toes-spread-out exercise following an 8-week intervention. They went on to show that the anatomical cross-sectional area of AbH was increased significantly by 24% (a 0.48cm^2 increase) for the group that wore orthoses while completing an 8-week toes-spread-out exercise training, whereas no change in the morphology of this muscle was found in the group that only wore orthoses (Kim et al., 2015). In addition, radiography showed a reduction of the Hallux Valgus angle by 19% (or ~3°), and by ~40% (6°) during active abduction (Kim et al., 2015).

Despite the beneficial effect of these exercises, the inability of some individuals to activate AbH may hamper their strengthening capacity. The voluntary activation of this muscle is particularly difficult to ascertain in people with Hallux Valgus (Arinci İncel et al., 2003) and often in healthy individuals (Boon & Harper, 2003; Knellwolf et al., 2019). The latter may be partly explained by the complex individual-specific morphology of this muscle, as discussed previously (see 1.2.1.1). Indeed, Tosovic et al. (2012) reported in their cadaveric study of 9 individuals that the multipennate segment of AbH was only present in 8 out of 12 studied specimens implying a potentially reduced ability for hallux abduction. In addition, the performance of these exercises often relies on contribution from the extrinsic musculature (Newsham, 2010; Lynn et al., 2012; McKeon et al., 2015; Yamauchi & Koyama, 2019b), which may mask the isolated contribution of AbH. For example, Yamauchi & Koyama, (2019b) measured the EMG of AbH during toe-flexion at different joint ankle angles (from 70° to 120° of plantarflexion) and found that its highest activation (at 120° plantarflexion) corresponded to only 41.1% of its maximal activation capacity. In contrast, the activation of the peroneus longus, gastrocnemius medialis, and soleus were ~84%, ~57% and 63% of their maximal capacities, respectively (Yamauchi & Koyama, 2019b). This suggests that the performance of the toe-flexion manoeuvre was mainly achieved by the activation of the larger and extrinsic muscles over the AbH.

Being a superficial muscle, AbH is the ideal candidate for the application of NMES as a training modality that could overcome these difficulties. NMES has been successfully

used to evoke sustained contractions in AbH (Gaillet et al., 2004; Kelly et al., 2014; James et al., 2013; 2018; Shimoura et al., 2020) with James et al. (2018) demonstrating its potential effectiveness for muscle strengthening.

1.3 Neuromuscular electrical stimulation

The delivery of electrical stimulation to the skin surface overlying a supplying nerve or the motor point of muscle as the means to elicit muscle contraction is underpinned by the biophysical properties of the neuromuscular system. The resting membrane potential of motor axons is determined by the gradient between the intracellular and extracellular ionic concentrations of Na^+, K^+ and Cl^-, where the resting potential conventionally equates to -70mV (Mortimer & Bhadra, 2015). Changes in this potential are regulated by the membrane's permeability to the flux of Na^+ and K^+ ions through their respective transmembrane voltage-gated channels, and it is restored by the action of the Na^+-K^+ pump (Clausen, 2003). When electrical stimulation is applied, an electrical potential field is created that induces the influx of Na^+. As a result, the outer space of the membrane underneath the cathode becomes more negatively charged as anions flow from cathode to anode, which repel the negatively charged ions against the outside of the membrane. This raises the resting potential; the intracellular space becomes more positively charged and an action potential is evoked when the membrane exceeds the depolarisation threshold (see section 1.1.1).

Three main approaches are used to evoke muscular contraction with electrical stimulation - transcutaneous electrical nerve stimulation, functional electrical stimulation and NMES (Doucet et al., 2012; Maffiuletti et al., 2011; 2018). Transcutaneous electrical nerve stimulation is mainly used to target low-threshold afferent nerve fibres in order to inhibit nociceptive transmission and thus manage pain perception with no evoked muscle contractions (Johnson et al., 2015). Functional electrical stimulation is applied to evoke

contractions from one or more muscles in a synergistic manner in order to perform a specific functional task (Howlett et al., 2015). NMES also evokes muscle contractions, but it does so with the aim of strengthening or preserving muscle mass and function (Jones et al., 2016).

Similar to voluntary training, NMES can prevent muscle atrophy (Dirks et al., 2014) and promote morphological and neurological strength adaptations (Gondin et al., 2011; Gondin et al., 2005; Minetto et al., 2013). For this reason, it has been used by healthy and athletic populations (Filipovic et al., 2011) as a mode of training as well as a rehabilitative modality (Quittan et al., 2001; Talbot et al., 2003; Stevens et al., 2004; Stevens-Lapsley et al., 2012a; Maddocks et al., 2016) for a wide range of clinical populations, whose capacity to perform voluntary activity or generate repetitive volitional contractions is reduced. For example, NMES has been used in bedridden patients due to critical illness (Maffiuletti et al., 2013), in people with impaired pulmonary (Maddocks et al., 2016) or cardiac (Quittan et al., 2001) function and following surgery (Stevens et al., 2004; Stevens-Lapsley et al., 2012a). Correspondingly, the current consensus for the clinical populations, and within the context of impaired capacity to generate voluntary contractions, is that extended exposure to NMES is an effective rehabilitative modality that can prevent muscle atrophy (Maddocks et al., 2013; Jones et al., 2016). Importantly, the magnitude of the force produced during the evoked contractions represents the major determinant of NMES effectiveness (Maffiuletti et al., 2018).

Muscle activation during NMES is fundamentally different to voluntary activation (see 1.1.1). NMES recruits MUs in a spatially fixed manner and in a non-selective order, where the most superficially located MUs are recruited first rather than following the Henneman' size principle (i.e. recruitment of MUs in a descending order of fatigue resistance) of voluntary actions (Bickel et al., 2011). As such, MU firing frequency is also different since the evoked action potentials are synchronised to each NMES pulse (Bickel et al., 2011). These differences impact the evoked force during muscle contraction, and

ultimately the effectiveness of this modality to induce strength gains (Maffiuletti, 2010; Barss et al., 2018; Maffiuletti et al., 2018).

The ability to elicit NMES-induced strength adaptations depends largely on the electrical charge used. Indeed, there is a linear relationship between the magnitude of the evoked force and current intensity, where the higher the current applied, the greater the number of MUs recruited, and correspondingly the larger the area of muscle activated (Adams et al., 1993; Gorgey et al., 2009; Mesin et al., 2010; Bickel et al., 2011; Stevens-Lapsley, 2012b). As a result, NMES has conventionally been applied in healthy individuals using the maximal tolerated current intensity (>50mA, 5-200mA range) or at an intensity capable to evoke contraction forces equivalent to ≥50% MVC (Filipovic et al., 2011; 2012). In addition to high stimulus intensity, varying other stimulation parameters, such as relatively short pulse durations (≤0.4ms) and low frequencies (≤50Hz), have been traditionally implemented (Collins, 2007; Vanderthommen & Duchateau, 2007). Although concentrated attention has been given to these external stimulation parameters, the main driver of muscle strengthening is the level of evoked force with respect to the force-generating capacity, which is in turn dependent on the tolerance of each individual (Alon & Smith, 2005; Vanderthommen & Duchateau, 2007; Maffiuletti et al., 2018). Tolerance depends on the perceived discomfort during the application of high intensity stimulation resulting from activation of nociceptor afferents in skin and/or muscle (Delitto et al., 1992), of which there is a high concentration within the foot (Schmidt et al., 1997; 2002). Since the sense of discomfort can reduce considerably adherence and limit NMES effectiveness as a strength training for AbH, this thesis pays particular attention to ensuring tolerability in its application.

An intuitive approach to reduce discomfort during electrical stimulation is to evoke muscle contractions by “mimicking” the voluntary activation of MUs (Bergquist et al., 2011b; Barss et al., 2018), which involves the central nervous system in the production of force (Collins et al., 2001, 2002; Collins, 2007; Mang et al., 2010). The concentrated

effort in the last decade using a low intensity, wide-pulse and high-frequency neuromuscular electrical stimulation paradigm showed the production of greater forces accompanied by greater H-reflex amplitudes (Collins et al., 2001; Klakowicz et al. 2006; Lagerquist et al., 2009; Lagerquist & Collins, 2010; Bergquist et al. 2011a; Wegrzyk et al., 2015b; Vitry et al. 2019). The occurrence of this phenomenon has been ascribed to the contribution of the sensory volley that is modulated via enhanced depolarisation of sensory axons (Colllins, 2007). Such centrally-mediated contribution takes advantage of the lower rheobase (intensity) and wider chronaxie (pulse duration) of sensory with respect to motor axons (Mogyoros et al., 1996; Burke et al., 2001; Collins, 2007), which would lower the intensity used and thus improve tolerability (Bergquist et al., 2011b). This means that by reducing the intensity at which NMES is delivered, it has the potential to preferentially recruit sensory fibres as they have a lower excitation threshold. It has also been suggested that the combination of these parameters (i.e. wide pulse duration, low intensity) with high frequency may further benefit from the bistability of MNs allowing the occurrence of persistent inward currents (see 1.1.1) and evokes excitation in a greater number of MUs that can contribute to force production (Collins et al., 2001; Dean et al., 2007). Therefore, optimising the stimulation parameters to maximise force production while maintaining tolerability may be an efficacious way to strengthen muscle, and in this context AbH.

1.3.1 Optimised NMES parameters and mode of delivery

Biphasic and monophasic square-shaped (or rectangular) NMES waveforms are most often used (Merrill et al., 2005). During monophasic pulsing, a negative charge is applied to the stimulated tissue by each pulse whereas during biphasic pulsing, a negative followed by a positive charge is delivered, which respectively generates an action potential and reverses the electrochemical processes induced (Merrill et al., 2005). The

reversal of the induced processes reduces the risk of tissue damage by electrochemical by-products and hyperpolarisation that may occur after long-term delivery of monophasic pulses (Merrill et al., 2005). Due to these benefits and given the extended exposure to NMES during training, biphasic pulses have been preferentially used (~67% of studies since 1994; Fillipovic et al., 2011) to achieve muscle strength gains (Gondin et al., 2005; 2006; 2011; Herrero et al., 2006; Colson et al., 2009; Mignardot et al., 2015; Kadri et al., 2017; Di Filippo et al., 2017; Natsume et al., 2018; Mancinelli et al., 2019; Moran et al., 2019; Langeard et al., 2021) compared to monophasic pulses (Jang & Seo, 2018; Vitry et al., 2019; Bouguetoch et al., 2021). However, the monophasic approach is considered more efficacious in evoking action potentials due to its unidirectional supply of negative charge and in preventing corrosion in the electrodes compared to biphasic pulses (Merrill et al., 2005). Hence, the studies carried out in the present thesis have implemented constant current NMES delivered using monophasic square-wave pulses.

1.3.1.1 Mode of delivery

NMES can be applied over the skin overlying the muscle belly or the peripheral nerve that supplies the target muscle. The selection between muscle and nerve mode of delivery largely depends on the superficiality of the target tissue since this influences the consistency in evoking a muscle contraction to produce force (Bergquist et al., 2011a). Superficial muscles such as the AbH are often more accessible than their supplying nerve. During muscle stimulation, the MUs closest to the skin surface are consistently recruited in a spatially-fixed manner and deeper MUs are progressively recruited when the intensity is increased (Adams et al., 1993; Farina et al., 2004; Mesin et al., 2010; Maffiuleti, 2010; Okuma et al., 2013). The recruitment of the same MUs at a given intensity puts this mode of stimulation at an advantage for evoking a more consistent and stable force during its application (Baldwin et al., 2006; Bergquist et al., 2012). In

contrast, nerve stimulation recruits MUs in a more evenly diffused pattern irrespective of the intensity (Okuma et al., 2013), which can lead to co-activation of muscles that share the same nerve supply (Place et al., 2010). This may influence the consistency of force production (Baldwin et al., 2006; Bergquist et al., 2012) and also the effectiveness of the NMES application due to the activation of MUs of different activation thresholds.

NMES is more commonly applied to the skin surface overlying the target muscle(s). The advantages of this approach are its accessibility to training (Baldwin et al., 2006; Gondin et al., 2005; 2011; Jones et al., 2016) and the ability to target the muscle's motor point area, which can be identified to reduce the intensity required for contraction and optimise force production (Gobbo et al., 2014; James et al., 2018). Nevertheless, direct-muscle stimulation may cause premature fatigue of the target muscle due to repetitive activation of the same population of MUs superficial to the stimulated area (Gregory & Bickel, 2005; Bickel et al., 2011). Application of nerve stimulation for strengthening purposes is scarce, possibly because nerve stimulation can be more uncomfortable (Klakowicz et al., 2006; Place et al., 2010; Bergquist et al., 2012; Neyroud et al., 2018). A recent study by Vitry et al., (2019) showed that 5-week stimulation of the tibial nerve using low intensities increases force-generating capacity in the triceps surae, whilst minimising discomfort; whereas discomfort from nerve stimulation has been reported even during low intensity (Klakowicz et al., 2006; Bergquist et al., 2012; Neyroud et al., 2018). Nevertheless, the prevailing evidence points out that careful selection of the stimulation parameters can promote the contribution of central pathways to force production, prevent premature fatigability and lower the discomfort with either approach (Bergquist et al., 2011b).

1.3.1.2 Current intensity and pulse duration

The stimulation current intensity (mA) and pulse duration (ms) are inversely proportional to the strength (current intensity)-duration properties of the muscle or nerve subjected to

stimulation (Geddes, 2004). As the current intensity increases to achieve a threshold for membrane depolarisation, the required pulse duration decreases, and vice versa (Bostock et al., 1998). From this relationship, the excitability properties of different tissues, which are the rheobase and chronaxie, can be identified. Theoretically, the rheobase represents the minimal current intensity to depolarise a given tissue using a pulse of infinitely long duration (Burke et al., 2001). The chronaxie is defined as the pulse duration required to achieve depolarisation using a current intensity equivalent to twice the rheobase value (Burke et al., 2001). Experimentally, the intensity-duration curve is transformed to a charge (duration x intensity)-duration linear relationship, by means of the Weiss's linear regression transformation, to accurately identify these properties (Fig. 1.5 A&B) (Mogyoros et al., 1996; Bostock et al., 1998).

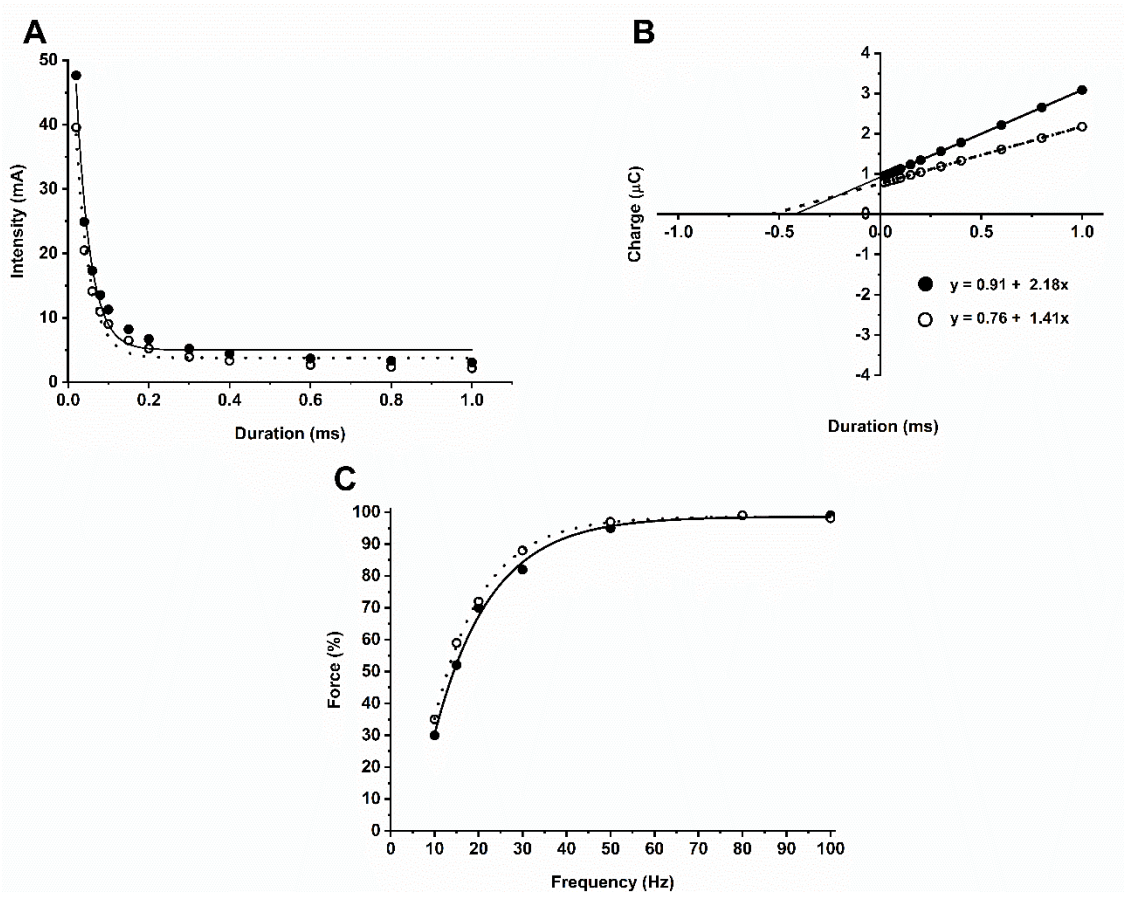

Figure 1.5. Intensity–duration relationship (**A**) for motor (filled circles) and sensory (unfilled circles) axons in the median nerve of a single subject, plotted as stimulus charge (intensity × duration)-duration (**B**), as per Weiss's linear regression transformation to determine chronaxie (from intercept on duration axis) and rheobase (from the slope of regression line). Reconstructed using data taken from Mogyoros et al., (1996). The force–frequency relationship in human skeletal muscle (filled circles for quadriceps; unfilled circles adductor pollicis) is presented in (**C**). Reconstructed using data taken from Edwards et al. (1977). The charge – duration plot in **B** shows the respective linear function y = b + mx for the motor and sensory axons, where the x-intercept corresponds to chronaxie, the slope (m) corresponds to rheobase and (b) represents the y-intercept. The chronaxie is determined by calculating the x-intercept from the linear regression equation, given y = 0. This is, the linear equation for motor and sensory axons are y=0.91 + 2.18x and y = 0.76 + 1.41x, respectively. So, if y = 0, then |x|=0.91/2.18=|x|=0.42 for motor, and |x|=0.76/1.41=|x|=0.54 for sensory axons. Therefore, the rheobase and chronaxie are equal to 2.18mA and 0.42ms, respectively, for motor axons, and to 1.41mA and 0.54ms for sensory axons.

The current intensity used for NMES is often expressed as a percentage of the force produced by the target muscle or muscle group during an MVC (Maffiuletti et al., 2018). This approach relies on the premise that 100% of voluntary contraction is possible and therefore can be impractical in participants with an impaired capacity to voluntary activate their muscles. Other approaches such as the determination of the individual motor threshold (MT) (James et al., 2018; Maffiuletti et al., 2018) or the maximally tolerated intensity (Filipovic et al., 2011) have been also used. However, the latter approach can result in great variability of current intensities used for inducing strength gains ranging from 10 to 200mA (Filipovic et al., 2011). This can also depend on the population; for instance, an average of ~70mA (range 32-120mA) was reported as the maximum

tolerated intensity for the triceps surae of healthy individuals (Gondin et al., 2006), whereas only ~20mA was considered maximally tolerable in the elderly (Langeard et al., 2021). In a similar way, healthy but sedentary individuals reported a maximally tolerated intensity at ~60mA compared to the ~80mA reported by active individuals when their quadriceps muscle group was being stimulated (Gondin et al., 2011).

The use of low current intensities minimises antidromic block in motor axons, and in combination with wide pulse durations (≥0.5ms) allows the preferential activation of sensory axons, due to their lower rheobase, compared to motor axons (Fig. 1.5B) (Kiernan et al. 2004; Veale et al. al. 1973). Combined, these parameters (i.e. wide pulse and low intensity) allow the evoked action potentials to reach the spinal cord (Bergquist et al. 2011b; Dean et al. 2007). Indeed, when delivered at a high frequency, these parameters cause the extra-force phenomenon and achieved forces as high as ~40% MVC compared to a target force of around only 5% (Collins et al. 2001, 2002). Nevertheless, NMES for strengthening has been typically delivered at a high intensity (e.g. ~60% MVC force along with a narrow pulse duration of ~0.3ms; Filipovic et al., 2011) or with a progressive increase of intensity, which results in the recruitment of more and deeper MUs, and therefore a higher force (Adams et al. 1993; Gorgey et al. 2006; Mesin et al., 2010; Bickel et al., 2011; Stevens-Lapsley, 2012b). Comparatively, low stimulation intensities (i.e. ≤40% MVC) have been implemented more rarely in healthy and athletic populations (Kadri et al., 2017; Natsume et al., 2018; (Jang & Seo, 2018; Bouguetoch et al., 2021) than high intensity protocols (i.e. >40% MVC) (Gondin et al., 2005; 2006; 2011; Herrero et al., 2006; Colson et al., 2009; Mignardot et al., 2015; Di Filippo et al., 2017; Natsume et al., 2018; Mancinelli et al., 2019; Moran et al., 2019; Langeard et al., 2021). These currents have been primarily delivered using commercially available stimulators (Filipovic et al., 2011), which often means that the parameter selection is fixed or has limited space for modulation (Lake, 1992).

Pulse duration (or width) represents the time over which a single pulse is delivered. Traditionally, NMES interventions have often used short pulses (≤0.5ms) in both the healthy (~0.3ms, range: 0.2-0.4ms; Filipovic et al., 2011) and clinical (~0.4ms, range: 0.2-0.7ms; Jones et al., 2016) populations. Following the intensity-duration relationship, increasing the pulse duration, which reduces the intensity required for activation, recruits a higher number of motor axons (Gorgey et al., 2006; Gorgey et al., 2008). For example, Gorgey et al. (2006) demonstrated that the evoked force via NMES increased significantly when a wide pulse (i.e. ~0.5ms) was used in comparison to pulses with a shorter duration (i.e. ~0.2ms). Furthermore, the evoked force was found to increase exponentially as the pulse duration was increased from 0.1ms to 0.6ms, potentially due to more efficient depolarisation of a higher number of MUs (Gregory et al., 2007). As previously mentioned, wider pulse durations would also increase the recruitment of sensory axons and force production with origin in the central nervous system.

1.3.1.3 Pulse frequency

According to the force-frequency relationship, the level of force production during NMES increases as the frequency at which the pulses are delivered increases (Edwards et al., 1977; Binder-Macleod & McDermond, 1992; Gregory et al., 2007) by partly increasing the firing rate of MUs until it reaches saturation at ~50Hz (Fig. 1.5 C) (Edwards et al., 1977). NMES has been conventionally delivered at a range of frequencies below saturation (i.e. 20-40Hz) in order to achieve a fused contraction that can be sustained for a long period of time and thus reduce fatigability (Fuglevand & Keen, 2003; Gorgey et al., 2009; Bergquist et al., 2011b; Doucet et al., 2012). This is because this range is within the physiological firing frequency of MUs during sustained contractions (i.e. <50Hz) (Del Vecchio et al., 2019). Force-generating capacity increments following interventions using low frequency stimulation can range from as low as ~9% (Talbot et

al., 2003) to as high as 47% (Moran et al., 2019). In order to reach maximal evoked forces, high frequencies (i.e. >50Hz) have also been used (Hainaut & Duchateau, 1992; Gregory et al., 2007; Dreibati et al., 2010). Interventions that have implemented high frequencies achieved an average of 20% increments in force-generating capacity (Gondin et al., 2005; 2006; 2011; Herrero et al., 2006; Colson et al., 2009; Mignardot et al., 2015; Kadri et al., 2017; Natsume et al., 2018; Mancinelli et al., 2019; Moran et al., 2019; Langeard et al., 2021; Bouguetoch et al., 2021).

The use of high frequencies is however associated with a rapid loss of force during stimulation (Gorgey et al., 2009; Grosprêtre et al., 2017; Wegrzyk et al., 2015a). This force loss has been observed to occur further in subsequent delivery of a number of trains of high frequency over a course of a session (Grosprêtre et al., 2017; Neyroud et al., 2014; Wegrzyk et al., 2015a). The associated mechanism with this force loss is an imbalanced ionic concentration within the muscle, where extracellular [Na^+] is decreased or [K^+] increased that ultimately impairs the initiation and transmission of the evoked action potentials (Jones et al., 1979; Jones, 1996). Other related mechanisms are an increased metabolic demand (Gorgey et al., 2009) and changes in excitability threshold that occurs in the motor efferents (Burke et al., 2001; Kiernan et al., 2004). The delivery of high-frequency trains may induce an imbalanced ionic distribution of Na^+ and K^+ across the motor efferents membrane, which in turn will activate the Na^+/K^+ pump and lead to axonal membrane hyperpolarisation (Burke et al., 2001). This hyperpolarisation results in a higher threshold for the excitation of the efferent membrane to secure transmission of the evoked action potentials. Consequently, a higher excitation threshold of the motor efferents would progressively reduce the number of the activated MUs to sustain the force production at this frequency (Papaiordanidou et al., 2014a; Papaiordanidou et al., 2014b; Matkowski et al., 2015; Martin et al., 2016).

The use of alternating frequency may preserve high force production during the tetanic evoked contraction. Indeed, the studies of Binder-Macleod & Guerin (1990) and Jones

et al., (1979) showed, respectively, that reducing or alternating the frequency within the train produces lower force losses due to fatigue than using only high frequency. Specifically, interruption of a train of 80Hz targeting the adductor pollicis with brief low frequency trains rapidly offset the force loss trend observed (Jones et al., 1979). Recent studies have also used protocols interspersing high and low frequency NMES bursts within the train (e.g. 20-100-20Hz) and showed better retention of the force increase from the high frequency stimulus (Collins et al., 2001; 2002; Dean et al., 2007 Lagerquist et al., 2009; James et al., 2018). In addition, recent evidence by Espeit et al., (2021) showed that the extra-force phenomenon can also be observed during trains of 1ms pulses delivered at 20Hz, to a similar extent to that achieved by 100Hz trains, in the plantarflexors. This represents further support for the potential benefit of using an alternating frequency paradigm targeting AbH via muscle stimulation.

Irrespective of the frequency used during prolonged/repetitive NMES however, force loss can occur as a result of the low-frequency fatigue phenomenon that is persistent for a prolonged period of time (e.g. hours) (Keeton & Binder-Macleod, 2006; Allen et al., 2008). The characteristics of this phenomenon include an impaired muscle excitability that results in the transmission failure of the action potentials at the neuromuscular junction or across membrane T-tubules, a reduced release of Ca^{2+} from the sarcoplasmic reticulum by the action potential and/or decreased Ca^{2+} sensitivity of the myofibrils (Keeton & Binder-Macleod, 2006; Allen et al., 2008). This phenomenon is prevalent during low frequency stimulation in line with the sigmoidal shape of the force-frequency and force-myoplasmic [Ca^{2+}] relationships, which indicate that a small change of [Ca^{2+}] at the slope of the sigmoidal curve results in a large effect on force production (Allen et al., 2008; Place et al., 2010). In order to quantify low-frequency fatigue, the force evoked using low (e.g. 10 Hz) and high (e.g. 100Hz) have been compared in a low-to-high frequency ratio as a fatigue index (Keeton & Binder-Macleod, 2006; Verges et al., 2009).

1.3.1.4 Duty-cycle

NMES is commonly delivered intermittently with stimulation trains separated with rest periods between them, where the duration of a train and the subsequent resting period represent an “on” and “off” cycle. In doing so, the evoked force can be preserved as the resting periods between trains allows the recovery of the MU’s resting state following each stimulating train (Boom et al., 1993; Dideriksen et al., 2015; Taylor et al., 2018), which in turn reduces the metabolic stress applied on the target muscle (Matheson et al., 1997; Taylor et al., 2018). The duty-cycle used in an NMES intervention is expressed as a ratio or percentage of the “on” time relative to total time (on and off times) (Packman-Braun, 1988; Herzig et al., 2015), where lower duty-cycles (e.g. 1:3 or 25%) preserve force to a greater extent than higher duty-cycles (e.g. 1:1 or 50%) (Holcomb, 2006; Packman-Braun, 1988; Rankin & Stokes, 1992; Matheson et al., 1997). Strengthening interventions for healthy individuals have often implemented a ~1:3 duty cycle using trains typically lasting 6s and separated by a 20s rest period (Maffiuletti et al., 2002; Gondin et al., 2005; Gondin et al., 2006; Jubeau et al., 2006; Gondin et al., 2011; Minetto et al., 2013; Grosset et al., 2014; Natsume et al., 2018; Letocart & Grosset, 2020). For use in clinical settings lower duty-cycles (i.e. 1:3 or 1:5) are considered more tolerable and are recommended (Talbot et al., 2003; Doucet et al., 2012; Herzig et al., 2015; Glaviano & Saliba, 2016).

1.3.2 Evidence of muscle strengthening via low-intensity NMES

Successful muscle strengthening has been achieved with low-intensity interventions with a median of ~20% (range 10-30%) MVC force increase (Table 1.1). Generally speaking, training regimes have lasted a median of 8 weeks (2-12 weeks), with 3 (3-7) weekly sessions, typically delivering paradigms of 25 trains (range: 15-40) with a duty cycle of ~1:3 (1:1-1:7.5) equivalent to 7s ‘on’ (2-20s) and 15s ‘off’ (6-50s) and consisting of pulses

delivered at 50Hz (20-100Hz) with 0.4ms (0.3-1ms) duration (Quittan et al., 2001; Talbot et al., 2003; Maddocks et al., 2016; Kadri et al., 2017; Natsume et al., 2018; Vitry et al., 2019; Bouguetoch et al., 2021).

Specifically, the low-intensity protocols have evoked an increased capacity to generate force by an average of 13% in the knee extensors (Quittan et al., 2001; Talbot et al., 2003; Maddocks et al., 2016; Kadri et al., 2017; Natsume et al., 2018), and by ~20% on the plantarflexors muscles (Vitry et al., 2019; Bouguetoch et al., 2021). Moreover, strength gains as high as 35.4% have been obtained in the knee flexors (Quittan et al., 2001), and 26.7% in the plantarflexors (Vitry et al., 2019). Neurological adaptations induced by these protocols showed ~5% increments in voluntary activation of the plantarflexors (Vitry et al., 2019). These adaptations precede morphological adaptations, such as an increase of ~15% of the cross-sectional area of the thigh muscles (Quittan et al., 2001), and rectus femoris (Maddocks et al., 2016). The muscle thickness of the quadriceps was also found to increase by 5%, and the cross-sectional area of the vastus lateralis muscle fibres was reported to increase by 7% and 11%, for the fibre type I and II, respectively (Natsume et al., 2018).

Table 1.1. Strength gains (% MVC) achieved following low-intensity NMES protocols with their respective electrical parameters.

KE: knee extensors; KF: knee flexors; TS: triceps surae.

Authors	Muscle (group)	Participants	Intensity (%MVC)	Intensity (mA)	Pulse duration (ms)	Frequency (Hz)	Trains	On:Off (s)	Duty-cycle	Strength (%MVC)
Quittan et al., 2001	KE/KF	Patients	25-30		0.7	50	225>450	2:6	1:3	23/35
Talbot et al., 2003	KE	Patients	22		0.3	50	15	10:50	1:5	9
Maddocks et al., 2016	KE	Patients	15-25		0.35	50	50	2:15; 5:20; 10:15	1:7.5; 1:4; 1:1.5	14
Kadri et al., 2017	KE	Healthy	20		0.38	50	23	7:7	1:1	12
Natsume et al., 2018	KE	Healthy	30		0.4	75	40	6.25:20	1:3.2	11
Vitry et al., 2019	TS (nerve)	Healthy	10	12	1.0	20/100	25	20:20	1:1	27/21
Bouguetoch et al., 2021	TS	Healthy	20	10-45	0.5	80	40	6:6	1:1	11

1.3.3 Wide-pulse, high-frequency neuromuscular electrical stimulation (WPHF)

In order to overcome the discomfort associated with the high intensities and the rapid fatigability associated with a spatially fixed recruitment of MUs during NMES, a wide pulse, high-frequency, low intensity paradigm has been proposed to maximise force production via centrally modulated pathways (Collins, 2007; Bergquist et al., 2011a), and has been shown to evoke acute peripheral adaptations in the AbH (James et al., 2018).

In a series of acute exposure to this paradigm, Collins et al., (2001; 2002) showed that force produced during the course of the train increased by up to 40% of MVC, but this increase in force production was removed when the nerve supplying the target muscle (i.e. tibialis anterior; triceps surae) was blocked (Lagerquist et al., 2009); thus suggesting a central origin for force enhancement. Higher forces using this paradigm in comparison to more conventional ones (e.g. narrow pulses and lower frequencies) have also been later reported (Collins, 2007; Bergquist et al., 2011a; Wegrzyk et al., 2015b; Neyroud et al., 2018); presenting this paradigm as more advantageous for engaging the central nervous system.

The evidence for the activation of afferent pathways through the application of this paradigm and the corresponding activation of MUs in a more physiological and asynchronous manner to produce force (Collins, 2007; Dideriksen et al., 2015) is drawn from EMG studies. For example, the asynchronous MU activity with respect to the pulses delivered has been used as a proxy for centrally mediated force production (Dean et al., 2014) following WPHF stimulation (Bergquist et al., 2011b). Indeed, a ~50% increase in asynchronous EMG activity was measured between pulses from a 20Hz burst that came immediately after a high frequency burst delivered to the triceps surae via muscle and nerve (Bergquist et al, 2011b). Furthermore, Donnelly et al., (2020) demonstrated that this EMG activity was inhibited when the stimulation was preceded by high-frequency transcutaneous nerve stimulation, as the latter potentially increased spinal inhibition,

which would thus support the central origin of force during WPHF. In addition, an increase in H-reflex amplitude was recorded after the delivery of a WPHF train or burst within a train (Baldwin et al., 2006; Collins, 2007; Bergquist et al., 2011b; Bergquist et al., 2012; Grosprêtre et al., 2017), as well as a post-activation depression following a session of a number of trains has been observed (Grosprêtre et al., 2017; Grosprêtre et al., 2018; Gueugneau et al., 2017; Wegrzyk et al., 2015a). Together, these results support the notion of the spinal contribution to the evoked force, which is enhanced by the use of this paradigm.

The force augmentation during WPHF NMES is likely due to post-tetanic potentiation (PTP) via central and peripheral mechanisms (Baldwin et al., 2006). Peripherally, WPHF NMES can cause force to summate and increase in a non-linear manner as a result of increased myoplasmic [Ca^{2+}] availability and increased myofibrillar sensitivity to Ca^{2+} (Allen et al., 2008; Frigon et al., 2011; Cheng et al., 2017). Centrally, the augmented extra-force phenomenon may be underpinned by mechanisms including evoked persistent inward currents (Collins et al., 2001, 2002; Baldwin et al., 2006; Dean et al., 2007), excitatory post-synaptic potentials (Dean et al., 2007) and temporal summation of subthreshold excitatory postsynaptic potentials of afferents (Dideriksen et al., 2015). A combination of these proposed mechanisms may contribute to the potentiation in force observed during NMES delivered at a high frequency.

Only two studies have implemented this paradigm for training in a longitudinal manner however, and their results are inconclusive. Specifically, Neyroud et al., (2019) targeted the plantarflexor muscles with 10x20s-trains (40s off; 1:2 duty cycle) of 1ms-pulses delivered at a constant frequency of 100Hz, and an intensity equivalent to ~5% MVC for 3 weeks (3 weekly sessions). However, only an increase in the evoked force during stimulation was found and no other neurological or morphological changes were induced. In contrast, Vitry et al., (2019) stimulated the tibial nerve to target the plantarflexors using 25x20s (20s off; 1:1 duty cycle) trains of 1ms pulses delivered at either 20Hz or 100Hz,

and an intensity of 10% MVC for a 5-week period (3 weekly sessions). The authors registered a significant increase of ~23% (26.7% for 100Hz; and 20.7% for 20Hz trains) in MVC force and ~5% (5.7% and 4.9% for 100Hz and 20Hz, respectively) in voluntary activation. In addition, they showed that the H-reflex and motor evoked potential amplitudes only increased after 100Hz trains.

Although both studies have implemented a WPHF paradigm, they have used different approaches. The latter study stimulated the nerve rather than muscle, and importantly, they did so at almost double the intensity. The intervention also included a higher number of trains and was implemented for a longer period of time (5 vs 3 weeks). In addition, the neurological adaptations after using 100Hz trains reported by Vitry et al., (2019) are expected based on what has been previously reported in acute nerve stimulation studies (see 1.3.1.3) but the scarcity of other longitudinal studies limits this agreement. What both of these studies demonstrate is that the selection of stimulation mode and parameters for an optimised paradigm for force production using low intensity requires further consideration.

As demonstrated by Vitry et al., (2019) there is virtue in using low frequencies for strengthening purposes. However, nerve stimulation has been shown to be almost twice as much uncomfortable as muscle stimulation (Neyroud et al., 2018), and therefore may reduce its utility. Recent evidence by Espeit et al., (2021) showed that the extra-force phenomenon can also be observed during trains of 1ms pulses delivered at 20Hz when delivered to the plantarflexors via muscle stimulation, which as discussed previously would indicate the benefit of using an alternating frequency pattern. Furthermore, the application of NMES independently of the intensity used, whether it is low (~20% MVC) or high (~60% MVC) can provide the sufficient stimulus to the central nervous system and muscle structure to induce adaptations that collectively contribute to the strength gains achieved for force production. Therefore, this training modality represents a potential solution for training AbH and overcoming its associated complexities with the

inability for voluntary activation. However, more clarity is required for the optimal paradigm to be used when targeting this muscle and therefore, this thesis will optimise the NMES paradigm (intensity, frequency, and duty-cycle) to strengthen AbH whilst maintaining the tolerability and effectiveness of its application.

2.0 General methods

This section presents the methods that are common to the subsequent chapters. First, the calibration and validation of the system to accurately capture the forces relevant to AbH are presented (section 2.1). Next, the optimisation of the procedures for targeted direct-muscle NMES of AbH is described (section 2.2). This is followed by a description of the experimental set-up and then an investigation into the optimal Hallux positioning for force production. Then, optimisation procedures for peripheral nerve stimulation (PNS) of the medial plantar nerve are described. This includes the description of the performance measures derived from the PNS-evoked responses, which will be used to assess the excitability and contractility of AbH. Finally, the results from the evaluation of the repeatability of these performance measures are reported.

The implementation of bespoke techniques, specific information concerning participants, ethical approval, study design, and statistical analyses will be presented in the respective experimental chapters. All procedures were conducted at London South Bank University.

2.1 Assessment of force production: validation and calibration of an uni-axial strain gauge transducer

The following describes a sequence of pilot procedures undertaken to establish a calibrated and validated system that enables the accurate measurement of the forces evoked from AbH.

2.1.1 Is a tri-axial force transducer necessary for recording the force produced by AbH?

Aim

To establish the contribution of the vertical component ($|F_Z|$) to the resultant twitch force ($|F_R|$) evoked by supramaximal PNS of the medial plantar nerve.

Methods

Four healthy participants (1F, 3M; mean±SD: 25.3±3.2 years, 76.0±10.9kg, 1.8±0.1m) were invited for this single-session study, following familiarisation. The AbH twitch force from the left foot was measured via a tri-axial force transducer (range: 0-50N, Applied Measurements Ltd, UK; sampling frequency: 1000Hz in each direction) in response to five 500μs single square-wave pulses, separated by 10s and delivered to the medial plantar nerve at supramaximal intensity (see section 2.4). The pulses were delivered by a constant-current stimulator (DS7A, Digitimer, UK), which was synchronised with the force data through an analogue to digital convertor (range: ±10V, Power1401-3, Cambridge Electronic Design Ltd., UK) and imported into Spike2 software (v7.12, CED Ltd., UK) for analysis. Participants remained seated throughout the procedures in the experimental apparatus (see section 2.3) with their Hallux suspended from the force transducer in slight dorsiflexion.

The peak of the resultant force $|F_R|$ along with each of the three orthogonal forces (vertical $|F_Z|$, medio-lateral $|F_Y|$ and anteroposterior $|F_X|$) evoked by each pulse were averaged across the five pulses. The orthogonal forces were then expressed as a relative (%) contribution to $|F_R|$. Only descriptive statistics are presented here.

Results

The population mean (±SD) $|F_R|$ evoked from supramaximal PNS was 3.2±1.5N of which 92.5% (range: 85.6-98.8%) - equivalent to 3.1±1.5N, was captured in $|F_Z|$ (Table 2.1). Only 5.0% (0.5±0.3N) and 2.5% (0.40±0.32N) were captured along the $|F_Y|$ and $|F_X|$ axes, respectively.

Table 2.1. Individual and population (*n*=4) mean (±SD) of the resultant and orthogonal twitch forces (N) evoked by supramaximal PNS. The orthogonal forces are reported relative (%) to $|F_R|$.

Participant	Orthogonal forces contribution to $\|F_R\|$						
	$\|F_R\|$	$\|F_Z\|$	%	$\|F_Y\|$	%	$\|F_X\|$	%
1	**1.0 (0.0)**	0.9 (0.0)	87.4	0.3 (0.0)	10.3	0.1 (0.0)	2.3
2	**3.3 (0.1)**	3.1 (0.1)	85.6	0.9 (0.0)	7.7	0.9 (0.0)	6.7
3	**4.1 (0.1)**	4.1 (0.1)	98.8	0.2 (0.0)	0.3	0.4 (0.0)	0.9
4	**4.2 (0.1)**	4.2 (0.1)	98.1	0.5 (0.0)	1.6	0.2 (0.0)	0.3
Mean	**3.2 (1.5)**	**3.1 (1.5)**	**92.5**	**0.5 (0.3)**	**5.0**	**0.4 (0.3)**	**2.5**

Interpretation

This study revealed an average contribution to $|F_R|$ of 92.5% (3.1N), 5.0% (0.5N) and 2.5% (0.4N) along the $|F_Z|$, $|F_Y|$ and $|F_X|$ axes, respectively. These findings were surprising as they indicate that the peak twitch force evoked from AbH via PNS occurs mainly along the $|F_Z|$ component with only 5% of total force representing Hallux abduction ($|F_Y|$). A radiating effect of the stimulus on m. flexor digitorum brevis and m. flexor hallucis brevis during PNS may perhaps be responsible for this greater flexion movement, as previously suggested by James et al., (2018). However, the population average of the peak twitch force found here is comparatively lower than reported by James et al., (2018) (4.3±1.6N) using an uni-axial force transducer. Specifically, the mean peak twitch force (*n*=4) investigated here is 3.2N but it is variable between participants, with the lowest force recorded being 1N (Table 2.1). As a result, the use of the tri-axial transducer over a uni-axial remains unjustified, and thus, an investigation is warranted to ensure that the discrepancy between studies and the low and variable forces reported here are not of mechanical origin. In addition, the low magnitude of forces recorded in response to PNS in this study and James et al., (2018) highlight the force range that is relevant for AbH and therefore if an uni-axial force transducer is to be used in future experimental studies, it should be calibrated in accordance to this range. Addressing these concerns will be the focus of the following pilot work.

2.1.2 Does a uni-axial and tri-axial force transducer record the same force output for a given input?

Aim

To simultaneously compare the force recordings of a uni-axial and tri-axial force transducer in response to a given input.

Methods

No human participation was necessary for this study. A uni-axial (F250) force transducer (range: 0-250N; RDP Electronics Ltd., UK; sampling frequency: 1000Hz) was firmly attached to the tri-axial (F50) force transducer for simultaneous capture of the output (V) to a given input (N) with the signals from both transducers synchronously digitised into Spike2 software via the analogue to digital converter (see 2.1.1). For F250, the voltage into force conversion was done using a standard (to laboratory) scale/offset configuration of y=24.826x -3.998, where 1V elicits 20.83N (Force (N)=(24.826 * Input (V)) -3.998). In the case of F50, the scale/offset (factory) configuration for the X, Y and Z axes were: y=5.0002x -0.0038, y=5.001x -0.0038 and y=4.9985x +0.0047, respectively, where 1V in one direction elicits 5N. The input used for this study was a "1kg" free-weight (measured as 9.6N, therefore an actual mass of 0.98kg; used as a representative force value evoked from AbH during NMES) which was suspended from both force transducers (Fig. 2.1) for 50s. After removing the weight, a period with no weight was recorded for baseline evaluation and subsequent correction of the force recorded. Only one attempt was captured from which the corrected mean force (N) was measured from a 5s window at the mid-portion of the 50s of weight suspension for each transducer. The corrected forces were then used to calculate the percentage difference ($\Delta\%$) between the measurements produced by the two transducers with the following equation: $\Delta\% = \left(\frac{F50-F250}{F250}\right) * 100.$

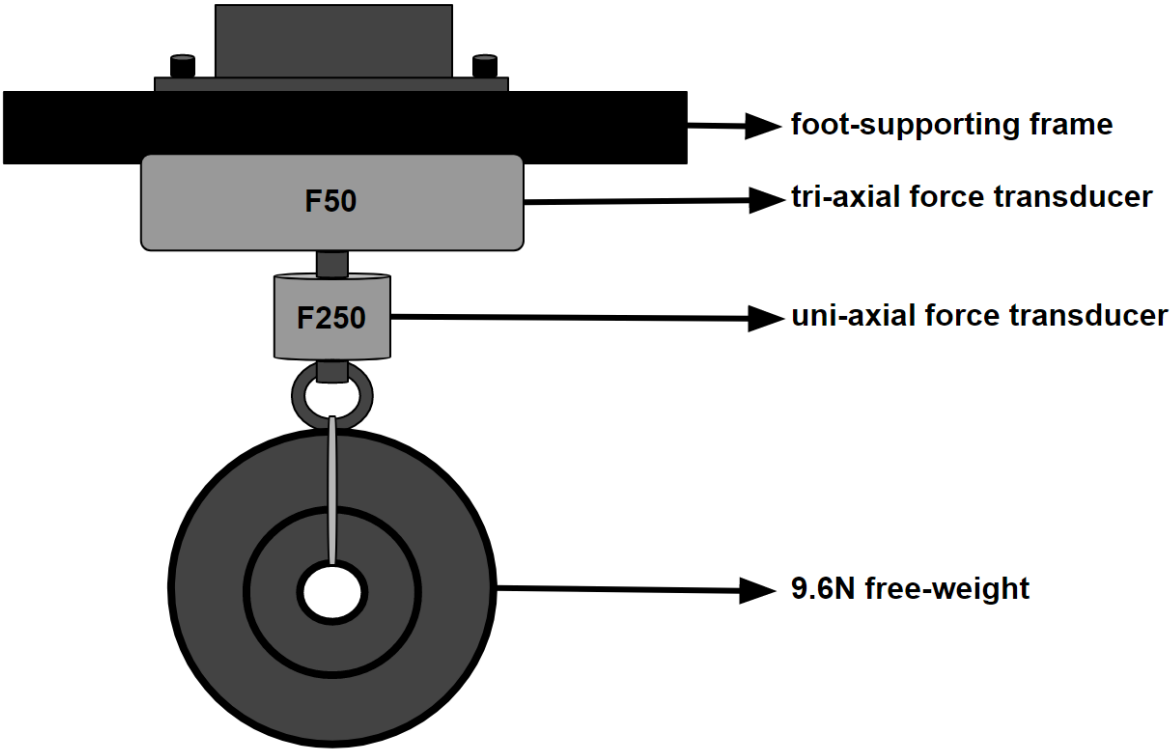

Figure 2.1. Experimental set-up for simultaneous measurement of the voltage output from the loaded (9.6N) tri-axial (F50) and uni-axial (F250) force transducers.

Results

The F250 recorded a mean force of 10.1N, whereas F50 recorded 9.9N. This represents a 1.7% variance between the transducers.

Interpretation

This finding suggests that the difference of 25.6% between the measured forces in section 2.1.1 (3.2 ± 1.5N) and those found by James et al, (2018) (4.3 ± 1.6N) cannot be attributed to a mechanical difference. The variance of 1.7% in the force recordings

between both transducers may instead be due to their respective ranges and prior calibration. For example, a force of 10.1N represents ~4% of the uni-axial transducer's full range capacity (250N), and it is possible that the calibration is not concentrated around the region corresponding to stimulation-evoked AbH force production (~0-10N). Therefore, the next stage of pilot work aimed to re-calibrate the uni-axial force transducer to capture forces that are relevant to AbH.

2.1.3 Calibration of the uni-axial force transducer

Aim

To adjust the scale/offset configuration of the uni-axial force transducer and ensure an adequate resolution for recording the low-level forces produced by AbH during NMES and PNS.

Methods

No human participation was necessary for this study. The standard (laboratory; linear) scale/offset configuration for the uni-axial transducer (see 2.1.2) was y= 24.826x - 3.0998. During focused (to the anticipated physiological range of forces) calibration testing, the sampling configuration set within Spike2 acquisition software to collect the analogue input data via the analogue-to-digital converter (see 2.1.1) was set to a scale= 1, and offset = 0. The voltage elicited from the loaded uni-axial force transducer was sampled at 500 Hz. A series of free-weights in the range of 0.2-44.5% of the transducer's full capacity (0.5, 1.0, 2.0, 3.0, 4.1, 6.1, 11.0, 16.1, 25.0, 37.8, 61.7, 111.2N) were suspended from the transducer (in a similar fashion as depicted in Fig. 2.1). A stepwise

addition of weight commenced following a 30s baseline period of no weight. Each load was suspended for ~30s and the respective mean voltage calculated within a 3s window at the mid-portion of the suspension. Once 111.2N had been achieved, the weights were successively removed completing an ascending-descending stepwise voltage profile. The output voltage was recorded against the input (N) for each stage of the profile and linear regression analysis was performed in order to obtain the slope (scale), y-intercept (offset) and coefficient of determination (R^2) of the regression line.

To validate the resolution of the obtained scale/offset configuration, a given (simulated) force (N) was first converted, based on the ranges of the force transducer (250N) and analogue-to-digital converter (10V), into output voltage ($Output\ (V) = \frac{Given\ force\ (N)}{250\ (N)} * 10\ (V)$). This voltage value was then inputted into the focused calibration configuration equation to calculate the expected force (N) to be elicited by the converted voltage. The simulated forces used for this were arbitrarily chosen and ranged between 2.9 to 235N (i.e. 2.9, 3.7, 4.3, 10, 30, 60, 100, 150, 200 and 235N), with the value of 4.3N used as a relevant force based on the evoked twitch force from AbH reported by James et al. (2018). The expected force (N) and the given force (N) were then used to calculate the relative ($\frac{Expected\ force\ (N) - Given\ force\ (N)}{Given\ force\ (N)} * 100$) and absolute ($Expected\ force\ (N) - Given\ force\ (N)$) errors of the calibration. Finally, the relative (%) and absolute (N) errors between expected and given force using the focused and standard scale/offset configurations were plotted for comparison.

Results

The focused scale/offset configuration and coefficient of determination after calibration of the uni-axial transducer was y= 24.673x + 0.1121; R^2 =1 (Fig. 2.2A). The relative error (%) between the simulated and expected forces ranged from 0.2 to 2.6% within the simulated range of 2.9 to 235N. The simulated force of 4.3N (James et al., 2018) produced a relative error of 1.3% (Fig. 2.2C, circled). For its part, the absolute error

ranged between 0.1 and 3.0N across the simulated range, with an absolute error of 0.1N at the simulated force of 4.3N (Fig. 2.2B, circled). In contrast, the relative error between the simulated and expected force using the standard calibration was large (~10 to110%) in the lower regions of simulated force, which progressively increased in accuracy at 50N and thereafter to full capacity (Fig. 2.2D)**.** At a simulated force of 4.3N specifically, the corresponding errors were 72.8% (Fig 2.2D, circled) and 3.1N, respectively.

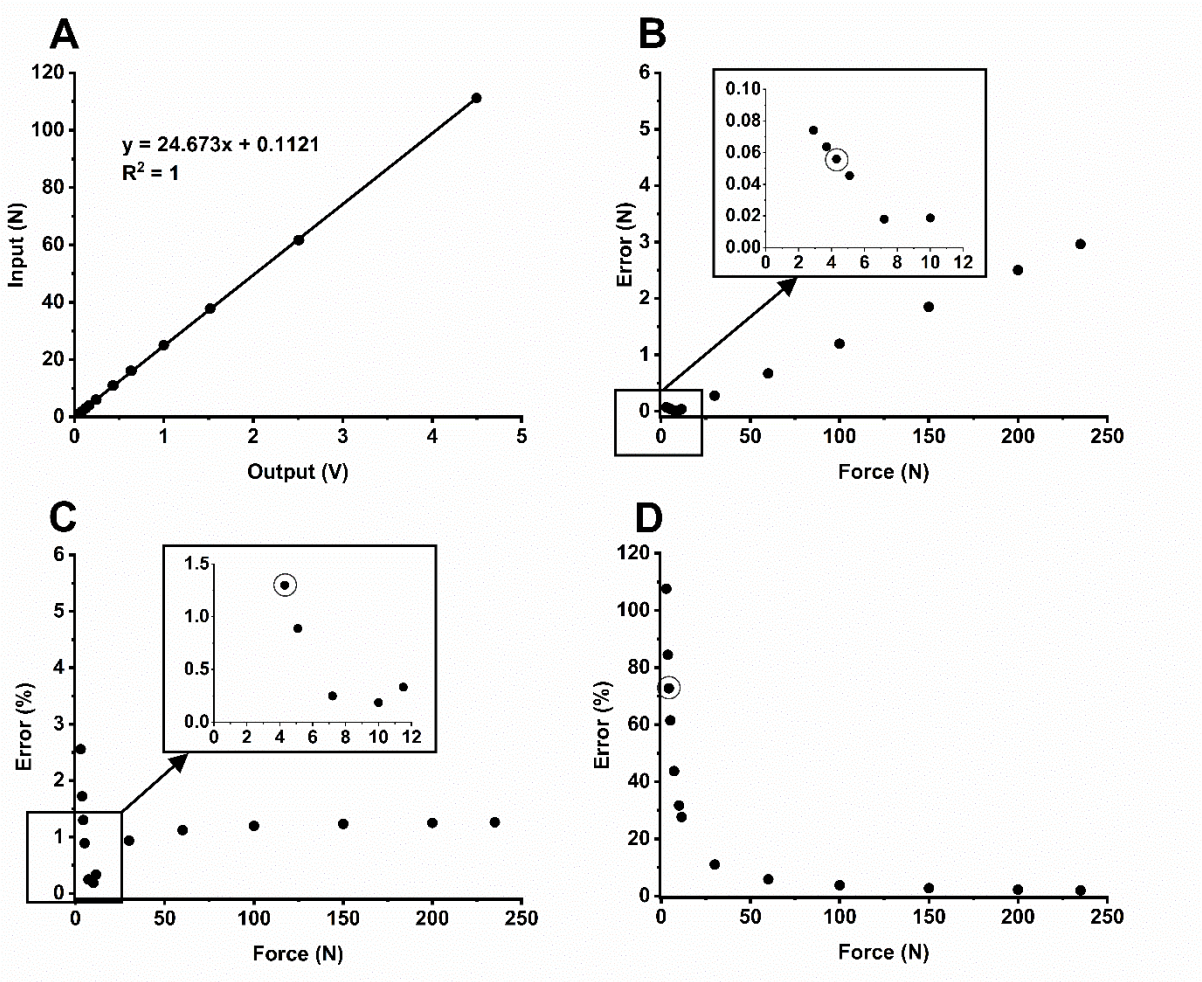

Figure 2.2. A: Slope (scale: 24.673), y-intercept (offset: 0.1121) and coefficient of determination (R^2=1) for the focused calibration configuration for the uni-axial force transducer. **B:** Absolute (N) and **C:** relative (%) errors between the given (simulated)

forces and the forces recorded using the calibration configuration obtained in A. **D:** The relative error (%) between the given (simulated) forces and the forces derived using the standard calibration configuration (James et al., 2018). The corresponding errors to the simulated force value representative of AbH (based on James et al., 2018) are circled and their comparison illustrates the improved accuracy of the focused (C) compared to standard (D) calibration.

Interpretation

The focused calibration of the uni-axial force transducer demonstrated low error across the range of simulated forces, unlike when the standard (laboratory) calibration is used. To illustrate this, a value of 4.3N was used as a representative force (James et al., 2018). The focused calibration configuration returns a value of 4.4N and a relative error of 1.3% (circled point in Fig. 2.2C). In contrast, the standard calibration equation returns a value of 1.2N and a relative error of 72.8%. These findings indicate that the standard calibration procedure does not produce sufficient accuracy of input-output conversion at low force levels (0-50N) and may have influenced the results of section 2.1.2. Therefore, the results reported in the previous section are now revisited. The revised F250 mean force in response to the given input of 9.6N now equates to 10.0N, which reduces its relative error of measurement with F50 (9.9N) to 1%. In other words, the focused scale/offset configuration validated in this study increased the similarity between the forces recorded by F250 and F50 transducers.

In summary, a systematic approach was taken to establish a calibrated and validated system for measurement of the forces produced by AbH contraction evoked either via electrical stimulation (section 2.1) or voluntarily (Chapter 5). First, it was revealed that 92% of the peak twitch force evoked from AbH by means of PNS occurs along the vertical ($|F_Z|$) component (section 2.1.1). Then, the accuracy of force measurement was shown

to improve significantly if calibration by a focused range rather than by a standard linearly incremental procedure is conducted (sections 2.1.2 and 2.1.3), and thus either force transducer can be used to measure the forces evoked from AbH confidently. Therefore, the uni-axial force transducer was used subsequently (unless otherwise stated) due to its flexibility for Hallux positioning at the optimal 1MPJ angle in the sagittal plane and for representing a vertical line of force (see section 2.3.2).

2.2 Method implemented for direct-muscle electrical stimulation (for training)

Delivering NMES directly to AbH as a percentage of the muscle's maximum capacity is problematic (Chapter 5), as is delivering it at maximally-tolerated intensity (section 1.3.1). One alternative is to normalise the stimulation current intensity to the muscle's MT. To do this accurately, the location of the AbH motor point needs to be first identified and the MT for the intended frequency of the training NMES determined. This section provides a description of the protocols implemented to optimise the delivery of NMES to AbH.

2.2.1 AbH motor point location

The motor point of a target muscle represents the skin surface area overlying the motor end-plates of a muscle, where the branches of the motor axons connect to the sarcolemma of the muscle fibres (location of ACh receptors). When stimulated at the motor point the muscle is readily depolarised, and the largest mechanical response can be evoked compared to other regions (non-motor point) of the skin overlying the muscle using the same stimulus intensity (Mandrile et al., 2003; Gobbo et al., 2014). The location of motor point prior to the delivery of NMES is therefore essential in order to reduce both the associated discomfort, which is often produced due to depolarisation of pain-conducting afferent axons, and the intensity required to depolarise motor axons to

achieve a forceful sustained contraction (Gobbo et al., 2011). The motor point location of AbH was therefore optimised at the commencement of every session that required NMES. This procedure was preceded by cleansing of the skin surface area overlying the AbH muscle belly and the 1MPJ with alcohol wipes (2% chlorhexidine gluconate in 70% isopropyl alcohol; Clinell, GAMA Healthcare Ltd, UK) in order to improve surface electrode-skin contact.

The motor point location procedure consisted of firstly drawing a 7x4cm matrix on the overlying skin of AbH muscle belly (James et al., 2018), which maps a total of 28 probing points 1cm equidistant and where the navicular tuberosity serves as the reference point (Fig. 2.3A). Then, participants were seated in the testing apparatus with their Hallux suspended in dorsal flexion (see section 2.3) from a uni-axial force transducer sampling at 500Hz. Next, a single square-wave (500μs) electrical pulse was systematically delivered at each of the probing points at a standard current intensity of 10mA through a custom-made pen-type cathode (Fig. 2.3A) using the constant-current stimulator (see section 2.1.1) which was digitally synchronised with the force data via the analogue-to-digital converter (see section 2.1.1) and imported into Spike2 acquisition software. A hypoallergenic surface electrode (79mm^2 uptake area; Ambu WhiteSensor WS, Ambu A/S, Denmark) acting as an anode was positioned over the 1MPJ to close the electrical loop (Fig. 2.3A). Consistent pressure, guided by feel and skin deformation, was applied to every point of the matrix, and a random ~5s period was kept between stimuli in order to avoid habituation. The point of the matrix resulting in the largest evoked twitch force was identified as the motor point of AbH (James et al., 2018), and an adhesive surface electrode (79mm^2 uptake area; Ambu WhiteSensor WS, Ambu A/S, Denmark) was subsequently positioned over this point area to act as cathode (Fig. 2.3B). The common location of motor point was 1cm posterior and 3cm inferior to NT.

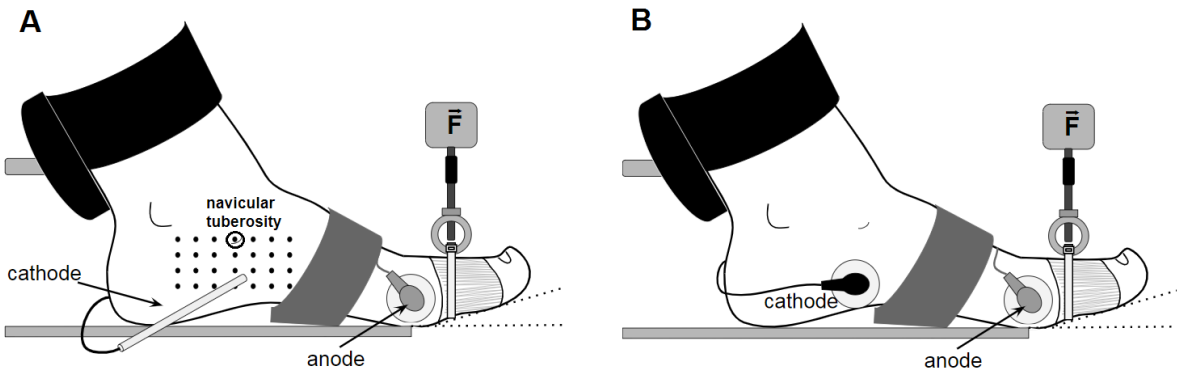

Figure 2.3. **A:** The 7x4cm matrix is drawn over the medial side of the foot with the navicular tuberosity (circled) as a reference point. A total of 28 points, 1cm equidistant, are systematically probed for motor point identification with a custom-made pen-type cathode electrode while an anode is positioned over the 1MPJ. **B:** A surface electrode is fixed over the matrix point identified as motor point for NMES.

2.2.2 AbH motor threshold (MT) determination

The MT of AbH was defined as the minimum stimulus current intensity required to evoke a twitch force (James et al., 2018). First and unless specified in respective chapters, five 1ms pulses were delivered to the previously identified motor point at 100Hz. The current intensity delivered was increased linearly in a stepwise manner in 0.5mA increments, with a starting current intensity of 0.5mA and random ~5s gaps between consecutive pulses to reduce electrical habituation and potentiation of the twitch force. This intensity was increased until a fused and visible twitch force was recorded that exceeded the baseline force by 2SD, which was measured from the signal within a 1s window and 1.5s prior to stimulation onset. A study investigating the repeatability of this procedure (MT determination) and motor point location is now presented.

2.2.3 Between-day repeatability analysis of motor point location and threshold

Aim

To establish the repeatability of motor point location and MT determination between days.

Methods

The motor point and MT of AbH in the left foot of eight healthy participants (7M/1F, mean±SD: 21.5±2.4 years, 75.6±13.5kg, 1.7±0.1m) were assessed on five different days. They were positioned in the experimental set-up as outlined in section 2.3, but on this occasion with the Hallux suspended from the uni-axial force transducer (sampling frequency: 500Hz) in slight dorsal flexion, enough to allow the flat surface of a manual goniometer to pass between the foot supporting surface and the Hallux. The NMES current intensity (mA) attained at MT was assessed to establish the between-day repeatability of AbH MT. In four of these participants (4M, 22.8±2.6 years, 78.3±18.2kg, 1.7±0.0m), a 3-dimensional motion capture system of three optical cameras (Oqus-3+, Qualisys AB, Sweden), sampling at 30Hz, was used to assess the repeatability of motor point location. Since motor point location depends on the accuracy of navicular tuberosity identification, the vector joining 2 x 4mm passive skin-mounted reflective markers positioned on the navicular tuberosity and mid-portion of the Hallux toenail was taken as an index for motor point repeatability, and calculated using the camera system's proprietary software (QTM, Qualisys AB, Sweden). The between-day repeatability of these measures was evaluated by calculating the intraclass correlation coefficient (ICC) (SPSS v.21, IBM, USA) with a two-way mixed effects model for single measurement $ICC_{[3,1]}$, where an ICC of <0.50, 0.50-0.75, 0.75-0.90 and >0.90 was considered poor, moderate, good and excellent repeatability, respectively (Koo & Li, 2016). Variability was measured by calculating the Coefficient of Variation (%): $(CoV\ (\%) = (\frac{SD}{Mean\ value\ for\ a\ given\ measure}) \times 100)$.

Results

The between-day repeatability of motor point location (*n*=4) was excellent ($ICC_{[3,1]}$=0.98) with a variability ranging between CoV=0.4-1.4%. The between-day repeatability of MT determination (*n*=8) was good ($ICC_{[3,1]}$=0.81) with a variability ranging between 5.2-22.4%.

Table 2.2. Mean (± SD) and CoV for motor point (MP) location (*n*=4) based on the distance (mm) between the markers placed on the navicular tuberosity and Hallux, and MT determination (mA; *n*=8). $ICCs_{[3,1]}$ demonstrate the repeatability in the measurements between testing sessions.

	MP (mm; *n*=4)	MT (mA; *n*=8)
Mean (SD)	156.7 (1.3)	2.9 (0.2)
CoV (%)	0.8 (0.4)	12.2 (6.0)
$ICC_{[3,1]}$	0.98	0.81

Interpretation

The motor point allocation of AbH is important in order to optimise the delivery of NMES. This section established a robust protocol for optimisation of NMES delivery to AbH. The results from the application of this protocol give confidence that the location of motor point can be identified consistently between-days, from which the MT can be identified with good repeatability (Table 2.2.).

In addition to identifying the motor point and MT as intrinsic muscle properties of importance, the force produced by AbH may also be influenced by muscle-joint

interactions about the ankle and forefoot. The next section will focus on the positioning of the ankle joint and the Hallux with respect to the testing apparatus in order to optimise the force produced by AbH.

2.3 Experimental set-up

This section introduces the testing apparatus used throughout the experimental chapters and documents the steps taken to optimise the Hallux position for force production.

2.3.1 Testing apparatus

Participants were seated and fastened in a custom-built testing apparatus. This testing apparatus, illustrated in Figure 2.4A, incorporates an inbuilt foot-supporting platform from which a force transducer can be suspended above the Hallux.

The foot was secured firmly at the ankle joint and forefoot to minimise movement during data collection (Fig. 2.4A). The ankle joint was positioned at 35º of plantar flexion from its neutral 0º position. At this specific joint angle, the extrinsic foot muscles are at mechanical disadvantage to produce force based on their joint moment–angle relationship (Goldmann & Brüggemann, 2012). The joint moment—angle relationship serves as a geometric proxy for the force-length relationship curve which is used to identify the optimal length for a muscle to produce force (Maganaris, 2001). Positioning the ankle joint at 35º of plantar flexion shortens the length of the extrinsic hallux flexor muscle - flexor hallucis longus, and its contribution to the force produced at 1MPJ is reduced in favour of isolating the force output due to activation of intrinsic hallux flexor muscles (eg, AbH). The positioning of the 1MPJ would also change the length of AbH, especially when the Hallux is suspended from the uni-axial force transducer (unless

specified). Therefore, investigating the optimal 1MPJ angle for AbH force production is warranted and will be the focus of the next section.

2.3.2 Identification of the optimum 1MPJ angle for AbH force production

Aim

This study was undertaken to identify the optimal 1MPJ angle for AbH force generation. The objectives of this study were: i) to investigate whether the force generation of AbH can be assessed in vivo using NMES in combination with dynamometry and at different muscle-tendon lengths achieved by varying the 1MPJ angle; and ii) to assess how the NMES-induced contractions impact on the 1MPJ axis of rotation and corresponding moment arm.

Methods

Sixteen healthy volunteers (12M/4F, mean ± SD: 25.6±5.8 years, 78.8±13.7 kg, 1.7±0.1 m) provided written informed consent to participate in the present study which was approved by the local ethics committee (SAS1806a). Participants visited the laboratory for a familiarisation visit and one main testing session. The familiarisation visit included motor point location and MT determination (see sections 2.2.1 and 2.2.2, respectively) for optimal delivery of NMES to AbH. The procedures performed for MT determination in this study were akin to those described in section 2.2.2 with the only difference of the use of the five (1ms) pulses at 20Hz frequency instead of 100Hz. This was done to determine the current intensity of the stimulus in accordance with the low-frequency trains that would be delivered during the main session. In the main session, motor point and MT were first verified, then a 7s train of 1ms pulses was delivered to AbH at low-frequency (20Hz) and an intensity of 150% MT (James et al., 2018) in the following 1MPJ sagittal plane angle configurations: neutral (0°) and 5°, 10°, 15° and 20° dorsal flexion.

The force generated in response to stimulation delivered at the neutral position was always measured first. Thereafter, the testing order of the remaining 4 joint configurations (5°- 20°) was determined by a Latin-square design randomisation.

Participants were positioned in the testing apparatus. A polymer gel support covered their left Hallux, which was suspended from the uni-axial force transducer (sampling frequency: 500Hz) through a semi-rigid thermoplastic cable fixed around the proximal phalanx, immediately distal to the 1MPJ (Fig. 2.4). Then, a system of five optical-based cameras (Oqus-3+, Qualisys AB, Sweden) was used to track the locations of 4mm passive skin-mounted reflective markers attached to the navicular tuberosity, the anode overlying 1MPJ (see section 2.2), and the interphalangeal joint of the Hallux (Fig. 2.4B). Tracking started after the positioning of each 1MPJ configuration and continued throughout each 7s train of electrical stimulation.

Two markers placed in series on the vertical rigid shaft of the force transducer described the force line of pull (Fig. 2.4B). The perpendicular distance between the line of pull and the 1MPJ axis of rotation represented the external moment arm (*r*). The force and raw marker positions (50Hz) were synchronously recorded through the analogue to digital convertor (see section 2.1.1) and imported using Spike2 acquisition software for analysis. Waveforms corresponding to 1MPJ angle (°), the external moment arm (m), and the recorded force were smoothed using a moving average function with a time constant of 0.1s. Then, the external joint moment evoked at each 1MPJ configuration was calculated using the equation:

$$\mathrm{M} = \mathrm{F} \bullet \mathrm{r}\,(\sin\theta)$$

where θ represents the sagittal plane angle formed by the line projected to the floor from markers d and e (Fig. 2.4B) and the horizontal distance from 1MPJ to the line of pull.

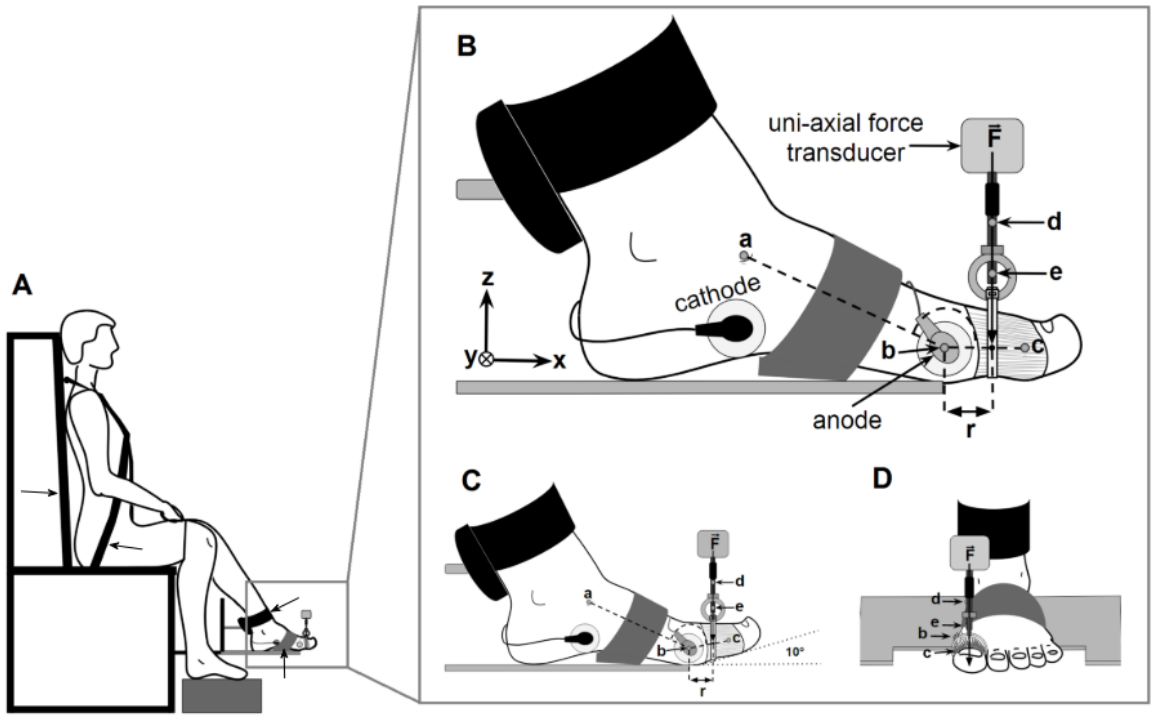

Figure 2.4. Experimental set-up and foot-hallux arrangement. **A:** Participant position on the custom-built apparatus with the left foot fixed to the foot platform and the ankle positioned at 35° plantarflexion. The arrows indicate the parts of the apparatus that are adjustable. **B:** Sagittal plane view of the experimental foot in the neutral configuration (0°): the Hallux is suspended from the uniaxial force transducer, and retro-reflective markers are placed at the: navicular tuberosity (a); first metatarsophalangeal joint (1MPJ, b); interphalangeal joint (c); and the proximal (d) and distal (e) shaft of the uniaxial force transducer. *r* represents the external moment arm length calculated as the perpendicular distance from the 1MPJ to the force line of pull ($\tan^{-1}\left(\frac{\Delta y}{\Delta x}\right)$ from markers d & e) along the x-axis. **C:** The experimental foot positioned in 10° 1MPJ dorsal flexion with respect to the neutral configuration (0°). **D:** Coronal plane view of the foot and Hallux arrangement. The anteroposterior axis of 1MPJ coincides with the end of the foot platform to achieve Hallux suspension from the uni-axial force transducer.

To assess the effect of sustained AbH contraction (evoked via NMES) on 1MPJ axis of rotation, the maximal force and average values of the joint angle, and corresponding external moment arm were calculated (within a 3s window) prior to (relaxed) and 1s into (contracted) each 7s-stimulation train for each 1MPJ configuration. The maximal external joint moment (N•m) was calculated twice for each 1MPJ configuration: using the external moment arm during the contracted condition (corrected joint moment), and during the relaxed condition (uncorrected joint moment).

Individual values (*n*=16) for 1MPJ angle and moment arm were normally distributed (Shapiro-Wilk, SPSS v.21, IBM, USA); therefore, a two-way repeated measures ANOVA, with condition (relaxed vs contracted) and 1MPJ configuration (0°, 5°, 10°, 15°, 20°) as the within-subject factors, was performed to assess for main and interaction effects of condition with effect size (η^2). Multiple comparisons were made using a Bonferroni correction factor and statistical significances were accepted when $p \leq 0.05$.

Individual values (*n*=16) for the external joint moments were not normally distributed, even following Log transformation; therefore, non-parametric Wilcoxon sign-rank tests were performed to compare the uncorrected vs corrected joint moments at the corresponding 1MPJ configuration. Statistical significance was accepted when $p \leq 0.01$ to account for the multiple comparisons. The corrected external joint moments were analysed using a Friedman test, followed again by Wilcoxon Signed-Rank tests to assess for an optimal 1MPJ configuration for force production. Statistical significance of differences was accepted when $p \leq 0.01$.

Results

The population average electrical stimulation intensity at 150% MT was 4.8 ± 2.2mA.

Significant interaction ($p<0.001$; $\eta^2=0.73$) and main effects of condition ($p<0.001$; $\eta^2=0.86$) and joint configuration ($p<0.001$; $\eta^2=0.99$) were found for 1MPJ angle (Fig. 2.5A). Post-hoc tests identified significantly different 1MPJ dorsal flexion between the

relaxed and contracted conditions at all investigated 1MPJ configurations except at 20° of dorsal flexion.

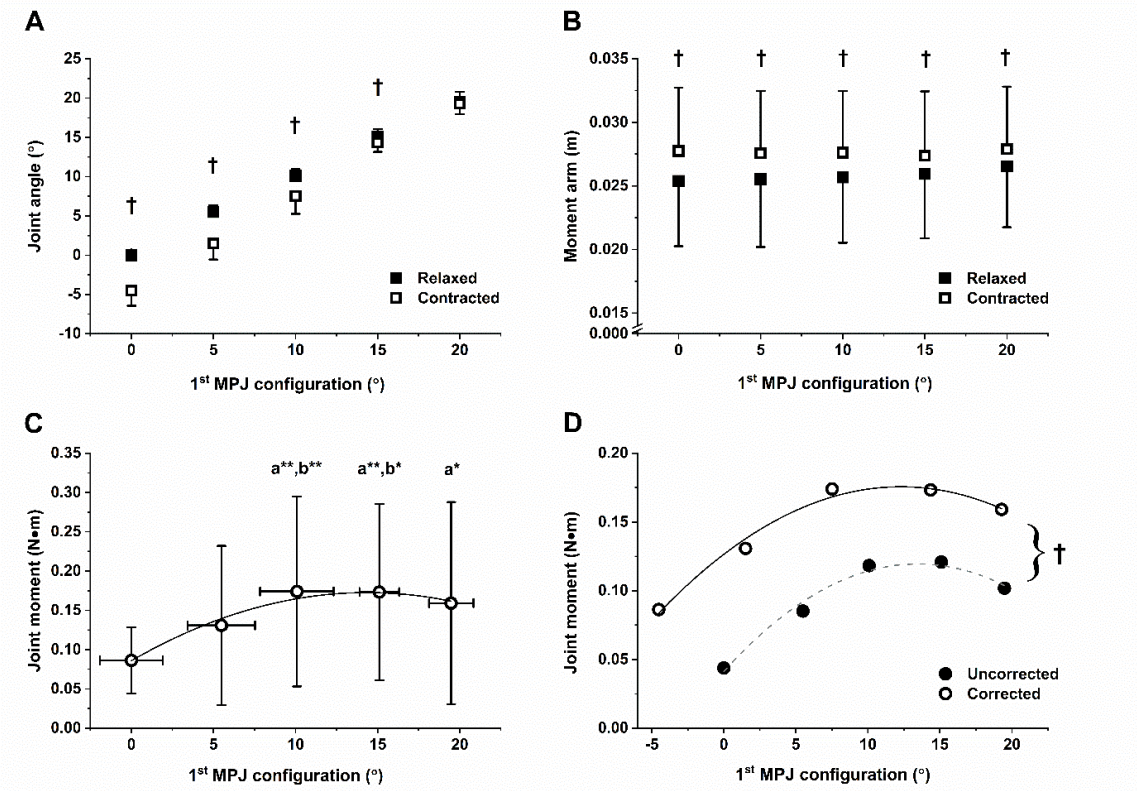

Figure 2.5. Population average (mean±SD, *n* = 16) responses for **A:** 1MPJ angle (°) during relaxed and contracted conditions; **B:** the external moment arm (m) during relaxed and contracted conditions; **C:** the corrected external joint flexion moment (N•m) at each 1MPJ angle configuration (x-error bars reflect the standard deviation values from y-axis in panel **A**; and **D:** comparison of the uncorrected (filled circles) vs corrected (unfilled circles) external joint moments. [a] indicates significantly different to 0°; [b]- significantly different to 5°; * - significantly different at p≤0.05 level; ** - significantly different at p≤0.01 level; † - significantly different between conditions at the respective 1MPJ configuration at p≤0.001 level.

The change in joint angle resulted in a significant difference ($p<0.001$; $\eta^2=0.83$, main effect of condition) in the external moment arm between relaxed and contracted conditions (Fig. 2.5B). Specifically, during contraction, the moment arm increased on average by up to 2mm. Therefore, the corrected external joint moment was significantly greater than the uncorrected joint moment at all investigated 1MPJ configurations (all $p\leq0.001$) (Table 2.3 for population mean moments; Fig. 2.5D for moment–angle relationship).

A significant main effect of 1MPJ configuration was found in the corrected external 1MPJ joint moment–angle relationship ($p<0.01$), which fits a parabolic-like curve (Fig. 2.5C). The external joint moments at 10° and 15° 1MPJ dorsal flexion were significantly higher compared to 0° (both $p<0.01$) and 5° ($p<0.01$, $p<0.05$, respectively), but not 20° (Table 2.3, Fig. 2.5C). The external joint moment at 20° 1MPJ dorsal flexion was significantly higher than 0° ($p<0.05$).

Table 2.3. Population average (mean ± SD, *n*=16) uncorrected vs corrected external joint moments (N•m) at each 1MPJ angle configuration. † - significantly different to the respective uncorrected joint moment at $p\leq0.001$ level; [a] - significantly different to the corrected joint moment at 0°; [b] - significantly different to the corrected joint moment at 5°; * - significantly different at $p\leq0.05$ level; ** - significantly different at $p\leq0.01$level.

	1st MPJ angle configurations				
	0°	**5°**	**10°**	**15°**	**20°**
Relaxed (N•m)	0.04 (0.03)	0.09 (0.08)	0.12 (0.08)	0.12 (0.08)	0.10 (0.09)
Contracted (N•m)	0.09 † (0.04)	0.13 † (0.10)	0.17 †,a**,b** (0.12)	0.17 †,a**,b* (0.11)	0.16 †,a* (0.13)
Δ (%)	49.3	34.8	32.1	30.3	36.1

Interpretation

The findings of this study suggest that the relationship between the force produced by AbH in response to direct-muscle NMES and the configuration of the 1MPJ follows a parabolic curve, and the highest 1MPJ moment is produced when positioned between 10° and 15° in Hallux dorsal flexion. In addition, a new method using NMES and dynamometry has been presented here for the assessment of AbH force generating capacity. An inherent cautionary note with this approach is an ensuing underestimation of the resulting joint moment due to a change in the 1MPJ moment arm as a result of joint rotation caused by sustained AbH contraction. This underestimation should be corrected to represent an accurate joint moment produced by AbH about 1MPJ.

Up to this point, the validity and scalability of the thesis's main techniques for data collection have been verified; the procedure and repeatability of NMES delivery documented, and the experimental set up presented. The following section reports how the PNS technique was implemented in the study to evaluate the performance/efficacy of NMES delivery.

2.4 Method implemented for peripheral nerve stimulation (for assessment)

PNS of the medial plantar nerve combined with surface EMG allows recording of the M_{wave} of AbH resulting from the depolarisation of its supplying motor axons beneath the stimulating electrode. As a result of the evoked excitation of the MUs a muscle contraction then ensues, which is recordable through a force transducer. Muscle excitability and contractility properties of AbH can therefore be assessed using this method. A description of the methodological protocols implemented to optimise PNS of the medial plantar nerve is given in this section.

2.4.1 Identification of medial plantar nerve location

Prior to location of the medial plantar nerve, the skin surface overlying AbH and posterior to the medial malleolus was prepared to reduce the skin impedance and improve the electrode-skin interface contact. For this, the skin surface was shaved (when necessary), abraded with clinical sandpaper (3M^{TM} Red Dot^{TM}, 3M UK PLC) and abrasive gel (NuPrep, Weaver and Co., CA, USA), and finally cleansed with alcohol wipes.

Then, a bi-polar EMG sensor (1 mm width, 10 mm pole spacing; CMRR> 80 dB; model DE2.1, DelSys Inc., USA) was positioned on the skin surface overlying AbH and distal to the cathode fixed at the motor point of AbH (Fig. 2.4B). A ground electrode (8cm^2 uptake area; Dermatrode, American Imex, CA, USA) was placed over the medial malleolus to reduce the interference of the power line and biological background noise in the EMG signal (Fig. 2.6). The quality of the EMG signal was confirmed when its root mean square amplitude was less than 10µV (within the range recommended by DelSys Inc., USA; De Luca, 1997), measured over a ~5s window, 5s after a voluntary contraction. The signal (sampling frequency: 2000Hz) was then amplified to a factor of 100 and band-pass filtered at the main amplifier unit (20-450Hz bandwidth; Bagnoli-8, DelSys Inc., Boston, MA).

Identification of the optimal location for medial plantar nerve stimulation was performed in a similar manner as identification of AbH motor point (see section 2.2.1). A 5x5 matrix of 0.5cm equidistant points was drawn posterior to the medial malleolus, the centre of the malleolus served as reference to draw the first row which was aligned to the transverse section of the lower leg (Fig. 2.6A). Then a single square-wave pulse (1ms) at a standard intensity of 10mA was delivered to each point of the matrix using the custom-made pen-type cathode (Fig. 2.6A) with an anode electrode (8cm^2 uptake area; Dermatrode, American Imex, CA, USA) attached over the lateral malleolus. The peak-to-peak amplitude (mV) of the evoked M_{wave} corresponding to each matrix point (if any)

was monitored and the point revealing the highest amplitude represented the optimal location for PNS of the medial plantar nerve. An adhesive cathode electrode (79mm^2 uptake area; Ambu WhiteSensor WS, Ambu A/S, Denmark) was then fixed over this skin area (Fig. 2.6B).

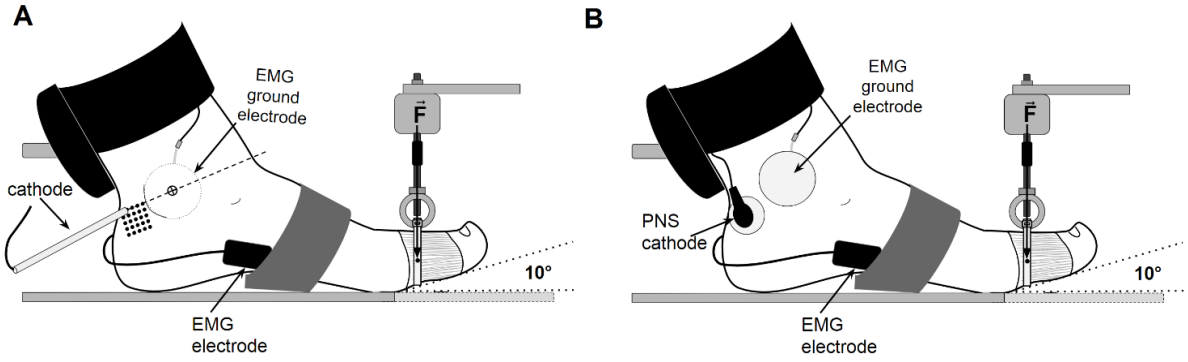

Figure 2.6. Foot-hallux arrangement for peripheral nerve stimulation (PNS). **A:** A 5x5cm matrix was drawn over the skin posterior to the medial malleolus for optimal medial plantar nerve location using a pen-type cathode. The first row of the matrix was aligned with the transverse section of the lower leg using the centre of the malleolus as a reference point. **B:** Positioning of an adhesive surface electrode on the optimised medial plantar nerve location for PNS. The anode electrode is positioned on the lateral malleolus and is not visible in this figure.

2.4.2 Maximum compound muscle action potential (M_{wave})

The supramaximal intensity for PNS of the medial plantar nerve was determined through the performance of an input-output response (recruitment) curve at the beginning of each session (Fig. 2.7A). Single square-wave (1ms) pulses at increasing current intensities in increments of 1mA, starting at 1mA, were delivered to the nerve until a well-defined M_{wave}

(clear depolarisation-hyperpolarisation profile) was recorded; upon which, three stimuli - 5s apart were delivered at each intensity thereafter. Maximum M_{wave} (M_{max}) was defined as saturation in its peak-to-peak amplitude despite increasing stimulation current intensity. The current intensity was then multiplied by 130% (M_{max130}) to compute supramaximal PNS intensity (James et al., 2018) to ensure complete activation of the MU pool innervating AbH.

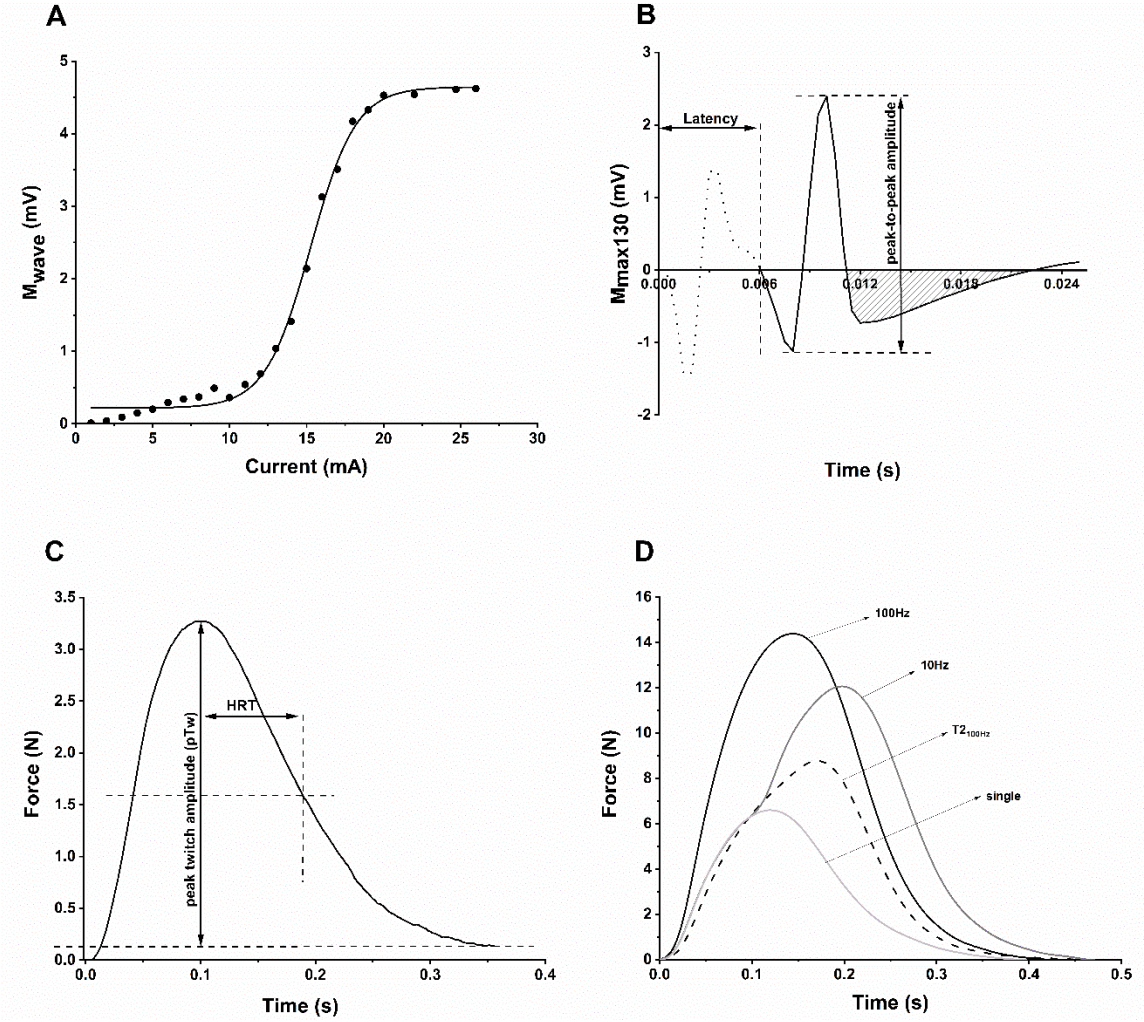

Figure 2.7. A: A fully constructed recruitment curve (sinusoidal shape) based on the amplitude of the M_{wave} to reveal M_{max130}. **B:** Exemplar of the M_{max130} with its corresponding excitability parameters: latency (ms), peak-to-peak amplitude (mV) and terminal phase area (TP; mV•ms) shaded in grey. The preceding stimulus artefact is shown as a dotted

waveform. **C:** Exemplar of a twitch force evoked by a single pulse at M_{max130} intensity with its respective contractility parameters: peak twitch amplitude (pTw; N) and half relaxation time (HRT; ms). **D:** Twitch forces (mean of three stimuli) evoked by a single pulse (light grey), paired stimuli at 10Hz (dark grey) and 100Hz (black) at M_{max130} intensity. The fourth trace (dashed black line) represents the potentiated $T2_{100Hz}$ force, which was obtained by digitally subtracting the force evoked during a single pulse from that of a doublet at 100Hz.

2.4.3 Performance measures associated with PNS

The peripheral excitability of AbH and processes underlying its capacity to contract can be assessed by parameters derived from the PNS-evoked M_{max130} and its corresponding twitch force, respectively.

2.4.3.1 M_{max130} (muscle excitability) evoked by PNS

Excitability is the property that reflects the capacity of a muscle to respond to a stimulus. When PNS is implemented at supramaximal currents, the stimulus propagates along the axon in the orthodromic direction towards the neuromuscular junction. Then, the compound muscle action potential propagates in opposite directions from the neuromuscular junction along the muscle fibre sarcolemma until it dissipates along the fibre-ends. The amplitude of the excitation propagation reflects the electrogenic Na^+-K^+ transport across the sarcolemma and T tubules (Clausen, 2003). If the amplitude of the excitation is high, M_{max130} conduction velocity decreases (increased conduction time) (Merletti et al., 1990) in turn broadening the duration of the potential (Bigland-Ritchie et al., 1979).

In this thesis, muscle excitability is assessed through the following parameters of the M_{max130} evoked in AbH by single pulse PNS (Fig. 2.7B): i) latency (ms), calculated as the time between stimulus onset and the beginning of the first positive phase; ii) amplitude (mV), calculated from the peak of the first positive phase to the peak of the negative phase, and iii) terminal phase area (TP; mV•ms), corresponding to the area between the horizontal threshold line (set at baseline ± 2SD) and the last positive phase of the waveform.

2.4.3.2 Twitch Force (muscle contractility) evoked by PNS

The contractility of AbH can be assessed through the evoked twitch force following M_{max130}. This is because the parameters derived from this mechanical response represent the continuum of events consisting of excitation-contraction coupling, muscle contraction and relaxation processes. Specifically, the peak twitch force (pTw) reflects the number of strongly bound cross-bridges formed to produce the contraction (Fitts, 1994), whilst the half relaxation time (HRT) of the twitch force represents the processes of Ca^{2+} re-uptake from the myoplasm and cross-bridge detachment (Hill et al., 2001). In this thesis, the pTw (N) was measured with respect to baseline; and the HRT (ms) was measured from the descending force profile in relation to the time concurring between pTw to the point equivalent to 50% of the ascending force profile (Fig. 2.7C).

In addition to single pulse evoked twitch force, paired stimuli were also delivered to investigate the effect of NMES exposure (specific to each subsequent chapter) on AbH's contractility and the potential induction of potentiation. For this, three stimuli (for paired pulses) were delivered pre- and post- NMES. The delivery of paired stimuli, i.e. two closely spaced pulses, results in an augmented twitch force response. Each of the pulses from paired stimuli is considered to evoke a different response: the first pulse evokes an unconditioned twitch force, equivalent to a single pulse response; and the second pulse

evokes a potentiated twitch force (T2) (Yan et al., 1993; Verges et al., 2009). The second pulse potentiates the force evoked by the first pulse in a non-linear fashion (Duchateau & Hainaut, 1986; Karu et al., 1995) and it is not due to the recruitment of additional muscle fibres by the second pulse since the evoked M_{max130} response for each pulse are equivalent (Duchateau and Hainaut, 1986; Karu et al., 1995). Rather, the mechanisms responsible for this twitch force potentiation are likely to be due to additional Ca^{2+} released from the sarcoplasmic reticulum into the myoplasm in response to the second pulse, and the concomitant prolongation of myoplasmic [Ca^{2+}] available for binding to troponin C (Cheng et al., 2013; Bakker et al., 2017). These mechanisms which describe cross-bridge formation for force generation during a paired stimuli are affected by the previous activation history of muscle (Binder-Macleod & Kesar, 2005; Allen et al., 2008); therefore, T2 from the paired stimuli delivered at 100Hz ($T2_{100Hz}$) can be used to assess the Ca^{2+}-dependent mechanisms responsible for force summation in AbH.

With paired stimuli delivered at two different frequencies (low and high), muscle fatigability was also quantified. Specifically, paired stimuli were delivered at 10Hz and 100Hz to compute the low-to-high frequency fatigue index ($F_{paired10/100}$). $F_{paired10/100}$ increases with high-frequency fatigue and decreases with low-frequency fatigue (Yan et al., 1993; Verges et al., 2009). The peak twitch force amplitude of the responses to paired stimuli (10Hz and 100Hz; N) and $T2_{100Hz}$ (N) was measured with respect to baseline (Fig. 2.7D). The force amplitude of the responses was then used to calculate the ratio $F_{paired10/100}$ by dividing the peak twitch force evoked through the paired stimuli at 10Hz by that of the peak twitch force corresponding to paired stimuli at 100Hz. In order to access $T2_{100Hz}$, the twitch force evoked by a single pulse stimulation was digitally subtracted from the twitch force evoked by the paired stimuli at 100Hz (Fig. 2.7D) (Yan et al., 1993; Verges et al., 2009).

2.4.4 Within-day repeatability analysis of PNS-evoked responses

Aim

To assess the within-day repeatability of the responses used to assess muscle excitability (M_{max130}) and contractility (twitch force) derived from PNS.

Methods

Four participants were tested to assess the within-day repeatability of the performance parameters derived from PNS (4M, 22.8±2.6 years, 78.3±18.2 kg, 1.7±0.0 m).

Optimisation procedures were undertaken at the commencement of the session for PNS of medial plantar nerve, which included: EMG electrode positioning, medial plantar nerve site location and construction of the recruitment curve (see section 2.4.2; Fig. 2.7A) to reveal the supramaximal intensity (M_{max130}). Then, five x M_{max130} were delivered to the medial plantar nerve, while participants were seated with their hallux suspended from a uni-axial force transducer (see section 2.3).

Cross-correlation analysis (*n*=4) was performed in Spike 2 software (v7.12; CED Ltd., UK) to assess the similarity of the M_{max130} and twitch force waveforms within-days (Fig. 2.8). M_{max130} and twitch force waveforms similarity within days serves as an indication of the stability of the respective parameters derived from these waveforms (see Fig. 2.7). The responses evoked by the first and fifth pulses within the session were compared for analysis. For this, the cross-correlation was set to have a maximum shift (absolute width of the x-axis) of 10ms and an offset (positive and negative temporal interval from and to zero) of 5ms for the M_{max130}, and a maximum shift of 100ms and an offset of 50ms for the twitch force. The phase-shift (lag) between the compared profiles and the Pearson's correlation coefficient (r) at zero time-shift are indicators of the similarity of the profiles to assess the stability of excitability and contractility responses and by proxy the repeatability of their parameters within-days.

Results

The within-day cross-correlations for each participant, performed to assess the variability in the M_{max130} and twitch force waveforms within a session (Fig. 2.8), indicate that the M_{max130} (Table 2.4) and corresponding twitch force (Table 2.5) were stable throughout a testing session in all participants. [1]

Interpretation

The results reported here show that the M_{max130} and twitch force waveforms had excellent within-day correlations. These findings suggest that the parameters derived from PNS to evaluate muscle excitability and contractility are stable and repeatable when assessed within-days.

[1] The between-day repeatability was analysed and the minimal detectable change (MDC) values calculated for each of the excitability and contractility parameters derived from PNS. This was done with the intention of providing an assessment criteria for the intervention study that was intended prior to the Covid-19 pandemic. The results from the between-day repeatability analysis and MDC data can be found in Appendix 1 (*2.4.5*).

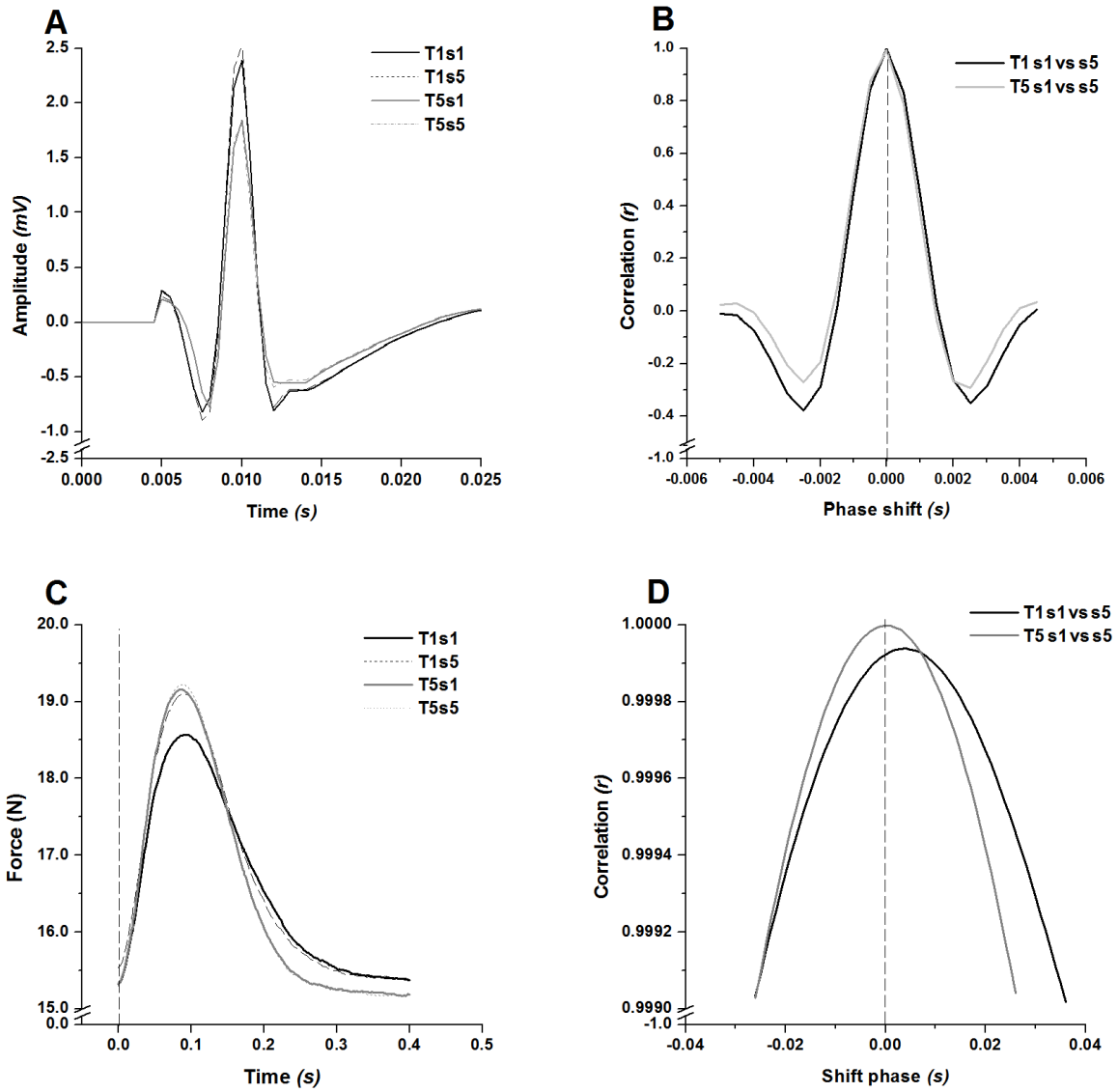

Figure 2.8. An exemplar of one participant's waveform within-day correlation of the first (s1) and fifth (s5) M_{max130} and corresponding force twitch from trials 1 and 5 (T1 & T5). **A:** Sample of the s1 and s5 M_{max130} responses for T1 and T5. **B:** Waveform correlation comparing the s1 vs s5. **C:** The s1 and s5 evoked twitch forces corresponding to M_{max130} for T1 and 5. **D:** Correlation between s1 and s5 force twitches in T1 and T5.

Table 2.4. Within-day correlation coefficients (r), lag and p value for M_{max130} are presented in this table for each trial and each participant. The waveform of the M_{max130} responses from all participants (*n*=4) showed excellent correlation within day.

	Participant 1			Participant 2			Participant 3			Participant 4		
	r	$lag^{(r@lag)}$	p value	r	$lag^{(r@lag)}$	p value	r	$lag^{(r@lag)}$	p value	r	$lag^{(r@lag)}$	p value
T1	1.00	$0.00^{(1.00)}$	<0.001	1.00	$0.00^{(1.00)}$	<0.001	1.00	$0.00^{(1.00)}$	<0.001	1.00	$0.00^{(1.00)}$	<0.001
T2	1.00	$0.00^{(1.00)}$	<0.001	1.00	$0.00^{(1.00)}$	<0.001	1.00	$0.00^{(1.00)}$	<0.001	1.00	$0.00^{(1.00)}$	<0.001
T3	1.00	$0.00^{(1.00)}$	<0.001	1.00	$0.00^{(1.00)}$	<0.001	1.00	$0.00^{(1.00)}$	<0.001	0.99	$0.00^{(0.99)}$	<0.001
T4	1.00	$0.00^{(1.00)}$	<0.001	1.00	$0.00^{(1.00)}$	<0.001	1.00	$0.00^{(1.00)}$	<0.001	1.00	$0.00^{(1.00)}$	<0.001
T5	1.00	$0.00^{(1.00)}$	<0.001	1.00	$0.00^{(1.00)}$	<0.001	1.00	$0.00^{(1.00)}$	<0.001	1.00	$0.00^{(1.00)}$	<0.001

Table 2.5. Within-day correlation coefficients (r), lag and p value for force twitch are presented in this table for each trial and each participant. The waveform of the twitch force responses from all participants (*n*=4) showed excellent correlation within day.

	Participant 1			Participant 2			Participant 3			Participant 4		
	r	lag$^{(r@lag)}$	p value	r	lag$^{(r@lag)}$	p value	r	lag$^{(r@lag)}$	p value	r	lag$^{(r@lag)}$	p value
T1	0.99	-0.005$^{(0.99)}$	<0.001	0.98	-0.005$^{(0.99)}$	<0.001	0.96	-0.011$^{(0.99)}$	<0.001	1.00	0.004$^{(1.00)}$	<0.001
T2	0.94	0.010$^{(0.97)}$	<0.001	0.93	0.012$^{(0.96)}$	<0.001	1.00	-0.001$^{(1.00)}$	<0.001	1.00	-0.001$^{(1.00)}$	<0.001
T3	1.00	-0.001$^{(1.00)}$	<0.001	1.00	0.003$^{(1.00)}$	<0.001	1.00	-0.001$^{(1.00)}$	<0.001	1.00	0.001$^{(1.00)}$	<0.001
T4	0.99	-0.002$^{(0.99)}$	<0.001	1.00	0.000$^{(1.00)}$	<0.001	1.00	-0.001$^{(1.00)}$	<0.001	1.00	0.001$^{(1.00)}$	<0.001
T5	1.00	-0.001$^{(1.00)}$	<0.001	1.00	-0.001$^{(1.00)}$	<0.001	1.00	0.001$^{(1.00)}$	<0.001	1.00	0.000$^{(1.00)}$	<0.001

Link to next chapter

High current intensity augments the recruitment of MUs within the target muscle (Bickle et al., 2011; Bergquist et al., 2011b) for muscle contraction. At the same time, high currents cause higher discomfort, which limits the utility of the NMES applied (Maffiuletti, 2010; Bergquist et al., 2011b). Using low current intensity may reduce discomfort and increase the applicability of NMES (Bergquist et al., 2011b). In addition to current intensity, pulse duration plays a role in MU recruitment for muscle contraction due to the current intensity-duration relationship and their product represents the charge being delivered (see section 1.3.1.2; Fig. 1.5A&B). The current intensity-duration relationship is intrinsic to the excitable tissue, and therefore it will depend on whether NMES is applied on the skin overlying a muscle belly or nerve trunk. Identifying which of these modes of stimulation and the pulse duration that requires the lowest current intensity to achieve a muscle contraction is an important consideration to minimise discomfort. Therefore, the next chapter will report the procedure for optimising low current intensity selection for a tolerable application of NMES targeting AbH.

3.0 Optimising the current intensity selection procedure and pulse duration for a tolerable and effective NMES training paradigm

3.1 Introduction

NMES can be delivered via muscle or nerve. In both cases, the evoked contraction is the result of the recruitment of MUs through the depolarisation of motor and sensory axons situated underneath the stimulating electrodes (Collins, 2007). Sensory axons have a lower rheobase compared to motor axons, and therefore require a lower current intensity to be depolarised (Bostock et al., 1998; Collins, 2007). In addition, chronaxie is inversely related to rheobase (see section 1.3.1.2) (Bostock et al., 1998), and therefore sensory axons are preferentially depolarised using wider pulse widths (Collins, 2007).

By exciting action potentials in the sensory axons (Ia afferents), NMES engages the spinal MNs and may activate centrally mediated mechanisms that contribute to the forces generated peripherally by the depolarisation of motor axons (Collins et al., 2001; Collins, 2007). Maximising the contribution of the central mechanism by using low current intensities is therefore beneficial for maintaining the tolerability to NMES and promoting force production.

Discomfort and the contribution of peripheral and central mechanisms differ between the modes of NMES application. At low current intensities, nerve compared to muscle stimulation has been shown to evoke forces with a greater central contribution (measured through H-reflex) (Klakowicz et al., 2006; Baldwin et al., 2006; Bergquist et al., 2011a; 2012). In contrast, muscle stimulation can evoke greater forces which are more consistent and stable during contractions compared to nerve stimulation (Baldwin et al., 2006; Neyroud et al., 2018) with indifferent (Bergquist et al., 2012) or higher asynchronous activity (Bergquist et al., 2011a). Interestingly, high discomfort during nerve stimulation at low intensities has been reported (Klakowicz et al., 2006; Neyroud et al., 2018), by up to twice the level of discomfort induced using muscle stimulation (Neyroud et al., 2018). These considerations are important when selecting the mode of stimulation used to target AbH.

In addition to different pulse durations, varying pulse frequencies have been used during both modes of stimulation to improve force production (Bergquist et al., 2011b). The inclusion of a high pulse frequency of 100Hz has been shown effective in enhancing the evoked afferent drive towards the central nervous system (Collins, 2007; Mang et al., 2010) and increasing the myofibrillar [Ca^{2+}] during contraction (Cheng et al., 2017), which are beneficial for facilitating plasticity of the central nervous system and for increasing cross-bridge formation during NMES, respectively. Therefore, whether nerve or muscle stimulation should be implemented to AbH for tolerable and efficient force production is

currently uncertain but may be discerned by optimising the procedure used for low current intensity selection.

In order to standardise current intensity selection to each individual, the current intensity has been previously expressed as a percentage of the force produced by the target muscle during an MVC (Maffiuletti et al., 2018). However, this approach is impractical for AbH due to its complex mechanical action (Tosovic et al., 2012; see section 1.2.1.1) and the inability for voluntary activation of this muscle even in healthy participants (Boon and Harper, 2003; Arinci Incel et al., 2003; see section 1.2.1.3). Instead, NMES intensity selection for AbH has been guided by its MT, which was defined as the minimum current intensity required to evoke a clear and recordable twitch contraction (James et al., 2013; 2018). Due to the use of low stimulation intensity, this approach overcomes both the problems associated with the requirement for maximal voluntary activation of AbH and minimises discomfort. To be successful, the MT determination protocol requires optimisation of the stimulation parameters selection (pulse intensity, duration and frequency) to achieve a recordable twitch force whilst maintaining its tolerability.

Therefore, the purpose of this study was to optimise the procedure of MT determination for NMES current intensity selection. To adopt a mechanistic approach for optimising the procedure, the threshold current intensity (rheobase) and pulse duration (chronaxie) required to excite the axons underneath the stimulating electrodes must be determined. For this, the current intensity-duration curves (Bostock et al., 1998) will be constructed and used to identify the optimal: i) mode of stimulation (muscle or nerve), ii) pulse duration, and iii) pulse frequency for MT determination in order for NMES delivery to be tolerable and effective.

3.2 Methods

3.2.1 Participants

Thirteen healthy volunteers (11M/2F; mean±SD: 23.2±2.6 years; 79.2±14.0kg; 1.7±0.1m) were recruited and provided written informed consent to participate in this study that had received prior local ethical approval (SAS1806) and was compliant with the Declaration of Helsinki (2013). All participants completed a health screen questionnaire and reported to be in good health, free from lower extremity injuries, underlying pathology or neurological problems.

3.2.2 Experimental procedure

Participants visited the laboratory twice: i) for familiarisation with the testing procedures, and ii) for the main testing session. As part of the familiarisation, optimisation procedures for direct muscle (motor point) and nerve (medial plantar nerve) stimulation were performed. These included identification of AbH motor point and medial plantar nerve location (refer to section 2.2.1 and 2.4.1, respectively) while participants were seated with their left Hallux suspended from a uni-axial force transducer (refer to section 2.3). The second visit started with the same optimisation procedures to verify the motor point prior to commencing the main testing procedures. The two modes of stimulation delivery were tested in a randomised order. Skin temperature was monitored throughout the session using a probe (Moor Instruments Ltd, UK/ RS Components Ltd, UK) fixed proximal to the medial plantar nerve stimulating area for each participant. This was done during muscle and nerve stimulation since skin temperature can influence the excitability properties of sensory (Burke et al., 1999) and motor axons (Kiernan et al., 2001).

3.2.3 Data collection

Five-pulse trains were delivered for each mode to identify the lowest current intensity (mA) that evokes a twitch of amplitude 2SD above the baseline (MT; see section 3.2.2). The current intensity was increased in a stepwise manner, from 0.2mA in 0.2mA increments, until MT was reached. This procedure was repeated using 0.05, 0.1, 0.2, 0.5, 1 and 2ms pulse durations, separated with a 1-minute rest in-between, to construct the intensity-duration curves. The 5-pulse trains were delivered at 10, 20 and 100Hz, therefore three intensity-duration curves were constructed for each mode (e.g., muscle stimulation:10 x 20 x 100Hz). The sequence direction of the pulse duration was alternated (i.e. narrow to wide or wide to narrow), and the order of the 5-pulse train frequency tested was randomised between modes and participants.

3.2.4 Data analysis

Each intensity-duration curve was plotted with intensity (mA) on the y-axis and duration (ms) on the x-axis (Fig. 3.1A & B). Then, rheobase and chronaxie values were calculated through a linear transformation following the charge (intensity x duration) – duration relationship and Weiss' law (Bostock et al., 1998) (Fig. 3.1C & D, for muscle and nerve stimulation respectively). This law dictates that the charge (μC) at activation threshold is directly proportional to the duration of the stimulus used (Bostock et al., 1998). Therefore, the intensity-duration curve can be transformed into a linear regression function: y = b + mx, where the x-intercept corresponds to chronaxie, the slope (m) corresponds to rheobase and (b) represents the y-intercept (Bostock et al., 1998). Correspondingly, chronaxie is derived by accepting y = 0; hence: $|x| = \frac{b}{m}$.

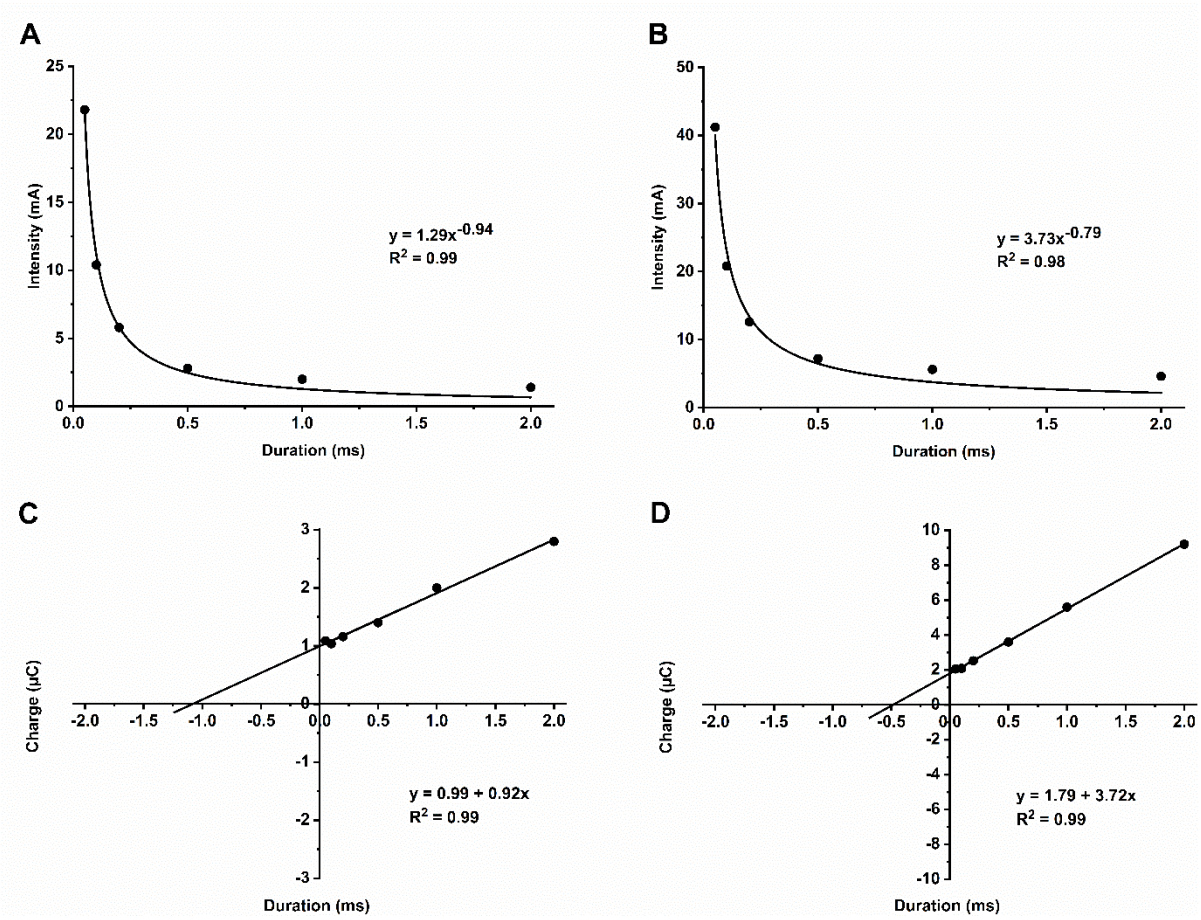

Figure 3.1. Determination of rheobase and chronaxie for muscle and nerve stimulation of a representative participant using a 5-pulse train at 100Hz. Intensity – duration curves for muscle (**A**) and nerve (**B**) stimulation, based on the current intensity required to elicit an AbH twitch force (i.e. MT) at each of the pulse durations tested. The corresponding charge (intensity x duration) – duration plots are shown in **C** (muscle) and **D** (nerve) following linear transformation. In each charge – duration plot and their respective linear function y = b + mx, the x-intercept corresponds to chronaxie, the slope (m) corresponds to rheobase and (b) represents the y-intercept. The chronaxie is determined by calculating the x-intercept from the linear regression equation, given y = 0. For this participant, the linear equation for muscle and nerve stimulation mode are y=0.99 + 0.92x and y = 1.79 + 3.72x, respectively. So, if y = 0, then $|x| = \frac{0.99}{0.92} = |x| = 1.08$ for muscle, and $|x| = \frac{1.79}{3.72} = |x| = 0.48$ for nerve stimulation. Therefore, the rheobase and chronaxie

are equal to 0.92mA and 1.1ms, respectively, for muscle (motor point of AbH), and to 3.72mA and 0.48ms for nerve (medial plantar nerve) stimulation.

The optimised pulse duration corresponds to the chronaxie obtained at the mode and frequency stimulation that resulted in the lowest rheobase. This pulse duration was then compared to 1ms, as previously used (James et al., 2018), by means of calculating the charge as the product of the intensity required to reach rheobase, and the optimised pulse duration or 1ms.

3.2.5 Statistics

Population average values (mean±SD, n=13;) for the rheobase were normally distributed (Shapiro-Wilk, SPSS v.21, IBM, USA); therefore, a two-way repeated measures ANOVA with mode of delivery (muscle vs nerve) and frequency (10, 20, 100Hz) as the within-subject factors, was performed to assess for interaction and main effects of mode and pulse frequency and their effect size (η^2). Pairwise comparisons for mode of stimulation were made post-hoc using a Bonferroni correction. If there was a significant interaction effect, a one-way repeated measures ANOVA with frequency as the within-subject factor was then performed for each mode. Statistically significant differences were accepted when $p \leq 0.05$.

In order to compare the charge calculated using the optimised pulse duration against the charge calculated using 1ms, a paired sampled t-test was performed to compare between charge values after normal distribution was confirmed (Shapiro-Wilk test). Statistical significance was accepted when $p \leq 0.05$.

3.3 Results

Tissue temperature. The recorded average skin temperature during muscle and nerve stimulation was 30.1±1.2°C and 30.0±1.2°C, respectively. These skin temperatures were stable and comparable throughout the session and between modes of stimulation.

Current intensity. Significant main effects of mode ($p<0.01$; $\eta^2=0.45$) and frequency ($p<0.001$; $\eta^2=0.63$) were found. Post-hoc tests revealed that nerve stimulation required more intensity to reach rheobase compared to direct muscle stimulation (Table 3.1).

Pulse frequency. Within the direct muscle stimulation mode, 100 Hz stimulation elicited a lower rheobase when compared to 10 ($p<0.01$) and 20Hz ($p<0.05$) trains. Similarly, during nerve stimulation, 100 Hz elicited a lower rheobase than 10 ($p<0.01$) and 20Hz ($p<0.05$) trains

Pulse duration. The chronaxie corresponding to muscle stimulation delivered at 100Hz was 1.15 ± 0.65ms (Table 3.1). No significant difference ($p>0.05$) was found between the charge calculated using the chronaxie obtained in this study (2.29 ± 0.52µC) and the charge calculated using the previously used pulse duration (1 ms) (2.47 ± 0.98µC).

Table 3.1. Population average (mean ± SD, n = 13) current intensity (rheobase) and pulse duration (chronaxie) at each train frequency (10, 20 or 100Hz) used for MT determination during muscle and nerve stimulation.* Indicates $p<0.05$; ** $p<0.01$; [a] significantly different to 10Hz; [b] significantly different to 20Hz.

	Muscle			**Nerve**		
	10 Hz	**20 Hz**	**100 Hz**	**10 Hz**	**20 Hz**	**100 Hz**
Rheobase (mA)	1.58 (1.01)	1.52 (0.99)	1.39 (0.88)[a]**,[b]*	3.64 (2.12)	3.39 (2.13)	3.00 (1.87) [a]**,[b]*
Chronaxie (ms)	1.06 (0.63)	1.07 (0.60)	1.15 (0.65)	0.57 (0.35)	0.63 (0.39)	0.75 (0.62)

3.4 Discussion

In this study, the construction of intensity-duration curves was used as a mechanistic approach to identify the mode of stimulation (muscle vs nerve), pulse duration (chronaxie, ms) and frequency (Hz) for MT determination that required the lowest rheobasic intensity (mA) in order to minimise discomfort and develop a low intensity NMES approach. The main findings from the present study are: i) NMES applied over the motor point of AbH requires less current intensity to achieve rheobase than when applied to the medial plantar nerve; and ii) wide pulses (1ms) delivered at high frequency (100Hz) require less current intensity to achieve rheobase than narrower pulses (i.e. 0.05, 0.1, 0.2, 0.5ms) delivered at low frequencies (10 and 20Hz). These stimulation parameters and mode of stimulation comprise an optimised approach of MT determination for a low intensity NMES training paradigm targeting AbH that can foster tolerability.

Stimulating at the motor point of AbH (muscle stimulation) or the medial plantar nerve (nerve stimulation) will recruit motor axons differently. During muscle stimulation, superficial and deeper axons are progressively recruited as intensity increases (Okuma et al., 2013; Nagakawa et al., 2020). In contrast, during nerve stimulation, superficial and deep motor axons are evenly depolarised irrespective of intensity and in a random fashion (Okuma et al., 2013; Nagakawa et al., 2020). This suggests that nerve stimulation would provide a more effective mode to activate muscle even at low intensity. However, this study found that muscle stimulation required lower rheobasic intensity to evoke a contraction in AbH than nerve stimulation. This may be explained by the greater proportion of low-threshold compared to high-threshold MUs situated at the superficial aspect of the muscle (Širca et al., 1990; Dahmane et al., 2005), which would make their recruitment readily achievable at low intensities (Fleshman et al., 1981). In addition, stimulating at the motor point of AbH ensures the targeted depolarisation of its main motor axonal branch, which optimises its isolated activation further (Del Toro & Park,

1996; Choi et al., 2017). Conversely, the medial plantar nerve also innervates the m. flexor hallucis brevis and m. flexor digitorum brevis, therefore the stimulation charge applied during nerve stimulation may have radiated to these muscles resulting in a shared contribution to the twitch contraction recorded. For example, AbH is a fatigue-resistant muscle with a low recruitment threshold (Kelly et al., 2013); in contrast, the flexor hallucis brevis has a relatively high recruitment threshold (Aeles et al., 2020), thus a higher overall intensity would be required if both muscles contribute to the contraction evoked by stimulating at the medial plantar nerve. This inhomogeneity in motor axons with different recruitment thresholds within the medial plantar nerve trunk may have affected the effectiveness for evoking a response in AbH during nerve compared to muscle stimulation.

High frequency reduces the intensity required to determine the MT of AbH. In this study, a stimulation train of five pulses of 1ms duration delivered at 100Hz required a significantly lower current intensity to reach rheobase compared to pulses delivered at lower frequencies (i.e. 10 and 20Hz). This finding concurs with the work of Grosprêtre et al., (2017) who found that the current intensity required to achieve in the triceps surae muscles a contraction level of 20%MIVC in response to a 1ms train (lasting 1s) was lowest when delivered at 100Hz compared to 20Hz and 60Hz. The likely mechanisms for 100Hz requiring lower current intensity for reaching a low level of force in both studies may be due to the force-frequency relationship of skeletal muscle (see section 1.3.1.3; Fig. 1.5C). Briefly, this relationship explains force summation as the result of increased Ca^{2+} released from the sarcoplasmic reticulum available for contraction (Binder-Macleod & Kesar, 2005) due to the higher rate of synchronous recruitment of MUs (Gorgey et al., 2006). Therefore, 100Hz promoted force production by summating the twitch force evoked by each pulse within the 5-pulse train.

In summary, this study found that trains of wide pulses delivered at high (100Hz) frequency to AbH via direct muscle stimulation require the lowest current intensity to reach the MT and achieve a recordable twitch contraction. The identified optimal chronaxie was found to be 1.15ms, which confirms the effectiveness of wide (1ms) pulses for promoting force contraction at low intensities shown in previous studies. Taken together, this set of stimulation parameters optimises the MT determination protocol to maintain the intensity low for comfort and to promote force production in AbH. This protocol will be used in the subsequent studies for an individualised and efficient MT determination. Furthermore, the findings of the optimal pulse duration, as well as the mode of stimulation, constitute part of the NMES protocol for an effective and tolerable targeted training of AbH.

Link to next chapter

This chapter has revealed that targeted NMES should be applied to AbH via muscle and using 1ms pulses. The frequency at which these pulses are delivered determines the force that is produced according to the force-frequency relationship (Edwards et al., 1977), where high frequency stimulation can be used to maximise force production and develop an effective NMES paradigm (Maffiuletti, 2010; Bergquist et al., 2011b). However, the fatigability associated with high frequency NMES is a limitation to its application, as the force produced decays rapidly (Jones et al., 1979; see section 1.3.1.3). In addition, the duration of NMES trains delivered also play a role in force maintenance and fatigue (Boom et al., 1993; Taylor et al., 2018). Therefore, the following chapter will compare different frequency patterns and train durations in order to optimise force production and minimise fatigability.

4.0 Optimising the stimulation frequency and train duration to maximise force production for an NMES training paradigm

4.1 Introduction

The level of force produced by the NMES-evoked contraction is considered the main determinant for muscle training effectiveness (Maffiuletti et al., 2018), and therefore force production should be maximised when selecting the pulse frequency for a strengthening intervention. When sustained high frequency NMES (i.e. 60-100Hz) is delivered in combination with pulses of 1 ms duration and low current intensity, facilitated recruitment of MUs via central nervous system pathways is observed (Collins, 2007; Bergquist et al., 2011b). Although the exact mechanisms responsible for this central contribution remain unclear (Collins, 2007), MN intrinsic mechanisms have been associated to this augmented force, namely the activation of persistent inward currents (Collins et al., 2001; 2002), synaptic PTP (Dean et al., 2007) and temporal summation of subthreshold excitatory postsynaptic potentials of Ia fibres (Dideriksen et al., 2015). The beneficial implication of engaging central mechanisms for force production is the recruitment of MUs in a more physiological manner (Bergquist et al., 2011b), however a rapid decay of force is a characteristic of using high frequency stimulation (see section 1.3.1.3) when applied to muscle (Gorgey et al., 2009; Wegrzyk et al., 2015a; Grospretre et al., 2017). This has been linked to increased metabolic demand (Gorgey et al., 2009), compromised neuromuscular transmission (Jones et al., 1979), axonal hyperpolarisation, and presynaptic inhibition (Martin et al., 2016; Grospretre et al., 2017; 2018). Accordingly, since fatigue or metabolic stress are not prerequisites for inducing strength gains (Folland et al., 2002; Gomes et al., 2019), this rapid fatigability provoked using high frequency NMES limits its utility in training muscle

In order to match the physiological discharging rate of MUs, NMES has conventionally been applied using low frequencies (20-40Hz) to produce fused forces and reduce

muscle fatigability (Fuglevand & Keen, 2003; Gorgey et al., 2009; Bergquist et al., 2011b). In contrast to high frequency stimulation however, low frequency NMES activates MUs mainly via direct recruitment of superficial motor axons (Collins, 2007) and it relies on higher stimulus intensity to evoke the same level of force achieved by high frequency stimulation (da Silva et al., 2015; Grospretre et al., 2018). Additionally, low frequency NMES may be less efficient in evoking anabolic processes to foster muscle hypertrophy (Mettler et al., 2018). In a compromise to optimise force production whilst keeping the intensity low to minimise discomfort, and avoid any presynaptic inhibition induced by the combination of high intensity and high frequency (Dideriksen et al., 2015), an alternating frequency approach (ALT) can be used. Indeed, by interspersing high frequency NMES bursts within a continuous low frequency train (e.g. 20-100-20Hz), the force enhancement from the high frequency stimulus is maintained by the consecutive low frequency stimulus (Collins et al., 2001; 2002; Dean et al., 2007 Lagerquist et al., 2009; James et al., 2018). This is due to an increased Ca^{2+} sensitivity (Frigon et al., 2011; Cheng et al., 2017) along with the abovementioned central mechanisms related to high frequency NMES (Dean et al., 2007; Lagerquist et al., 2009). As a result, alternating NMES can progressively produce higher force within a stimulation train (Lagerquist et al., 2009), which is further maximised when the stimulating trains are sustained over several seconds (Dean et al., 2007; Bergquist et al., 2011a).

In addition to frequency, the total number of pulses delivered to muscle in an NMES train will also affect the sustainment of force during NMES (Mettler & Griffin, 2010; Mettler et al. 2018). This would suggest that longer train durations consisting of high frequency pulses would increase the effectiveness of force production during stimulation. However, stimulation trains of medium duration (e.g. 10s) of high frequency pulses delivered repetitively show the force output decaying within and between contractions (Gorgey et al., 2008) due to fatigue of the activated MU pool (Binder-Macleod et al., 1995; Gorgey et al., 2008). Additionally, shorter 100Hz trains with >20 pulses (e.g. 6s) are not

necessarily more effective in preventing MU hyperpolarisation and consequent force decay (Dideriksen et al., 2015; Martin et al., 2016; Grospretre et al., 2017; 2018; Luu et al., 2021). Nevertheless, the fatigue that ensues during or following NMES application can also be the result of low frequency fatigue, which is not frequency dependent (Jones, 1996; Russ & Binder-Macleod, 1999).

Low frequency fatigue is a phenomenon in which the reduction in force persists long after cessation of contraction and represents a major limitation to NMES application (see 2.3.1.3) (Jones, 1996; Keeton & Binder-MacLeod, 2006). Given its impact on muscle performance, NMES frequency and train duration combination can be optimised by monitoring low frequency fatigue occurrence. A low-to-high frequency ratio between the force evoked by paired stimuli at 10Hz and 100Hz has been previously computed as a fatigue index ($F_{paired10/100Hz}$) to detect low frequency fatigue when this ratio decreases (Yan et al., 1993; Verges et al., 2009).

Therefore the purpose of this study was to identify an NMES pattern of pulse frequency and train duration that promotes high AbH force production, counteracts rapid fatigue and minimises discomfort. To achieve this, NMES was delivered at three frequency patterns (low, high and alternating) and three train durations (short, medium and long).

4.2 Methods

4.2.1 Participants

Fifteen healthy volunteers (12M/3F, mean ± SD: 24.3±5.7 years, 76.3±14.9 kg, 1.7±0.1 m) provided written informed consent to participate in the study that had received prior local ethical approval (SAS1807) and was compliant with the Declaration of Helsinki (2013). Prior to participation all volunteers completed a health screen questionnaire and

reported good health and absence of lower extremity injuries, underlying pathologies and neurological problems.

4.2.2 Experimental procedure

Participants visited the laboratory on four different occasions: once for familiarisation with the testing procedures, and then for three main sessions. During the familiarisation, the motor point and the MT of AbH were identified (see sections 2.2.1 and 2.2.2, respectively) with the participant seated with the ankle at 35° of plantar flexion and the hallux suspended from a uniaxial force transducer (range: 0-250N; RDP Electronics Ltd., UK) at 10° of dorsal flexion (see section 2.3.2). Three 6s-trains of wide pulses (1ms), low intensity (150% MT) direct muscle electrical stimulation were delivered at 20Hz, 100Hz and alternating (20-100-20Hz) frequency to the motor point of AbH to habituate the participants to the stimulation patterns used in the study.

The motor point and MT were verified at the beginning of each main session (see section 2.2.1 and 2.2.2, respectively). In the session investigating NMES with 20Hz pulse frequency, the MT was identified using trains of 5-pulses delivered at 20Hz. The optimal point for medial plantar nerve stimulation and the supramaximal current, equivalent to 130% of the intensity producing the maximal compound muscle action potential (M_{max130}), were identified using surface electromyography (see sections 2.4.1 and 2.4.2, respectively). During each main session, five NMES trains interspersed with a 45s rest period (James et al., 2018) were delivered to AbH at one of the three pulse frequencies: continuous 20Hz or 100Hz, or alternating 20-100-20Hz (2s each). Three different train durations were investigated, short (6s; Martin et al., 2016), medium (10s; da Silva et al., 2015), and long (22s; Neyroud et al., 2014; Wegrzyk et al., 2015ab), for each frequency pattern within the same session, with at least 5 minutes periods in between. The order

of the frequency pattern, as well as the train durations tested within the session, were randomised to eliminate any potential order effect.

Before (PRE) and immediately following (POST) each protocol, three single pulse, three low frequency (10Hz) and three high frequency (100Hz) paired stimuli were delivered to the medial plantar nerve at M_{max130} (Verges et al., 2009) (Fig. 4.1). A rest period of at least 20s separated each stimulus and the order of delivery was always in the sequence as described to avoid possible potentiation following the high frequency paired stimuli and to reduce habituation.

4.2.3 Data analysis

The parameters of the M_{max130} and corresponding twitch force evoked by the single pulses were recorded to assess AbH peripheral excitability and muscle contractility, respectively. Specifically, M_{max130} latency (ms), amplitude (mV) and terminal phase area (mV•ms) were measured (see section 2.4.3.1) for excitability assessment. The peak twitch force amplitude (N) and half relaxation time (ms) were measured (see section 2.4.3.2) for contractility assessment.

The peak twitch force evoked by the 10Hz and 100Hz paired stimuli were measured to compute the $F_{paired10/100Hz}$ as a fatigue index (see section 2.4.3.2). The amplitude of the twitch force evoked by the second pulse of the paired stimuli at 100Hz ($T2_{100Hz}$) was calculated (see Fig. 2.7 D from General Methods) for assessing PTP following NMES (see section 2.4.3.2).

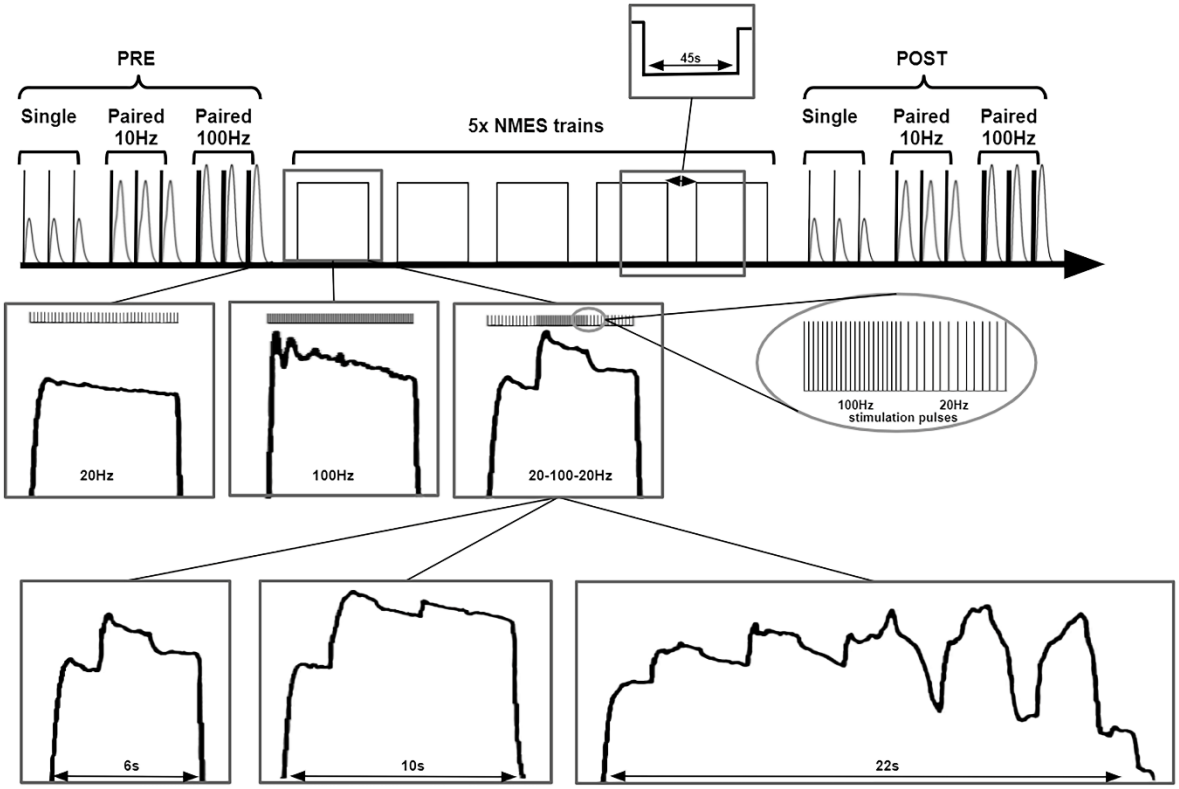

Figure 4.1. Experimental design: five NMES trains at 20Hz, 100Hz or alternating (20-100-20Hz) frequency were delivered using trains with a duration of 6, 10 or 22s. The NMES trains were with 45s rest periods between trains and delivered at an intensity of 150%MT to AbH. Single and paired (10Hz and 100Hz) pulses were delivered before (PRE) and immediately after (POST) via peripheral nerve stimulation at M_{max130} to assess peripheral nerve excitability and contractility of AbH and for the assessment of fatigue and PTP, respectively, in response to NMES.

4.2.4 Statistics

Individual values (*n*=15) for the terminal phase area derived from the M_{max130} were normally distributed (Shapiro-Wilk, SPSS v.21, IBM, USA), whilst the M_{max130} latency and amplitude values reached normal distribution following log transformation. The values

for the twitch half relaxation time and the $F_{paired10/100Hz}$ and $T2_{100Hz}$ derived from the paired stimuli were all normally distributed. The peak twitch amplitude was normally distributed following log transformation. Therefore, a three-factor repeated measures ANOVA was performed on each outcome measure to test for significant main and interaction effects of time (PRE vs POST), frequency (20Hz vs 100Hz vs alternating) or train duration (6s vs 10s vs 22s). Significance was accepted when $p \leq 0.05$. For each pulse frequency, the main and interaction effects of time (PRE and POST) and train duration (6s, 10s, and 22s) were analysed via a two-way repeated measures ANOVA. Significant effects were assessed by post-hoc pairwise comparisons. Statistical significance was adjusted to $p \leq 0.017$ to account for the multiple comparisons (alpha value/number of pairwise comparisons).

4.3 Results

The population average (*n*=15; ±SD) NMES current intensity delivered to participants for muscle stimulation and M_{max130} for the testing measures were similar between days. Specifically, the current intensity delivered to AbH at 150% MT for each session was 4.6±1.7mA for 20Hz, 4.7±1.8mA for 100Hz and 4.6±1.3mA for alternating frequency. The average current intensity used to achieve M_{max130} in each testing session was 23±7.8mA for 20Hz, 22.1±5.2mA for 100Hz and 22.7±5.7mA for alternating frequency. The current intensity used for delivering the stimulation trains and the M_{max130} and corresponding twitch force were therefore similar between days and between pulse frequencies investigated. In addition, there was no significant main condition effect for frequency ($p>0.05$) or train duration ($p>0.05$) for any of the parameters measured, which confirms non-different between-day measurements.

A significant main time effect (POST vs PRE; $p=0.043$; $\eta^2=0.261$) was found for $F_{paired10/100Hz}$, but this effect was abated in post-hoc analyses ($p>0.05$; Table 4.1).

Similarly, there were no significant time effects ($p>0.05$) of pulse frequency or train duration on any of the parameters derived from M_{max130} and the corresponding evoked twitch force (Table 4.1). However, $T2_{100Hz}$ amplitude showed a significant main time effect ($p=0.005$; $\eta^2=0.441$), where PTP was measured at POST. Post-hoc pairwise comparisons showed that there was no time effect for 20 or 100Hz, but a significant time effect for alternating frequency ($p=0.003$; $\eta^2=0.486$) was found. Specifically, a significant increase of $T2_{100Hz}$ (12.4±15.8%; $p=0.012$) was found for alternating frequency at trains lasting 22s (Table 4.1).

Table 4.1. Population average (mean ± SD, n = 15) values of the parameters measured for each frequency (20Hz, 100Hz, alternating) and train duration (6, 10, 22s). The relative change (%) from POST to PRE values are also expressed. TP: terminal phase area; pTw: peak twitch force amplitude; HRT: half relaxation time; $T2_{100Hz}$: force amplitude corresponding to the second stimulus from the paired stimuli at 100Hz.

	20Hz						**100Hz**						**Alternating (20-100-20Hz)**					
	6s		**10s**		**22s**		**6s**		**10s**		**22s**		**6s**		**10s**		**22s**	
	PRE	**POST**	**PRE**	**POST**	**PRE**	**POST**	**PRE**	**POST**	**PRE**	**POST**	**PRE**	**POST**	**PRE**	**POST**	**PRE**	**POST**	**PRE**	**POST**
Latency (ms)	7.3 (0.5)	7.3 (0.5)	7.3 (0.5)	7.3 (0.5)	7.2 (0.6)	7.2 (0.6)	7.3 (1.1)	7.3 (1.0)	7.2 (0.7)	7.3 (0.9)	7.1 (0.9)	7.1 (0.9)	7.2 (1.0)	7.2 (1.0)	7.1 (0.9)	7.1 (0.9)	7.2 (0.9)	7.2 (0.9)
Amplitude (mV)	6.7 (5.1)	6.6 (4.9)	6.8 (5.4)	6.9 (5.1)	6.7 (5.0)	6.7 (4.9)	6.3 (4.5)	6.3 (4.5)	6.1 (4.6)	6.1 (4.4)	6.8 (4.4)	6.3 (4.4)	6.7 (4.6)	6.8 (4.6)	6.6 (4.6)	6.5 (4.6)	6.9 (4.6)	6.7 (4.7)
TP (mV•ms)	9.3 (4.6)	9.0 (4.4)	9.3 (4.7)	9.2 (4.4)	9.4 (4.4)	9.2 (4.0)	8.7 (3.9)	8.8 (3.7)	9.1 (4.0)	9.3 (4.3)	9.9 (4.3)	9.2 (4.4)	9.4 (4.2)	9.4 (4.1)	9.3 (4.3)	9.0 (4.1)	9.8 (4.4)	9.4 (4.3)
pTw (N)	7.1 (2.6)	7.1 (2.7)	7.6 (2.8)	7.6 (2.5)	7.5 (2.7)	7.6 (2.8)	6.8 (2.5)	6.6 (2.6)	7.0 (2.7)	6.9 (2.9)	6.6 (2.2)	6.5 (2.4)	7.0 (3.8)	6.8 (3.8)	7.0 (3.8)	6.8 (3.8)	6.4 (2.5)	6.3 (2.4)
HRT (ms)	88.3 (25.1)	88.1 (21.7)	90.4 (22.4)	84.7 (19.3)	90.1 (20.6)	90.5 (21.4)	90.6 (20.5)	88.6 (20.9)	91.6 (29.1)	89.1 (24.3)	88.3 (21.4)	85.0 (22.2)	92.7 (24.8)	88.6 (24.9)	89.0 (25.1)	90.5 (26.0)	93.2 (27.1)	90.2 (22.6)
$F_{paired10/100}$	0.83 (0.07)	0.83 (0.07)	0.82 (0.06)	0.80 (0.09)	0.81 (0.08)	0.80 (0.10)	0.79 (0.09)	0.79 (0.11)	0.80 (0.09)	0.78 (0.11)	0.79 (0.07)	0.78 (0.07)	0.80 (0.10)	0.79 (0.09)	0.79 (0.08)	0.79 (0.08)	0.79 (0.11)	0.77 (0.10)
$T2_{100Hz}$ (N)	7.7 (2.8)	8.0 (3.0)	8.2 (3.0)	8.3 (3.2)	8.7 (3.6)	8.6 (3.4)	7.6 (2.1)	7.7 (2.0)	7.9 (3.2)	8.1 (3.0)	7.3 (1.7)	7.7 (1.8)	7.5 (3.1)	8.2 (3.2)	7.7 (2.7)	7.9 (2.8)	6.9 (2.0)	7.8 (2.4)

4.4 Discussion

This study aimed to identify a pulse frequency pattern and train duration combination that maximises NMES evoked force and minimises low frequency fatigue occurrence. The findings indicate that: i) five 22s trains of NMES delivered at alternating frequency resulted in a significant PTP of force as measured by $T2_{100Hz}$; and, ii) the peripheral excitability and contractility of AbH, as well as the $F_{paired10/100Hz}$ index, were unchanged following NMES irrespective of the different frequency and train duration combinations used. These measurements were also not significantly different between frequency patterns (100Hz vs 20Hz vs alternating) or train durations (6s vs 10s vs 22s). These findings indicate that there was no evidence of fatigue following the five trains delivered, and that post-tetanic-potentiation of the force depended on the frequency and train duration, with only the alternating frequency pattern and longest trains resulting in an increase of $T2_{100Hz.}$

The peripheral excitability and contractility of AbH were unaffected by the neuromuscular patterns investigated in this study. Since no significant changes in time or between frequency and train duration combinations were found for the parameters (latency, amplitude and terminal phase area) derived from the M_{max130} (Table 4.1.), the integrity of the mechanism for propagation of the potential along the nerve to the muscle (Na^+-K^+ transport across the sarcolemma and T tubules; see section 2.4.3.1) remained stable. Similarly, the parameters derived from the corresponding twitch force (i.e. pTw and HRT; Table 4.1.) to assess contractility (Ca^{2+} uptake kinetics and cross-bridge interaction; see section 2.4.3.2) in response to a single pulse stimulation were intact following the NMES trains delivered. Nevertheless, these measures do not reflect the entire effect of the NMES exposure on post-tetanic potentiation or the force-frequency relationship (for low frequency fatigue assessment). Therefore, these aspects were also assessed by calculating the $T2_{100Hz}$ and $F_{paired10/100Hz}$ index, respectively.

Low frequency fatigue results in a prolonged reduction in the force production underpinned by an impaired muscle excitability, reduced release of Ca^{2+} from the sarcoplasmic reticulum and/or decreased Ca^{2+} sensitivity (see section 1.3.1.3) (Keeton & Binder-Macleod, 2006; Allen et al., 2008). The $F_{paired10/100Hz}$ can be used to assess for low-frequency fatigue, which would be indicated by a reduction of the ratio (Verges et al., 2009). The results from this study suggest that low frequency fatigue did not occur following NMES at any of the frequency and train duration combinations tested. These findings along with the unaltered excitability and contractility of AbH may be explained by the low number of NMES trains delivered as well as other parameters used compared to previous studies. For example, an acute impairment of the peripheral excitability and contractility was induced in AbH, whereby the M_{max130} terminal phase area was increased, and the HRT of the twitch force lengthened, following twenty-four trains (15s) of NMES at alternating frequency (James et al., 2018). Similarly, decreased single pulse force was found in the triceps surae muscles following twenty trains (20s) delivered at high (100Hz; 1ms) or low (25Hz; 0.05ms) frequencies (Neyroud et al., 2014). A reduction in the $F_{paired10/100Hz}$ (by 12%) has also been observed following forty trains (6s) delivered at 100Hz (0.4ms) to the knee extensors (Foure et al., 2014). Since no low frequency fatigue was found in this study, no discrimination between the frequencies or train durations can be made based on the fatigue index or the excitability and contractility parameters measured.

In addition to fatigue, the possible occurrence of PTP was also assessed in this study by measuring the peak twitch force from single stimulation and the $T2_{100Hz}$. PTP at the muscle level (i.e. peripheral PTP; Baldwin et al., 2006) represents a transient increase in force production due to changes in the contractile function that occur following an electrically-evoked contraction (Sale et al., 2002). Specifically, this potentiation in force may occur as a result of increased myoplasmic $[Ca^{2+}]$ and myofibrillar Ca^{2+}-sensitivity, which increases the likelihood of actin-myosin interaction during consecutive pulses

(O'Leary et al., 1997; Allen et al., 2008; Frigon et al., 2011; Cheng et al., 2017). In this study however, no force potentiation was found in pTw following NMES at any frequency and train duration combination tested. In contrast, the force contribution of $T2_{100Hz}$ was found to increase significantly following 22s NMES trains at alternating frequency. The $T2_{100Hz}$ reflects the additional Ca^{2+} released from the sarcoplasmic reticulum into the myoplasm in response to the second pulse of a paired stimuli, and the concomitant prolongation of myoplasmic [Ca^{2+}] available for contraction (Cheng et al., 2013; Bakker et al., 2017). Since these mechanisms are affected by the previous activation history of muscle (Binder-Macleod & Kesar, 2005; Allen et al., 2008), $T2_{100Hz}$ can be used to indicate a possible PTP occurrence (Baudry et al., 2005). Indeed, an increased $T2_{100Hz}$ was previously found following 6s of MIVC in young adults (Baudry et al., 2005). Therefore, the findings of the present study suggest that the alternating frequency pattern potentially engages the Ca^{2+}-dependent mechanisms for force potentiation more efficiently than its constant frequency counterparts, perhaps due to the combination of low frequencies that are able to sustain the force produced following the 100Hz burst (Cheng et al., 2013; Frigon et al., 2011; Cheng et al., 2017) and preventing fatigue.

The long stimulation duration may have also influenced the level of the possible PTP occurring in AbH after alternating NMES. A 22s NMES train may enhance force potentiation due to its higher number of pulses compared to 6s or 10s, which may have increased the overall Ca^{2+} available for cross-bridge formation, and the potentiation effect may have been maintained by alternating Ca^{2+} saturation levels between high and low frequencies (Mettler & Griffin, 2010). This is, the saturation in Ca^{2+} achieved during high frequency may have been reduced during the low frequency sections of the alternating frequency pattern allowing for a greater potentiation effect measured by the $T2_{100Hz}$ (Mettler & Griffin, 2010). Given the coexistence of potentiation and fatigue, the findings from this study suggest that alternating NMES may help overcome any fatigue induced by a paradigm with a higher number of trains. Therefore, 22s trains of NMES delivered

at alternating frequency is the optimised candidate for maintaining force production in AbH.

The inclusion of long trains and high-frequencies (i.e. 100Hz) in the delivery of NMES has previously resulted in the “extra-force” phenomenon, increased H-reflex amplitudes, and a residual asynchronous EMG activity (Klakowicz et al., 2006; Baldwin et al., 2006; Bergquist et al., 2011a). As a likely contributor to these phenomena, centrally-sourced PTP has been proposed (Baldwin et al., 2006). It results from an increased likelihood of neurotransmitter release from the presynaptic membrane terminal (potentially due to a residual elevation in presynaptic Ca^{2+}) of MNs induced by the high-frequency stimulation (Zucker & Regehr, 2002). In addition, the repetitive depolarisation of the MN’s membrane can activate persistent inward currents, which can amplify and prolong the depolarisation of the MN and the consequent increased firing of action potentials (Heckman & Enoka, 2012). In combination with the latter MN property, the temporal summation of sub-threshold excitatory post-synaptic potentials evoked using pulses that have an inter-stimulus interval shorter than their duration (high-frequency) also contributes to the responses recorded after high frequency NMES (Dideriksen et al., 2015). The activation of persistent inward currents occurs after multiple seconds of stimulation (Dean et al., 2007; Bergquist et al., 2011a), whereas the temporal summation of excitatory post-synaptic potentials can occur after just two pulses at 100Hz (Dideriksen et al., 2015). However, since the “extra-force” phenomenon, H-reflex amplitudes, and asynchronous EMG activity were not measured in this study, the contribution of the centrally-sourced PTP to the results from this study could not be verified.

Link to next chapter

This study has shown that the alternating frequency in combination with trains of long duration may induce post-tetanic potentiation more effectively than constant frequencies and shorter train durations. This is an important finding for the development of an NMES paradigm that promotes force production and minimises fatigue, where alternating frequencies (20-100-20Hz) and 22s trains should be used. However, force production is only partly dependent on these parameters, where the intensity used will also influence the overall force produced. Indeed, a dose-response exists where the level of evoked force related to intensity will determine the overall NMES effectiveness to induce strength gains (Maffiuletti, 2010; Fillipovic et al., 2011). Therefore, the next study will investigate the minimal NMES intensity required to foster strength gains to maintain a low level of discomfort.

5.0 Optimising and identifying minimum the training intensity for strengthening benefits from an NMES paradigm

5.1 Introduction

During a voluntary muscle contraction, the central nervous system modulates the force output by means of MU recruitment and discharging rates. In contrast, during an NMES-evoked contraction, the force modulating mechanisms depend upon the stimulus frequency (≥20Hz; Bergquist et al., 2011b) to produce fused contractions, and intensity to maximise the number of MUs being recruited (Bickle et al., 2011; Bergquist et al., 2011b). Accordingly, a proportional relationship between intensity and strength gains exists (Alon & Smith, 2005; Filipovic et al., 2011), where maximally tolerated NMES intensity is recommended (Bickel et al., 2011) and has been used by many studies with

positive results. Indeed, neurological as well as morphological gains have been reported after an extended exposure to NMES using this approach (Gondin et al., 2011). However, the associated participant discomfort with high intensities represents an important consideration for designing an NMES protocol (Bergquist et al., 2011b).

When used for muscle strengthening, NMES intensity is typically expressed as a percentage of the force produced by the target muscle or muscle group during an MVC (Maffiuletti et al., 2018; Natsume et al., 2018). For NMES to be efficacious, an intensity equivalent to 20% MVC and above (see section 1.3.2) promotes strength gains in both healthy (Alon & Smith, 2005; Maffiuletti et al., 2019) and clinical (Talbot et al., 2003; Maddocks et al., 2016) populations. However, this approach for selecting NMES intensity is impractical for AbH because its voluntary activation is a challenge for many individuals due to its complex architecture (see section 1.2.1; Fig. 1.4B) (Arinci Incel et al., 2003; Boon & Harper et al., 2003; Kelly et al., 2013). Instead, an alternative approach, that overcomes these problems, is expressing intensity as a percentage of individual MT (Chapter 3) (James et al., 2013; James et al., 2018). James et al., (2018) demonstrated fatigue-induced adaptations in AbH peripheral neural drive and contractility following a 30-min NMES protocol. The stimulus intensity used was low and equivalent to 150% MT in order to attenuate against antidromic transmission in motor axons (Bergquist et al., 2011b) and minimise discomfort. Voluntary resistance training at a low intensity level has been shown to be as effective as high intensity for strength gains (section 1.3.2) since greater discomfort and fatigue are not prerequisites (Folland et al., 2002; Gomes et al., 2019). However, it is currently unknown how 150% MT relates to the MVC force of AbH, and whether this achieves the 20% MVC training intensity to achieve NMES-induced strength gains.

Therefore, the aim of the present study is to identify a minimum stimulus intensity, when expressed as a percentage of MT, for training AbH via NMES. It is hypothesized that an

intensity equivalent to 150% MT is an acceptable stimulus intensity to be effectively used for NMES strengthening of AbH.

5.2 Methods

5.2.1 Participants

Thirteen healthy volunteers (10M/3F, mean ± standard error of the mean [SEM]: 25.2±1.7 years; 74.0±3.5 kg; 1.7±0.0 m) signed a written informed consent to participate in this study that received prior local ethical approval (SAS1807) and complied with the Declaration of Helsinki (2013). Prior to participation, all volunteers completed a health screen questionnaire and reported good health and absence of lower extremity injuries, underlying pathologies and neurological problems.

5.2.2 Experimental procedure

5.2.2.1 Study design

Participants visited the laboratory on three separate occasions: for familiarisation and for two main testing sessions. The familiarisation session served to acclimate participants to all experimental procedures and to optimise the delivery of NMES to AbH (see below for protocol). In the first main session, the optimisation procedures were repeated for verification purposes, then participants' ability to maximally activate AbH voluntarily was quantified using the interpolated twitch technique. During the second main session and following verification of AbH motor point location and MT (see sections 2.2.1 and 2.2.2, respectively), the force evoked by 7s trains of NMES delivered to AbH at different stimulus intensities was recorded.

In each visit, participants were seated with their left foot securely fixed at the ankle and forefoot and positioned in 35º plantar flexion with respect to foot flat (Goldmann & Brüggemann, 2012), and the Hallux suspended in 10° dorsal flexion (Fig. 2.4). During the familiarisation sessions and the first main trial a uni-axial force transducer (1000Hz sampling frequency, range: 0-250 N; RDP Electronics Ltd, UK), calibrated for measuring low forces and mounted to the experimental apparatus above the foot was used to record the voluntary and interpolated twitch forces (Fig. 2.4). In the second main trial, a tri-axial force transducer (1000Hz sampling frequency, range: 0-50N; Applied Measurements Ltd, UK) was used to account for the abduction force elicited from direct-muscle NMES. The force data was collected through an A/D convertor (1401power, Cambridge Electronic Design Ltd., UK) and imported into Spike2 software (v7.12, CED Ltd., UK) for analysis.

5.2.2.2 Procedures for NMES optimisation

The procedures for optimisation of the direct-muscle NMES delivery involved AbH motor endpoint zone location and MT determination (see sections 2.2.1 and 2.2.2 for protocol, respectively). Once the motor point was identified, trains of 5 x 1ms pulses were delivered to this location at 20Hz pulse frequency and increasing current, starting at 0.5mA with increments of 0.5mA. AbH MT represented the lowest current, which evoked a twitch force that exceeded the baseline force level by 2 standard deviations (as in 2.2.2) (James et al., 2018).

To identify the stimulus intensity capable of recruiting the full range of AbH muscle force, a twitch force recruitment curve in response to single square-wave (1ms) pulses delivered to the motor point at increasing current intensities was constructed (Fig. 5.1A). The stimulation started at 1mA current intensity with 1mA increments until saturation of

the evoked twitch force amplitude was reached. Finally, the recorded current at this point was multiplied by 130% to ensure supramaximal stimulation intensity (James et al., 2018) for the interpolated twitch technique delivery (Allen et al., 1995; Gandevia & McKenzie, 1988).

5.2.2.3 Voluntary activation testing

Participants attempted 3 x ~5s 1MPJ flexion MVCs separated by 5 minutes rest. In each, participants concomitantly attempted abduction of the Hallux in order to fully engage AbH contraction. Upon reaching the force plateau, a supramaximal (130%) 1ms 100Hz doublet stimulus (Gandevia et al., 1996) was delivered over the motor point of AbH (Fig. 5.1B). The additionally evoked twitch force represents the engagement of MUs that have not been activated through voluntary command and therefore are excited by the interpolated stimulus (Shield & Zhou, 2004). Participants were instructed to maintain maximal effort until instructed to relax, following which, a second supramaximal twitch (same stimulus parameters) was evoked 1-2s into rest to take into account the possible potentiation of neural drive to the muscle (Allen et al., 1995). Visual feedback and appropriate encouragement were provided as well as demonstration, instruction and practice trials prior to recording the MVCs (Gandevia, 2001).

5.2.2.4 Sub-maximum evoked (NMES) AbH force testing

7s NMES trains of 1ms pulses were delivered to AbH at 20Hz pulse frequency with increasing current intensity starting at 150% MT with 25% MT increments up to 300% MT (Fig. 5.1C). One minute rest was given between each train to avoid cumulative fatigue. Participant's perceived discomfort was quantified for each NMES intensity with

a 10cm visual analogue scale (VAS), where 0 represents 'no discomfort' and 10 represents 'maximal discomfort' (Maffiuletti et al., 2014).

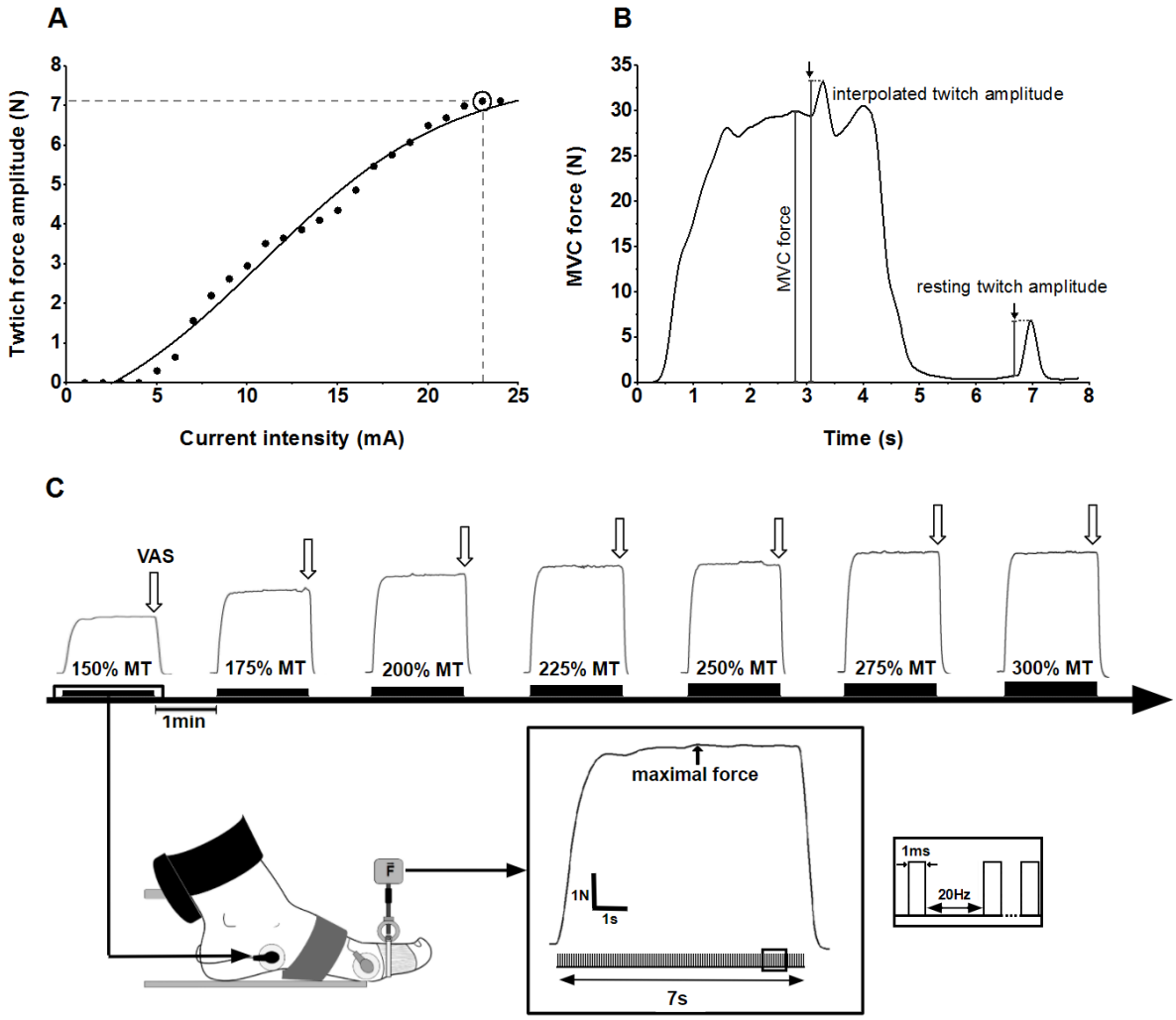

Figure 5.1. Examples of the stimulation protocols used in the study and the respective evoked AbH forces. **A:** Twitch force recruitment curve constructed by gradually increasing stimulus strength to identify the current intensity (mA; vertical dashed line) corresponding to maximal twitch force (circled); **B:** Twitch interpolation evoked by 1ms 100Hz paired pulse stimulation delivered during and following a maximum voluntary 1MPJ flexion contraction with abduction of the Hallux. The arrows indicate the stimulation time points and the vertical lines mark the interpolated, resting and MVC force amplitudes used to calculate the voluntary activation ratio; **C:** NMES-evoked force from 7s 20Hz

trains of 1ms pulses delivered to AbH motor point with stimulus intensities increasing from 150% to 300% of MT. At each intensity, maximum AbH evoked force was recorded (filled vertical arrow) as well as the level of perceived discomfort (VAS; open vertical arrows).

5.2.3 Data analysis

The voluntary activation ratio (VAR) for AbH during each MVC was calculated using the following equation (Allen et al., 1995):

$$VAR = 1 - \left(\frac{interpolated\ twitch\ amplitude - MVC\ force}{resting\ twitch\ amplitude}\right)$$

where the *interpolated twitch amplitude* is the extra force evoked from AbH in response to the supramaximal doublet stimulus during MVC and *MVC force* is the maximal force measured prior to stimulus onset (Fig. 5.1B). The highest VAR and corresponding MVC force achieved out of the 3 attempts from each participant were considered for analysis. Participants were deemed "*able*" to fully activate AbH if their VAR was ≥0.9 (e.g., 90% of full capacity) (Herbert & Gandevia, 1996). Correspondingly, those with a VAR that was <0.9 comprised the "*unable*" group.

The maximum force (N) evoked during each of the 7s NMES trains (Fig. 5.1C) was entered for analysis. In the *able* group (participants with a VAR ≥0.9) the maximum force (N) was normalized (%) to the MVC force from the contraction that produced the highest VAR and then plotted against the respective NMES stimulus intensity (150% to 300% MT). The minimum stimulus intensity required to achieve evoked contractions with a force ≥20%MVC was identified from the minimum value within the range of *able* participant responses at each stimulus intensity.

The mean (±SEM) of NMES current (mA) required at each stimulus intensity was plotted against the evoked force (N) and VAS score to assess the relationship between the stimulus intensity, force production and participants' discomfort, respectively.

5.3 Results

The interpolated twitch technique identified that only 3 participants (23%) in the cohort were able to activate AbH ≥90% of its full capacity (mean VAR (range): 0.93 (0.91 – 0.95); Fig. 5.2A). The average VAR of the remaining 10 participants was 0.69 (0.36 – 0.83). Despite this difference between the groups, the average MVC force was comparable (34.8 (29.8 – 41.2)N vs 31.8 (17.6 – 75.4)N, respectively). However, the higher range recorded in the *unable* group MVC force suggests an alternative force-generating strategy in certain individuals.

In the *able* group, the NMES stimulus intensity needed to achieve a force ≥20% MVC corresponded to 200% MT (Table 5.1, Fig. 5.2B) and this was delivered at an average current intensity of 7.9 (6.0 – 10.8)mA (Fig. 5.2C). The corresponding perceived level of discomfort at this intensity was 3.3 (2 – 5) (Fig. 5.2D).

Table 5.1. Mean (range) NMES-evoked force delivered at increasing stimulus intensities and expressed as a percentage of MVC in *able* participants (VAR ≥0.9; *n*=3).

	NMES stimulus intensity relative to AbH MT						
	150%	**175%**	**200%**	**225%**	**250%**	**275%**	**300%**
% MIVC	14 (4-32)	26 (17-44)	31 (21-45)	38 (26-46)	43 (24-57)	49 (31-66)	54 (38-72)

Despite not being able to activate AbH to its full capacity, the *unable* group produced comparable NMES-evoked forces to the *able* group during the graded NMES protocol (Fig. 5.2C). This was achieved at lower current intensities (Fig. 5.2C), but with a slightly higher pain score (Fig. 5.2D). For example, at 200% MT, the *unable* group generated an average force of 11.8 (2.0 – 27.8)N compared to 11.2 (7.0 – 18.5)N in the *able* group, which was delivered at a current intensity of 6.5 (2.4 – 16.4)mA (compared to 7.9 (6.0 – 10.8)mA) and elicited a VAS of 4.5 (1 – 6.5) (compared to 3.3 (2 – 5)).

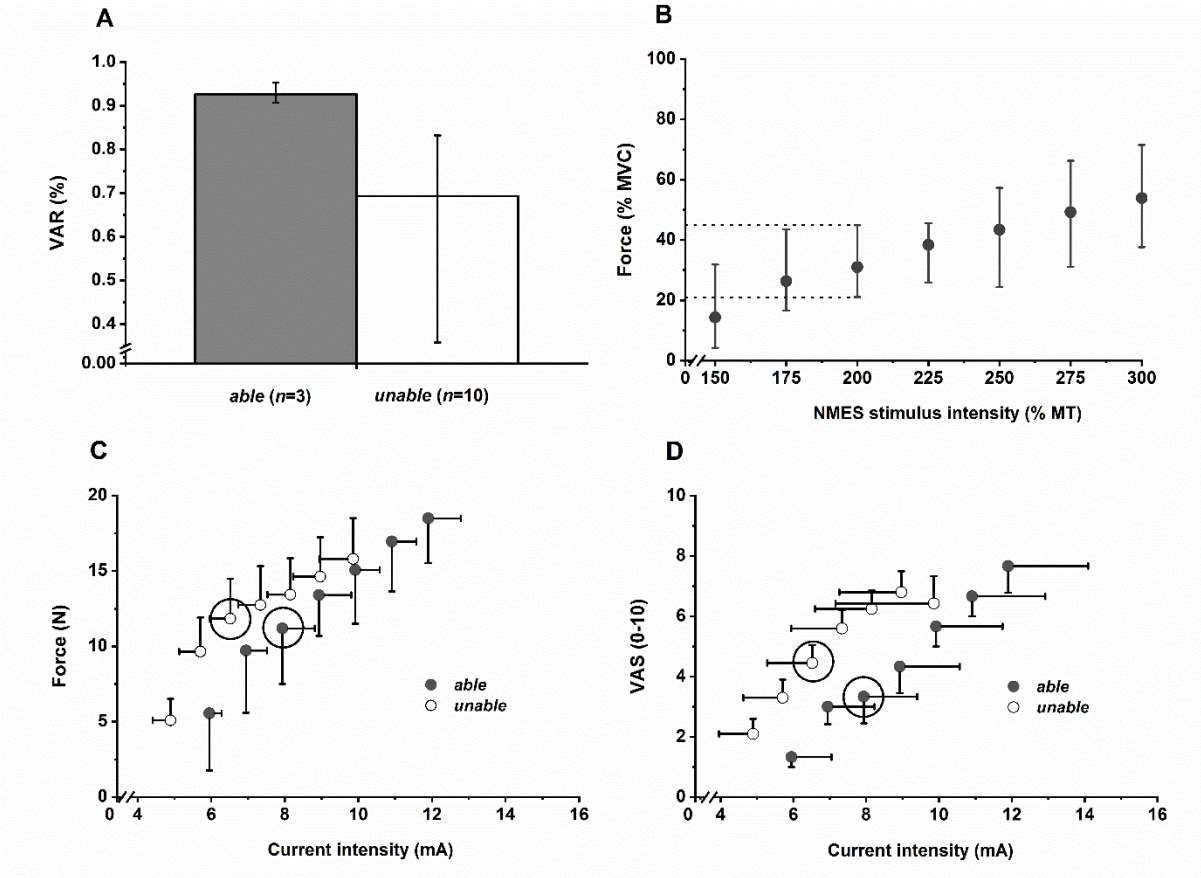

Figure 5.2. A: Mean (range) participant responses for voluntary activation ratio (VAR); **B:** Mean (range) % MVC plotted against NMES stimulus intensity in the *able* group (*n*=3). The dashed horizontal lines illustrate that 200% MT is the minimum stimulus intensity required to evoke forces ≥20% MVC; **C:** Mean (±SEM) NMES-evoked force (N) plotted against mean (±SEM) current intensity (mA) in *able* (filled circles) and *unable* participants (*n*=10; unfilled circles); **D:** Mean (±SEM) perceived level of discomfort (visual analogue

scale; VAS) plotted against mean (±SEM) current intensity (mA) in *able* and *unable* participants. The current intensity corresponding to 200% MT is circled in Figures C and D.

5.4 Discussion

The aim of this study was to identify a minimum stimulation intensity for NMES training of AbH based on its maximum isometric force generating capacity. Using the twitch interpolation technique and a cohort of healthy individuals this study demonstrated that: (i) a small proportion (23%) of the participants were able to activate AbH to near full capacity as ascertained by achieving a high voluntary activation ratio (≥0.9) during maximum 1MPJ flexion contraction with abduction; ii) a current of twice (200%) the AbH MT has the potential to activate the muscle to a sufficient level for promoting strength gains via NMES training; this finding rejects the experimental hypothesis posed; (iii) NMES at this stimulus intensity causes low-to-medium discomfort level; and (iv) NMES is applicable independently on the individual's ability to voluntarily activate AbH muscle.

Training via evoked muscle contractions is different to voluntary activation of muscle because MU discharge patterns are non-selective and spatially fixed (Bickel et al., 2011). Despite this, previous research has showed the use of NMES for muscle strengthening benefits at intensities which evoke muscle contractions of ≥20% MVC (section 1.3.2) (Alon & Smith, 2005; Maddocks et al., 2016; Maffiuletti et al., 2019; Talbot et al., 2003). Indeed, a chronic period (~8 weeks) of high-intensity NMES training (~80% MVC) of the quadriceps has been shown to result in strength gains via transitions in the myosin heavy chain isoforms in both active and sedentary individuals (Gondin et al., 2011). Similarly, NMES training of quadriceps at lower stimulus intensities, but above the recommended training level (~30-60% MVC), proved sufficient to induce beneficial adaptations in

muscle morphology and concomitant strength gains (Natsume et al., 2018), whereas NMES training at 5-10% MVC (in the same muscle) was not (Natsume et al., 2015). In the present study, the NMES current intensity at which all *able* participants exceeded the 20% MVC threshold was 200% MT (mean: 31% MVC; range: 21-45% MVC) and this was achieved with low-to-mild discomfort (Fig. 5.3D; circles). In previous work applying NMES to AbH a lower dose was adopted, equivalent to 150% MT (James et al., 2013; James et al., 2018) and observed peripheral excitability (M_{max130}) and contractile (twitch force) adaptations indicative of fatigue following an acute exposure to an NMES paradigm (James et al., 2018). The present study findings suggest that the potential for training AbH at 150% MT for strength gains, with regular exposure, may be reduced for certain individuals. Indeed, two of the three *able* participants in the present study only managed to voluntary activate AbH to 4% and 7% MVC at 150% MT (mean: 14% MVC; range: 4 - 32% MVC; Table 5.1), implying that this NMES stimulus intensity would be insufficient to cause meaningful muscle strengthening.

Training muscle at a low intensity of electrical stimulation can enhance the central contribution to force production (Bergquist et al., 2011b; Collins, 2007). Training muscle at low intensity NMES and combining wide pulse widths (1ms) takes advantage of the rheobase of sensory muscle afferents and minimises the potential for antidromic transmission of the stimulus in the motor axon, which would otherwise cancel the signal emanating from sensory pathways. If these electrical pulses are delivered in sequences of low and high frequency trains (Baldwin et al., 2006; James et al., 2013; James et al., 2018), the potential to increase force production is enhanced as a result of the effective current delivered to MNs and resulting post-tetanic potentiation of synaptic drive to the muscle (Baldwin et al., 2006; Bergquist et al., 2011b; Collins, 2007). Thus, NMES training of AbH at the minimum suggested threshold for strength gains (20% MVC; Alon & Smith, 2005; Maddocks et al., 2016; Maffiuletti et al., 2019; Talbot et al., 2003) may not only be effective but is also tolerable, which suggests a potential clinical utility for this approach

to alleviate or combat common foot pathologies in which the integrity of AbH is impaired, such as Hallux Valgus (Nix et al., 2010).

The finding that a large proportion of participants, or 77% of the present study cohort, were unable to voluntary activate AbH to at least 90% of its maximal force generating capacity was not surprising. This finding is consistent with the study performed by Arinci Incel et al. (2003), who found in 70% (*n*=14) of their healthy cohort that MU action potentials during AbH voluntary contraction were contaminated with cross-talk from the synergistic flexor hallucis brevis muscle. Boon & Harper (2003) also noted that ~19% of their cohort were in fact unable to voluntarily activate AbH. The cause of this inability is uncertain and can be perhaps due to one or more factors. Potentially, there may be an insufficiency in the central drive to fully activate AbH. Decreased synaptic transmission of the supraspinal input to the muscle via spinal MNs is another possibility, and finally, there may be a deficit in the muscle's ability to convert the excitatory input into an effective contraction. This latter point is particularly noteworthy since AbH has a complex morphology with differing architectural arrangements (unipennate, bipennate and multipennate) within distinctive segments along its length (see 1.2.1.1; Fig. 1.4B) (Tosovic et al., 2012). There is also considerable morphological variability between individuals within each of the segments. Indeed, Tosovic et al. (2012) noted in a small cohort of cadaveric specimens that ~11% were missing the typical multipennate arrangement at the proximal segment of the muscle and went on to show that this segment of AbH had the largest physiological cross-sectional area (~520mm^2) of all 14 muscle segments investigated from four intrinsic foot muscles. An absence of this predominant force generating segment of the muscle may have an impact on the magnitude of the force produced by some participants when attempting to activate AbH to its full capacity.

Importantly, it is likely that neural factors due to AbH morphological specificity can explain the large number of *unable* participants in the present study. A feature of muscles with broad origins and distinctive segments, such as AbH, is the selective recruitment of MNs to fine-tune a movement and control the differentiated lines of force within the differing segments (functional differentiation) (Paton & Brown, 1994; Tosovic et al., 2012). Evidence for this non-uniform activation of motor units is also found in the pectoralis major (Paton & Brown,1994) and trapezius (Falla & Farina, 2008), where their distinct segments are selectively activated to match the force required for a given task. For example, the upper segments of the pectoralis major are preferentially activated during forward flexion of the shoulder whilst inferior segments are preferred for forward extension (Paton & Brown, 1994). Furthermore, different motor unit behaviour (recruitment and firing rate) available to control force has also been found to be muscle segment dependent (Falla & Farina, 2008). Indeed, motor units from the upper segments (multipennate architecture) of the trapezius were found to be preferentially recruited during sustained shoulder abduction, whilst the lower segments relied on discharge rate. Additional motor units are recruited in the upper segments to compensate for decreased discharging rates within the lower segments to maintain the force level over time (Falla & Farina, 2008).

Accordingly, in AbH, the proximal multipennate segment will be characterised by distinct populations of MUs to perform 1MPJ flexion and abduction of the Hallux independently of each other, and activating AbH to its full capacity would require the recruitment in synchrony of both of these pools of MUs as well as of those from other distal segments. Thus, the instruction to participants during data collection was to perform Hallux abduction concomitant to maximum 1MPJ flexion by encouraging them to displace a small ball of plasticine, placed on the dorsal aspect of 1MPJ, away from the digits during the MVC. A number of participants could not achieve this voluntarily; therefore, one can

speculate that the supraspinal drive of others was insufficient or inefficient to innervate the abduction MU pool for full activation of AbH.

Despite the inability to perform the contraction as instructed, the *unable* participants still exerted a comparable MVC to the *able* participants (31.8N vs 34.8N, respectively). Since VAR confirmed that AbH activation capacity had not been reached in the *unable* group, it is likely that they performed the instructed movement with greater activation of the prime Hallux flexor intrinsic (i.e. flexor hallucis brevis) and extrinsic (i.e. flexor hallucis longus) muscles (Arinci Incel et al., 2003; Bruening et al., 2019; Gooding et al., 2016; Yamauchi & Koyama, 2019b). The inability to voluntary activate AbH to its full capacity may have functional consequences. More specifically, an inability to produce abduction force compromises 1MPJ stability during the propulsion phase of gait, which in turn will lower forefoot stiffness and place a greater demand on more proximal joints for propulsive power (Farris et al., 2019). Hence, the benefit of training AbH to produce a mechanically correct movement of the Hallux, which is possible with NMES-evoked contractions, seems intuitive not only for the pathological foot but also for healthy individuals to ensure appropriate forefoot loading during gait. Indeed, direct-muscle NMES evoked comparable (absolute) force generation in all participants in this study independently of their ability to fully activate AbH by will (Fig. 5.3C); and this was achieved with a stimulation intensity causing relatively low discomfort. This finding implies that the peripheral contractility of AbH is intact irrespective of the inability to voluntary contract AbH to its full capacity; therefore, it might be possible to increase the voluntary activation capacity of the muscle with targeted NMES exposure.

This study is not without limitations that need to be acknowledged and considered when interpreting the present findings. Firstly, the small sample size limits the capacity of this study to statistically compare the results between *able* and *unable* groups. However, the results highlight the difficulty to activate this muscle to its full capacity in the healthy

population, which is prevalent and may not necessarily be overcome with a higher number of participants. Secondly, the twitch interpolation technique represents a standard method to assess for voluntary activation that requires its own practical considerations. Namely, the technique has been noted to be less sensitive at high levels of muscle activation (Herbert & Gandevia, 1999) or influenced by changes in the joint-angle configuration (Bampouras et al., 2006). The calculation of VAR also relies on the assumption that full activation capacity is achieved when it equates to 1 (i.e. VAR = 1; de Haan et al., 2009). Additionally, the antidromic potentials evoked by the interpolated twitch stimulus collide with the voluntarily produced potentials that discharge orthodromically, which in turn influences the magnitude of the interpolated twitch force and the voluntary activation measured (Gandevia, 2001). Furthermore, the contribution from other agonistic muscles (i.e. flexor hallucis brevis, flexor hallucis longus) to the MVC force recorded needs to be considered in relation to the implementation of the twitch interpolation technique and when relating this force to the NMES-evoked forces.

The study attempted to overcome these practical considerations by optimising the experimental protocol. Specifically, the use of a conditioning followed by test pulse (doublet) maximises force production due to the recruitment of the motor units which may have been in the refractory period if only one test stimulus were used (Belanger & McComas, 1981; Herbert & Gandevia, 1999). This, in turn, overcomes the antidromic collision and reduces the variability in force produced when using only single pulses (Oskouei et al., 2003). For its part, the sensitivity to joint-angle configuration was addressed by positioning the 1MPJ at 10° of dorsal flexion to optimise force production by AbH (see section 2.3.2). Furthermore, the foot was positioned at 35° of ankle plantar flexion specifically to minimise the contribution to the MVC force from the flexor hallucis longus, since this muscle and other plantar flexors would be at a less favourable condition to produce force due to the force-length relationship (Goldmann & Brüggemann, 2012). Participants were also instructed to perform Hallux abduction

concomitant to the 1MPJ flexion to minimise the activation of the flexor hallucis brevis. However, the contribution of this flexor muscle to the MVC force is likely and difficult to negate, so this limitation should be considered when interpreting the results. Therefore, if one assumes that VAR ~1 (i. e. ~100%) represents full activation capacity, the implementation of the twitch interpolation technique as reported in this study represents a robust method to quantify insufficiencies in AbH activation.

In conclusion, the findings of the present study have shown that a large number of (healthy) participants are unable to activate AbH to its full capacity, which may be due to the complex muscle morphology and/or a neural activation deficit. Despite this, targeted NMES applied directly to AbH can be used to alleviate these deficits and evoke comparable forces in all individuals, which may have practical implications for both restoring function in the healthy foot and offsetting weakness in the pathological foot. NMES stimulus intensity equivalent to 200% of individual AbH MT has the potential to evoke forces above 20% MVC and may be used to promote muscle strengthening in AbH whilst mitigating discomfort.

Link to next chapter

This study has shown that NMES delivered at 200% MT of AbH evokes forces above 20% MVC, which has the potential to foster the strengthening of AbH. This intensity was found to also be tolerable in those that can and cannot activate AbH voluntarily and therefore this intensity can be used as part of the NMES paradigm. Nevertheless, force production will also rely on the duty-cycle used as the rest intervals between evoked contraction can help minimise the fatigability of NMES application. Therefore, the next study will investigate the NMES duty-cycle required to preserve force production.

6.0 Optimising the duty cycle for enhanced training benefits from an NMES paradigm

6.1 Introduction

NMES is delivered in bursts or trains of pulses interspersed with rest periods of no stimulation. Such cyclic stimulation delivery allows for the relaxation of the muscle fibres between evoked contractions, as any induced ionic imbalance in the Na^{+}-K^{+} pump that affects muscle excitability (Jones et al., 1979; Jones, 1996) is restored. In addition, during this recovery period, the Ca^{2+} is removed from the myoplasm to reduce its concentration, which leads to Ca^{2+}-disassociation from troponin and cross-bridge sliding cessation (Westerbland et al., 1997; Allen et al., 2008). Beyond the muscle membrane, the metabolic substances altered during adenosine triphosphate hydrolysis are replenished and the intracellular acidity resulting from metabolite accumulation return to pre-evoked contraction status (Vanderthommen et al., 2003; Ratkevicius et al., 2004). During fatigue induced by repetitive activation of muscle via NMES training, the aforementioned mechanisms are altered leading to impaired muscle excitability and contractility, and a consequent decline in force production (Allen et al., 2008). Since the level of evoked force is the main stimulus of NMES training efficacy (Maffiuletti et al., 2018), the duty-cycle used can be manipulated to allow sufficient rest time between repetitive contractions in order to minimise fatigue and preserve force production for longer.

The preservation of the evoked force by NMES depends on the duty-cycle used. An NMES duty-cycle is often expressed as a contraction (on) to rest (off) intervals ratio (i.e. on:off), or a percentage of the time when the stimulation is ‘on’ to the sum of ‘on’ and ‘off’ times (Packman-Braun, 1988; Lake, 1992). For example, NMES protocols consisting of 20s of stimulation followed by either 20s (Wegrzyk et al., 2015a) or 90s (Wegrzyk et al., 2015b) of rest represent duty cycles of 1:1 (50%) or 1:4.5 (~18%), respectively. Low

duty-cycles (i.e. longer time off) are found to better preserve force production throughout the NMES protocol compared to high duty-cycles (e.g. 1:5 vs 1:1) (Packman-Braun, 1988; Rankin & Stokes, 1992; Matheson et al., 1997; Holcomb, 2006). Indeed, earlier studies reported that a duty-cycle of 1:1 (5s on, 5s off) failed to sustain a force level above 50% of the initial value within the first 10 minutes of a 30-minute session (Packman-Braun, 1988). The force loss using high NMES duty-cycles is associated with a higher metabolic cost evidenced by an increased adenosine triphosphate production, higher inorganic phosphate to phosphocreatine ratio, and reduced intracellular pH (Matheson et al., 1997), all of which contribute to an inability to contract and generate force (Vanderthommen et al., 2003; Ratkevicius et al., 2004; Allen et al., 2008; Kent-Braun et al., 2012). Conversely, this metabolic cost and the consequent force decay are progressively mitigated when 1:3 (Packman-Braun, 1988) and 1:5 (Packman-Braun, 1988; Matheson et al. 1997) NMES duty-cycles are used instead. Accordingly, in clinical settings and in order to reduce fatigue, minimise discomfort and promote force preservation, NMES is applied using a duty-cycle between 1:3 (Quittan et al., 2001; Doucet et al., 2012) and 1:5 (Talbot et al., 2003; Glaviano & Saliba, 2016). Similarly, significant strength gains are achieved after prolonged exposure to NMES with duty-cycles of 1:3 (6.25s on, 20s off) (Gondin et al., 2005; 2011; Natsume et al., 2018) or 1:5 (4s on, 20s off) (Maffiuletti et al., 2002).

Along with metabolic cost, an impaired excitability and contractility contribute to force decay during NMES. Alterations occurring at the muscle level that reduces excitability and contractility are also associated with fatigue after NMES (Papaiordanidou et al., 2014; James et al., 2018), and the extent of these alterations may also be modulated by the duty-cycle used (Neyroud et al., 2016). Indeed, a recent study by Neyroud et al. (2016) showed that when fatiguing protocols are applied to the adductor pollicis muscle, using a high duty-cycle of 3:1 (3s on, 1s off) produced a significant reduction (~55%) in the evoked force, reduced contractility (~70% reduction in peak twitch force), and

impaired excitability (~65% reduction in M_{wave} amplitude; 7% increase in M_{wave} latency). However, when a lower duty-cycle of 1:2 (1.5s on, 3s off) was used, such reduced preservation of force was minimal or halved (~25% of force produced) with additional induced ischemia (Neyroud et al., 2016). Correspondingly, reduced contractility (~55% in peak twitch force) and excitability (<25% decrease in M_{wave} amplitude) were reported for the latter duty-cycle but to a lower extent. Only one study has reported the effect of an NMES training session on the excitability and contractility of AbH, where a 1:3 (15s on, 45s off) duty-cycle induced an increase in M_{wave} latency and area, and an elongation of half relaxation time of the corresponding evoked twitch force following 24 trains (James et al., 2018). A ~75% reduction in force preservation from the first to the last stimulating train was observed to accompany these peripheral fatigue adaptations (James et al., 2018). Taken together, these findings suggest that although a reduction in the preservation of force is observed in both high and low duty-cycles, the use of longer rest periods can be used to mitigate fatigue.

Therefore, the purpose of this study was to identify the optimal NMES duty-cycle delivered to AbH which minimises fatigue and preserves force production. The hypothesis tested was that a low duty cycle will preserve force generation, minimise muscle fatigue and maintain contraction dynamics.

6.2 Methods

6.2.1 Participants

Eight healthy male volunteers (mean ± standard deviation [SD]: 27.1±8.7 years, 76.8±8.6 kg, 1.8±0.1 m) provided written informed consent to participate in the study that had received prior local ethical approval (SAS1807) and was compliant with the Declaration of Helsinki (2013). Prior to participation all volunteers completed a health screen

questionnaire and reported good health and absence of lower extremity injuries, underlying pathologies and neurological problems.

6.2.2 Experimental procedure

Participants visited the laboratory on two occasions ~7 days apart: once for familiarisation with the testing procedures and once for the main session. During the familiarisation session, the motor point and MT were identified (refer to sections 2.2.1 and 2.2.2, respectively) while participants were seated with the ankle at 35° of plantar flexion and the hallux suspended from a uniaxial force transducer (range: 0-250N; RDP Electronics Ltd., UK) at 10° of dorsal flexion (section 2.3.2). To accustom the participants to the NMES used in the main session, a 6s train of wide pulse (1ms), low intensity (200% MT; see Chapter 5) direct muscle electrical stimulation was delivered at ALT frequency (20-100-20Hz; 2s each; see Chapter 4) to the motor point of AbH.

At the beginning of the main session, the identification of the motor point and MT were verified. Then, the medial plantar nerve was located and the supramaximal intensity for PNS was identified (see section 2.4.1 and 2.4.2). Next, three sets of five x 22s trains of wide pulse (1ms) NMES were delivered to the motor point of AbH at an intensity of 200% MT and ALT frequency. Each set had a different resting period between stimulation trains of either 22s (Wegrzyk et al., 2015a), 44s (James et al., 2018) or 88s (Neyroud et al., 2016; Espeit et al., 2021) corresponding to duty-cycles of 1:1, 1:2 and 1:4, respectively. The sets were delivered at random order across participants to eliminate any potential order effect. A rest period of at least 5 minutes was used between the sets.

Before (PRE) and immediately after (POST) each NMES set, three single pulse stimulations, three low frequency (10Hz) and three high frequency (100Hz) paired stimuli were delivered to the medial plantar nerve at a supramaximal intensity to compute

$F_{paired10/100Hz}$ (Verges et al., 2009) (Fig. 6.1). A rest period of at least 20s separated each individual stimulation and the order of delivery was always in the sequence as described to avoid cumulative force potentiation.

6.2.3 Data analysis

The M_{max130} and corresponding twitch force evoked by the single pulses were recorded to assess AbH peripheral nerve excitability and muscle contractility, respectively. Specifically, the M_{max130} latency (ms), amplitude (mV) and terminal phase area (TP; mV•ms) were measured (see section 2.4.3.1) for excitability assessment. The peak twitch force amplitude (pTw; N) and half relaxation time (HRT; ms) were measured (see section 2.4.3.2) for contractility assessment.

The $F_{paired10/100Hz}$ was computed as the ratio between the peak twitch forces evoked by the 10Hz and 100Hz paired stimuli as a fatigue index (see section 2.4.3.2). In addition, the FTI (N•s) corresponding to the first and fifth NMES trains within a set were calculated and compared to assess for preservation of force production during NMES and between the duty-cycles tested.

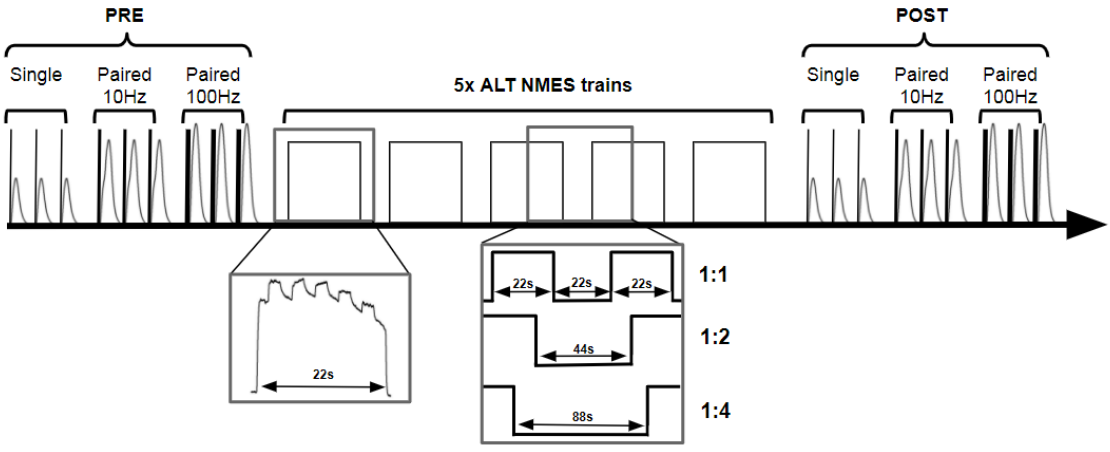

Figure 6.1. Experimental design: three sets of five 22s NMES trains, interspersed with either 22, 44 or 88s rest periods, were delivered to AbH at an ALT frequency (20-100-20Hz; 2s each) and an intensity of 200% MT with a 5min rest period between sets. Single and paired (10Hz and 100Hz) PNS pulses were delivered before (PRE) and immediately after (POST) the NMES set at a supramaximal intensity to assess peripheral AbH muscle excitability, contractility, and fatigue caused by NMES.

6.2.4 Statistics

Each parameter derived from the three M_{max130} and corresponding twitch force evoked by the single pulses, as well as the three peak twitch forces from each of the paired stimuli were pooled for each participant. Individual values (n=8) for the M_{max130} latency (ms) and HRT (ms) were normally distributed (Shapiro-Wilk, SPSS v.21, IBM, USA). In addition, the M_{max130} amplitude (mV), but not the TP (mV•ms), pTw (N) or $F_{paired10/100Hz}$, values were normally distributed following log transformation.

A two-factor repeated measures ANOVA was performed on each outcome measure that was normally distributed for main and interaction effects of duty-cycle (1:1, 1:2, or 1:4) and time (PRE and POST). Significance was accepted when $p \leq 0.05$. For the parameters not normally distributed, non-parametric Wilcoxon sign-rank tests were performed to compare PRE vs POST values for each duty-cycle. Statistical significance was increased to $p \leq 0.017$ to account for multiple comparisons (alpha value/number of pairwise comparisons).

The individual values (n=8) of the FTI corresponding to the first and fifth NMES trains were normally distributed, therefore, a two-factor (duty-cycle condition: 1:1, 1:2, 1:4 vs time: first train, fifth train) repeated measures ANOVA was performed for main effects of condition and time, or a condition x time interaction effect, with inclusion of effect size

(η^2). Post-hoc pairwise comparisons were adjusted with a Bonferroni correction. Significant differences were accepted when p≤0.05.

6.3 Results

The population average (*n*=15; ±SD) NMES current intensity delivered to participants for stimulation of AbH at 200% MT was 3.2±0.9mA, and the supramaximal intensity delivered via PNS to evoke M_{max130} was 19.0±4.6mA.

Significant interaction (p<0.05; η^2=0.35) and main effects for duty-cycle condition (p<0.05; η^2=0.47) and time (p<0.001; η^2=0.92) were found for the FTI data. Bonferroni-adjusted post-hoc pairwise comparisons indicated that the FTI was significantly reduced (p≤0.001; Fig. 6.2 A) from the first to the fifth NMES train (Fig. 6.2B) for all duty-cycles tested. They also indicated that the force loss using a duty-cycle of 1:1 (-66.8±10.9%) was not significantly different to using 1:2 (vs -39.8±13.6%; p>0.05), but it was significantly greater than the use of 1:4 (vs -35.0±17.3%; p<0.05). In addition, no significant difference between 1:2 and 1:4 was revealed (p>0.05).

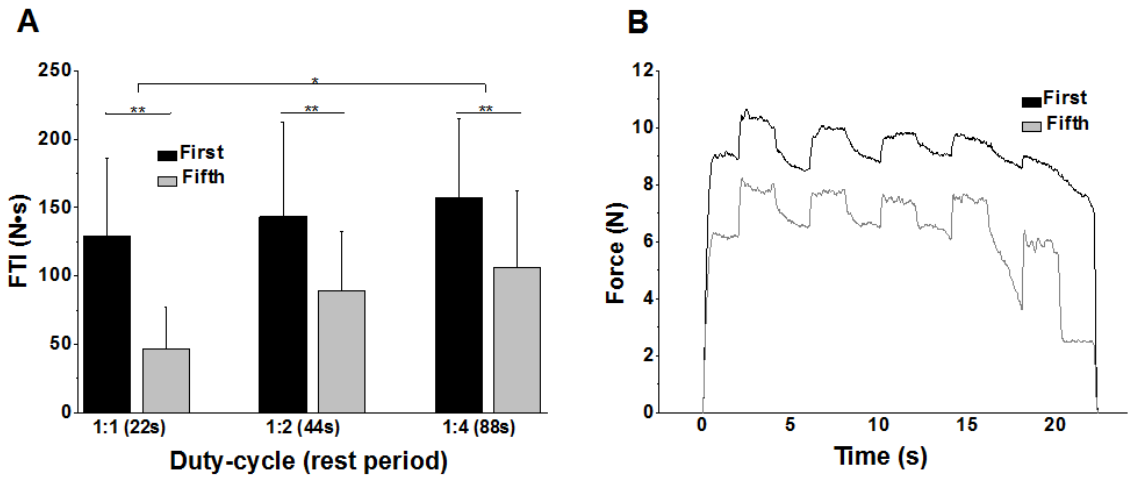

Figure 6.2. A: Force-time integral (N•s) corresponding to the first (black) and fifth (grey) NMES trains with duty cycles of 1:1, 1:2 or 1:4 (rest periods of 22s, 44s or 88s,

respectively). * Indicates p<0.05 (post-hoc comparisons); ** p<0.001 (ANOVA time effects). **B**: Exemplar of the force profile evoked by the first (black) and the fifth (grey) NMES trains delivered to AbH using a duty-cycle of 1:4 at an ALT frequency (20-100-20Hz; 2s each) and an intensity of 200% MT.

There were no main or interaction effects (p>0.05) between the duty-cycles tested for the latency, amplitude or TP derived from Mmax130, nor for the pTw or HRT derived from the corresponding twitch force (Table 6.1). Similarly, there were no significant main or interaction effects (p>0.05) for Fpaired10/100Hz (Table 6.1).

Table 6.1. Population mean (± SD, n=8) for the parameters evaluating excitability, contractility, fatigue using each duty-cycle tested: 1:1 (22s rest), 1:2 (44s) and 1:4 (88s). TP: terminal phase; pTw: peak twitch force amplitude; HRT: half relaxation time.

	Alternating (20-100-20Hz)					
	1:1 (22s)		**1:2 (44s)**		**1:4 (88s)**	
	PRE	**POST**	**PRE**	**POST**	**PRE**	**POST**
Latency (ms)	8.4 (1.4)	8.3 (1.4)	8.6 (1.5)	8.6 (1.6)	8.6 (1.5)	8.6 (1.8)
Amplitude (mV)	6.3 (3.8)	6.0 (3.2)	5.6 (2.8)	5.9 (3.0)	5.9 (3.1)	6.1 (3.3)
TP (mV•ms)	7.1 (4.3)	6.5 (3.8)	6.5 (3.4)	6.7 (3.3)	6.6 (3.5)	6.6 (3.4)
pTw (N)	9.4 (3.1)	9.6 (2.9)	9.3 (1.3)	9.2 (0.9)	9.2 (1.5)	8.9 (2.2)
HRT (ms)	101.4 (17.2)	103.2 (15.4)	100.2 (13.4)	103.5 (13.0)	105.9 (12.4)	103.9 (12.3)
$F_{paired10/100}$	0.88 (0.05)	0.88 (0.05)	0.89 (0.05)	0.88 (0.04)	0.89 (0.04)	0.87 (0.06)

6.4 Discussion

This study aimed to optimise the NMES duty-cycle implemented to minimise fatigue and preserve force production in AbH. The findings from this study indicate that five NMES trains induced a reduction in force production irrespective of the experimental duty-cycles (1:1, 1:2, and 1:4, with 22s, 44s and 88s rest periods, respectively) used. Indeed, the FTI was significantly lower from the first to the fifth train (Fig. 6.2), though to a lesser extent for the lowest duty-cycle (i.e. 1:4). In spite of this, AbH excitability and contractility measured immediately after the NMES trains remained unchanged since the parameters derived from the M_{max130} and corresponding twitch force, respectively, were no different to PRE values. Similarly, no significant change in the $F_{paired10/100Hz}$ index was found following any of the duty-cycles tested, which indicates that the five NMES trains delivered did not induce low frequency fatigue. Therefore, these findings indicate that from the duty-cycles tested, the one with the longest rest period (88s) showed signs of allowing better force preservation, which is in agreement with the study's hypothesis.

The FTI evoked by NMES was progressively reduced during the three duty-cycles investigated in this study. The FTI evoked during NMES can be used to reflect the preservation of force across evoked contractions (Rankin & Stokes, 1992; Gorgey et al., 2009; Gondin et al., 2010; Wegrzyk et al., 2015a), where higher duty-cycles induce progressively greater force decay (Packman-Braun, 1988; Rankin & Stokes, 1992; Matheson et al., 1997), in line with the findings of this study. Indeed, an early study by Rankin & Stokes (1992) compared the effect on the FTI of 10 trains of NMES delivered to the quadriceps using duty-cycles of 1:1 (10s on, 10s off), 1:5 (50s off) and 1:12 (120s off). They went on to show that the FTI was significantly reduced from the first to the tenth contraction for all duty-cycles, specifically by 51.3%, 38.3% and 25.8% for 1:1, 1:5, and 1:12, respectively. Furthermore, the FTI reduction was significantly greater using 1:1 compared to 1:12. Consistent with this, the present study also showed an FTI decay in

all of the duty cycles tested but to a greater extent in the highest duty cycle of 1:1 (-66.8%) compared to the lowest of 1:4 (-35.0%). These findings also concur with previous studies by Packman-Braun (1988) and Matheson et al. (1997) in which the higher duty-cycles tested lead to a greater force decay. In the former, duty-cycles of 1:1 (5s on, 5s off), 1:3 (15s off), and 1:5 (25s off) were compared in maintaining a force level above 50% of the initial force or meet the 30-minute treatment target. Out of the three duty-cycles tested, only 1:5 maintained the target force level for more than 20 minutes in 78% of their cohort (*n*=18). The latter study also compared duty-cycles and went on to show that force decay likely results from an increased metabolic stress in the stimulated muscle, especially during high duty-cycles (Matheson et al., 1997).

Indeed, Matheson et al., (1997) compared the energy metabolites and intracellular pH following 12 evoked contractions using a duty-cycle of 1:1 (10s on, 10s off) against a duty-cycle of 1:5 (50s off). They found that the former duty-cycle resulted in a significantly greater force loss (~30% vs ~13%) of triceps surea muscles than the latter one. Importantly, they went on to show that the higher duty-cycle (i.e. 1:1) induced a greater phosphocreatine depletion during anaerobic glycolysis to produce adenosine triphosphate, which in turn increased the ratio of inorganic phosphate to phosphocreatine significantly compared to the lower duty-cycle (210% vs 50%) (Matheson et al., 1997). In addition, the shorter rest periods minimised the capacity for mitochondrial oxidative phosphorylation to resynthesise adenosine triphosphate, which led to an increased intracellular acidity (i.e. drop in pH to 6.8 vs 7.03) (Matheson et al., 1997). As a result, the higher concentration of inorganic phosphate and adenosine diphosphate within the muscle, along with the associated accumulation of H^+, interfered with glycolysis and impeded the binding of Ca^{2+} to troponin to produce force (Matheson et al., 1997; Kent-Braun et al., 2012). The significantly greater force loss for 1:1 vs 1:4 (66.8% vs 35.0%) found in the present study is in line with the findings reported by Mathenson et al., (1997),

and is likely underpinned by the same processes since no other changes in muscle function were found.

The peripheral excitability and contractility of AbH were unchanged following five NMES trains irrespective of the different duty-cycles used. Since the latency (ms), amplitude (mV) and TP (mV•ms) derived from the M_{max130} showed no significant changes in time or across duty-cycles (Table 6.1), the Na^+-K^+ transport across the sarcolemma and T tubules responsible for the propagation of the potential (see section 2.4.3.1) may have been unaffected, even after the 1:1 duty-cycle. Similarly, the parameters derived from the corresponding twitch force (i.e. pTw and HRT; Table 6.1) were not altered, indicating that Ca^{2+} uptake kinetics and cross-bridge interaction in response to a single pulse stimulation (see section 2.4.3.2) were intact following the duty-cycle protocols tested presently. These findings are in agreement with what has been reported recently in terms of contractility and excitability following NMES. For example, a significant reduction in peak twitch force (-55%) and M_{wave} amplitude (-25%), and an increased latency, were found in the adductor pollicis following 28 trains of NMES (30Hz) using a 1:2 duty-cycle (1.5s on, 3s off) (Neyroud et al., 2016). These findings are indicative of impaired excitability and contractility in the muscle but were only evident from the 22nd evoked contraction for M_{wave} latency and from the 25th for amplitude. Similarly, the corresponding twitch force peak was only significantly lower after the 28th contraction. Even when a higher and more fatiguing duty-cycle was used (3:1), the M_{wave} amplitude and latency were significantly reduced from the 13th and increased from the 10th contraction, respectively, and the peak twitch force was reduced from the 22nd contraction. The previous study partly concurs with the findings from Papaiordanidou et al. (2014) in which a reduced peak twitch force was found only after the 15th, but not the 5th or 10th NMES (30Hz) train delivered using a 1:1 (2s on, 2s off) duty-cycle to the triceps surae from participants with complete spinal cord injury. However, this study also showed an increase in M_{wave} amplitude across the protocol perhaps due to the paralysed status of

the muscle tested from their cohort. In addition, a 24-train NMES (20-100-20Hz) protocol using a 1:3 (15s on, 45s off) delivered to AbH also showed indication of fatigue, as the M_{wave} latency and area increased, and half relaxation time was elongated (James et al., 2018). Taken together, these findings suggest that in order to observe the impaired excitability and contractility due to low frequency fatigue, a higher number of trains than in the present study may be required.

Indeed, no significant changes in the low frequency fatigue index $F_{paired10/100Hz}$ were detected following the duty-cycles tested. In contrast, a study where 40 NMES (100Hz) trains delivered using a 1:7 (5s on, 35s off) duty cycle to the knee extensors did report a significantly reduced fatigue index (-12%) immediately and up to 1 day later, which also accompanied a reduced ptw (-36%) and MVC (-28%) force for a prolonged period (Foure et al., 2014). In addition, Foure et al. (2014) reported an immediate and prolonged (up to 4 days) reduction in the peak force during the doublet stimuli at 10Hz (-38%) and 100Hz (-30%), which explain the reduced index. In a similar way, as previously discussed regarding the peripheral contractility and excitability of AbH, the 5-train protocol may have not loaded the muscle so as to induce low frequency fatigue. In fact, in the present study, the $T2_{100Hz}$ was calculated and compared to pre-NMES values as a follow up measure, and a moderate effect size (Cohen's d=0.3) was found only for the 1:4 duty-cycle. This is perhaps an indication that the 1:4 allowed the muscle to recover and potentiate the evoked force, as it has been observed when only a train of NMES is delivered (da Silva et al., 2015). In addition, this would also indicate that the longer resting period avoided to a greater extent the possible hyperpolarization of the MN that can also contribute to the reduced FTI (Papaiordanidou et al., 2014b), which its occurrence cannot be ruled out in this study. For example, the NMES paradigm used in the current study (i.e. WPHF) along with the 1:4 duty-cycle may have allowed the fast-twitch muscle fibres from AbH to recover and the MNs to repolarise, which resulted in a moderate increase in $T2_{100Hz}$ to combat fatigue. Therefore, using 88s rest allows sufficient

time for recovery following NMES evoked contractions and may be beneficial for maximising the force production achieved by ALT frequencies.

Finally, it is also noteworthy that although in accordance with the findings from previous literature and current study longer duty-cycles are recommended, these should be also selected in consideration of the overall duration of the NMES session (Lake, 1992). For instance, a full cycle (on+off times) from the current study using 1:4 lasts 1 minute and 50s, where a session of 15 or 22 trains would last ~30 or ~40 minutes, respectively. This is an important consideration for improving adherence and therefore effectiveness of NMES application.

Link to the next chapter

This study has shown that a duty-cycle of 1:4 with 88s rest periods allows for greater preservation of force between NMES trains and can help in the promotion of force production during a longer training session. The force produced during NMES is the main determinant for its strengthening effectiveness. Therefore, the practical implication of using a low duty-cycle, along with the other parameters together comprise a wide pulse (1m), low intensity (200% MT) and alternating frequency (20-100-20Hz) NMES paradigm, can promote the production force and foster the associated strength gains when delivered to the motor point of AbH.

7.0 General discussion

The studies reported in this thesis were undertaken with the overarching aim to systematically establish a tolerable NMES paradigm to target and strengthen AbH. In this chapter, the main findings of these studies and their implications for the application of NMES to AbH are discussed.

7.1 Main findings

7.1.1 An inability to voluntary activate AbH exists in asymptomatic feet

An atrophied AbH has been shown to be symptomatic in a number of prevalent lower limb pathologies including pes planus (Angin et al., 2014; Zhang et al., 2019), lesser toe deformities (e.g. claw/hammer toes; Mickle et al., 2018), chronic plantar heel pain (Franettovich-Smith et al., 2019) and Hallux Valgus (Steward et al., 2013). In turn, these pathologies are associated with overuse injury occurrence in the young (Zhang et al., 2019) or an increased likelihood of falling in the elderly (Menz & Lord, 2005) populations. In advanced Hallux Valgus, for example, the deformed bony prominence at the medial aspect of the 1MPJ leads to a reduced mechanical capacity for abduction of the Hallux and a consequent AbH dysfunction (Arinci İncel et al., 2003; Stewart et al., 2013). As a result, Arinci İncel et al. (2003) noted that most participants with Hallux Valgus were unable to voluntary activate AbH in its mechanical line of action. This inability was found to extend to their healthy control group, the majority of which also showed compensatory activation from the flexor hallucis brevis muscle during AbH voluntary contraction attempts. Boon & Harper (2003) also reported an inability to voluntary activate AbH in ~20% of an elderly and young healthy cohort. These findings indicate that an inability to voluntary activate AbH exists not only in the pathological but also in the healthy feet. Indeed, the work presented in this thesis (Chapter 5) confirmed and quantified a high

prevalence of this inability in the healthy population. Specifically, it was quantified that ~80% (*n*=10) of the cohort tested were unable to voluntary activate AbH to at least 90% of its maximal force generating capacity when assessed via the twitch interpolation technique.

A likely contributor to the prevalent voluntary activation insufficiency is the complex morphology of AbH, which is arranged in segments with distinct architecture and corresponding force generating capacity (Tosovic et al., 2012). Having morphologically different sections within the same muscle may lead to a non-uniform neural activation of MUs for flexion and/or abduction of the Hallux (Tosovic et al., 2012), which needs to be coordinated in order to directionally tune the force in its oblique line of action. Accordingly, AbH has a morphology that permits to fine-tune activation of its different segments to produce force, but the ability to recruit and synchronise their corresponding MU pools for full activation in its line of action may be lost even in healthy individuals.

7.1.2 NMES can be used to overcome the inability to voluntary activate the muscle as the AbH contractility is preserved

The inability to activate AbH to its maximal capacity may have functional consequences in healthy individuals. More specifically, an inability to produce force compromises 1MPJ stability during the propulsion phase of gait, which in turn will reduce forefoot stiffness and place a greater demand on proximal joints such as the hip to compensate during forward progression (Farris et al., 2019). The prevalent inability to fully activate AbH on demand also makes its training problematic, as AbH's contribution during gross foot exercises can often be diminished in favour of larger extrinsic foot (ankle) muscles to perform the majority of the work (McKeon et al., 2015; Yamauchi & Koyama, 2019b). Nevertheless, Chapter 5 also provides evidence showing that targeted NMES is capable

of overcoming this problem as it evoked comparable forces from AbH irrespective of the ability to voluntary contract to full capacity. Importantly, this finding indicates that the contractility of AbH is intact irrespective of ability and hence NMES can be used to train AbH to increase its voluntary activation capacity. The implication of this finding is that the application of targeted NMES to AbH may be beneficial not only for the pathological foot but also for the asymptomatic foot to ensure appropriate forefoot loading during gait.

7.1.3 An NMES paradigm has been optimised for targeted strengthening of AbH

7.1.3.1 Direct-muscle NMES requires lower intensity to evoke contractions from AbH than nerve stimulation

In order to enhance the clinical utility of training via evoked muscle contractions, finding a low NMES intensity level that can also be effective in promoting strengthening in AbH was imperative for this thesis. To do this, an approach for stimulation intensity selection based on MT of AbH (Chapter 3) was adopted rather than its MVC as it has been traditionally done (Maffiuletti et al., 2018; see section 1.3.1.2). The strength of adopting this approach is that it overcomes the dependency on the ability to fully activate AbH voluntarily. The MT identification was optimised, based on rheobase, to deliver NMES using the least stimulus intensity. In doing so, direct-muscle NMES was identified as the optimised mode of delivery since it required lower stimulus intensity than nerve stimulation. A lower stimulus intensity may be required to recruit AbH via direct-muscle stimulation since it is primarily composed of slow-fatiguing and low-threshold MUs (Kura et al., 1997; Širca et al., 1990; Kelly et al., 2013), some of which with smaller axon diameter could also be located in the superficial layers of the muscle (Mesin et al., 2010). This mode of stimulation also overcomes the inhomogeneous depolarisation of motor axons that occurs during nerve stimulation, which would also recruit the MUs of the

higher-threshold flexor hallucis brevis muscle (Aeles et al., 2020), thus increasing the stimulus intensity used to recruit AbH. The subcutaneous fat thickness (Madeiros et al., 2015) and the physical distance from the electrode to the depolarised tissue (muscle vs nerve) (Enoka et al., 2020) may have also contributed to finding direct-muscle stimulation as the mode that required lower intensities to recruit AbH.

7.1.3.2 MT determination optimises current intensity selection and identified 1ms as the optimised pulse duration

The minimal stimulus intensity approach used in Chapter 3 optimised not only the stimulation mode but also the pulse duration and frequency that should be used for MT determination. The intensity-duration curve transformed into the Weiss linear regression revealed that when direct-muscle NMES was delivered using 100Hz trains, the chronaxie (pulse duration) of AbH corresponding to the lowest rheobase (intensity) was 1ms. Wide pulse durations such as 1ms recruit a higher number of MUs than narrow pulses (Gorgey et al., 2006; Gorgey et al., 2008) because as the duration of a given pulse is increased, the intensity of the current required to depolarise an excitable tissue decreases (intensity-duration relationship) (Bostock et al., 1998). For its part, the pulse frequency that required the lowest intensity for MT determination was 100Hz. Indeed, trains of 5 x 1ms wide pulses delivered at 100Hz were more efficient at achieving rheobase for MT determination because high-frequencies maximise force production as the MU firing rate is increased and the force evoked per pulse summate in a non-linear manner (force-frequency relationship) (Edwards et al., 1977; Allen et al., 2008). The findings from Chapter 3 have therefore informed the mode of NMES delivery and MT determination approach that was used in subsequent studies. In addition, 1ms was identified as the optimised pulse duration to also be used during NMES delivery.

7.1.3.3 An NMES training intensity of 200% MT can be used to ensure strength gains while maintaining tolerability

An NMES intensity of 200% MT was selected in Chapter 5 as part of the optimised paradigm. This selection was not trivial as this NMES intensity corresponds to a force level equivalent to 20% MVC, which in turn represents a minimum intensity dose to achieve muscle strengthening (Tabolt et al., 2003; Alon & Smith, 2005; Maddocks et al., 2016; Maffiuletti et al., 2019). It is so because morphological and neurological strength adaptations are consistently being achieved when NMES is delivered at intensities which evoke muscle contractions of ≥20% MVC (section 1.3.2) (Alon & Smith, 2005; Maddocks et al., 2016; Maffiuletti et al., 2019; Talbot et al., 2003). Conversely, training intensities below this level (e.g. 5-10% MVC) are found to be futile in inducing strengthening adaptations (Natsume et al., 2015; Neyroud et al., 2019), possibly because the magnitude of the force evoked at this intensity when coupled with high-frequencies present a high interindividual variability (Wegrzyk et al., 2015b; Neyroud et al., 2018). Importantly, an NMES intensity of 200% MT delivered to AbH was perceived as tolerable when assessed via VAS. Therefore, the NMES intensity selected can achieve a tolerable NMES application whilst also ensuring its capacity to evoke forces that can efficiently induce strength adaptations in AbH. Nevertheless, the frequency pattern and the length of the trains will also contribute to the evoked forces and their maintenance during NMES, and correspondingly to its effectiveness.

7.1.3.4 Long trains (22s) delivered with an alternating frequency pattern (20-100-20Hz) promote force production during direct-muscle NMES via PTP

Long-lasting NMES trains (22s) delivered at alternating frequency pattern (20-100-20Hz) capitalise on the peripheral and central mechanisms underpinning PTP occurrence

during evoked forces. PTP has been proposed to have central and peripheral sources (see section 1.3.3; Chapter 4) (Baldwin et al., 2006), which contribution is influenced by the use of high-frequency (low inter-stimulus intervals; e.g. 10ms) and long NMES trains. Centrally-sourced PTP is underlined by a number of mechanisms that include pre- and post-synaptic processes occurring in the central nervous system (Zucker and Regehr, 2002; Dean et al., 2007; Bergquist et al., 2011b; Dideriksen et al., 2015), and which ultimately affect the force produced (Heckman & Enoka, 2012). For its part, the peripherally-sourced PTP can also enhance the magnitude and sustainment of evoked force during long-lasting NMES and is underpinned by an increase in the likelihood of actin-myosin interaction during consecutive pulses (O'Leary et al., 1997; Frigon et al., 2011; Cheng et al., 2017). The 22s trains of alternating high frequency may therefore provide the time frame and inter-stimulus intervals required for PTP to take place and enhance force production during NMES.

The work presented in this thesis however did not record the H-reflex, "extra-force" or asynchronous EMG activity phenomena from AbH to directly point to the specific mechanism(s) responsible for finding the 22s trains and alternating frequency pattern as an optimised combination. Instead, the $T2_{100Hz}$ was used to quantify the capacity of AbH in producing potentiated force following NMES delivery. Indeed, delivering a paired stimuli at 100Hz can provide an indication of the Ca^{2+} dependent mechanisms linked to peripherally-sourced PTP (Cheng et al., 2013). Although these mechanisms are considered to be muscle dependent, as it is more readily found in fast-fatigable muscles (O'Leary et al., 1997), and it is still shown in slow-fatigable muscles, such as AbH, although to a smaller and delayed extent (Gordon et al., 1990). In addition, the alternation of 20 and 100Hz may have permitted the maintenance of Ca^{2+} saturation levels relatively lower than if a constant high frequency was used (Mettler & Griffin, 2010). This may also have contributed to an increased, but not saturated, Ca^{2+}-sensitivity. Indeed, previous work showed that the "extra-force" phenomenon can be induced during wide pulses

delivered at a low frequency when preceded by a high frequency that increased the Ca^{2+}-sensitivity (Frigon et al., 2011; Cheng et al., 2017), or when using low-frequency NMES alone (Espeit et al., 2021). Therefore, the increased $T2_{100Hz}$ may partly provide an indication that the peripherally-sourced PTP was involved during the delivery of the NMES paradigm being tested.

7.1.3.5 The decay of the force evoked between contractions can be minimised by using a duty-cycle of 1:4

Although the evoked force within a stimulating train may have been optimised by promoting the involvement of central and peripheral mechanisms, its decay across contractions within an intervention session can still be manifested. Specifically, the force decays across evoked contraction as a function of the rest intervals between trains. Indeed, duty-cycles consisting of a lower resting time between contractions result in a greater reduction in force, whereas duty-cycles with long rest periods mitigate this force decay (Packman-Braun, 1988; Rankin & Stokes, 1992; Matheson et al., 1997). This reduction in force is linked to an increased metabolic demand placed on the muscle during NMES (Matheson et al., 1997), which is not necessarily dependent on frequency or pulse duration (Gondin et al., 2010). The increased metabolic cost results in a more acidic muscle environment which interferes with glycolysis and impedes the binding of Ca^{2+} to troponin to produce force (Matheson et al., 1997; Kent-Braun et al., 2012). The optimised duty-cycle of 1:4, with an NMES train that lasts 22s and a rest interval of 88s, allows a sufficient resting period for recovery of the metabolic changes incurred during repetitive contractions and therefore enhanced the excitation-contraction coupling dynamics in AbH for subsequent contractions. Importantly, this duty cycle is within the range of duty cycles implemented in strengthening interventions (i.e. 1:3) and the recommended for clinical settings (i.e. 1:5) (see 1.3.1.4).

7.1.4 The potential strength gains induced by the developed NMES paradigm can be quantified by constructing the joint moment–angle relationship of AbH

The NMES paradigm developed in this thesis can be used to overcome the inability to activate AbH for training; however, this inability also compromises the functional assessment of strength adaptations resulting from an intervention as the performance of an MVC is still problematic. Maximal toe flexion protocols have been previously used to measure muscle strength (Goldmann & Brüggemann, 2012; Kurihara et al., 2014; Latey et al., 2018; Yamauchi & Koyama, 2019ab), but this is far from an isolated movement of AbH as it includes the contribution of other intrinsic and extrinsic muscles. Given its superficiality, ultrasonography has also been used to assess the morphology of AbH (Mickle et al., 2013), but the expected strength gains may fall within its resolution. In Chapter 2 (see section 2.3.2), a new method using NMES and dynamometry has been presented for the assessment of AbH force generating capacity by means of plotting the joint moment–angle relationship between the evoked force and the angle configuration of the 1MPJ. This method, however, has its own limitations as alterations in the moment arm of the reaction force acting about the joint due to the evoked activation may in turn lead to a misrepresentation of the joint moments measured via dynamometry against those calculated using inverse dynamics (Arampatzis et al., 2004; 2005). Chapter 2 showed that this misrepresentation does happen when plotting the joint moment–angle relationship for AbH, but it can be corrected by calculating and accounting for the change in moment arm from rest to contraction. The findings also show that AbH may operate on both the ascending and descending limbs of the force–length curve, as its joint moment–angle relationship was parabolic, with the highest moments being produced at 10-15° 1MPJ dorsal flexion. Therefore, this approach provides an optimised 1MPJ angle configuration for measuring evoked forces from AbH and a method to assess functional post-intervention strength gains.

7.2 Limitations and future directions

The work undertaken within this thesis, as well as the interpretation of the findings, are not without limitations that must be acknowledged.

Firstly, participants were asked to remain in a seated position during the delivery of the stimulation across all studies reported here. Although the comfort of being in this position was monitored through participants' verbal feedback, and stretch breaks were given when necessary, it is possible that sitting for a relatively prolonged period of time may have impacted the relaxed status of participants and consequently the results obtained. Future research should further minimise the sitting time required during the experimental procedures by optimising the iterative processes involved in the studies presented.

Secondly, only 5 NMES trains per condition tested were delivered in Chapters 4 and 6, which may have precluded inducing recordable changes in peripheral contractility and excitability of AbH. Indeed, changes in both muscle properties were found in AbH (James et al., 2018) and other muscles (Neyroud et al., 2016) when a higher number of trains was used. The number of NMES trains delivered per session is another aspect that should be optimised taking into account the trade-off between force maintenance for strengthening effectiveness and session duration for intervention adherence.

Thirdly, no measurements were taken to directly assess mechanisms associated with spinal excitability (i.e. H-reflex) in any of the studies presented. The reasons for this were that H-reflexes are difficult to evoke in AbH due to the distance between the medial plantar nerve and the EMG electrode, and also because it is absent in a high proportion of the population (Versino et al., 2007). In addition, H-reflexes are recommended to be evoked during low levels of sustained voluntary contractions (~5-10% MVC; Knikou, 2008), but this would be difficult to achieve and standardise in AbH as recording a response is not guaranteed (Versino et al., 2007; Burke, 2016). A method to assess the

spinal excitability of muscle (i.e. recurrent inhibition), where a low intensity stimulus (to evoke an H-reflex) is delivered at an interval of 10ms (i.e. 100Hz) before a supramaximal stimulus, was proposed by Pierrot-Deseilligny et al., (1976). Although this method was developed with the soleus, future research could investigate whether the spinal excitability assessment of AbH may benefit from this method as it can be implemented at rest (Knikou, 2008).

Fourthly, the small sample size (*n*=13) in the study reported in Chapter 5 impeded the statistical comparison of the results between *able* and *unable* groups, and therefore warrants certain caution in drawing general conclusions. Considering this limitation, the results still highlight the prevalent difficulty to activate AbH voluntary to its maximal capacity. As discussed earlier, an indication of this difficulty has been previously reported in the works by Arinci İncel et al. (2003) and Boon & Harper (2003). Indeed, Arinci İncel et al. (2003) reported that the majority of their participants were unable to perform an isolated and maximal contraction of AbH. Similarly, Boon & Harper (2003) reported that ~20% could not activate this muscle voluntarily. However, the level of effort sustained in the contractions was not reported in the latter study but given that they were monitoring motor unit potential activity via EMG, this may have not been necessarily maximal. In addition, the former study did not quantify the level of effort nor the specific prevalence of inability for voluntary activation. Therefore, including a larger number of participants may influence the magnitude of the prevalence of *unable* individuals reported here, but would not overcome the inability to activate this muscle as reported.

Furthermore, although the twitch interpolation technique, as used in Chapter 5, represents a standard method to assess for voluntary activation, it is not without its own practical limitations. In order to minimise the impact of these, the experimental protocol was optimised to maximise force production and overcome the antidromic collision and the variability in force produced during the interpolated twitch, via the delivery of doublets

(Belanger & McComas, 1981; Herbert & Gandevia, 1999) instead of single pulses (Oskouei et al., 2003). In addition, positioning the 1MPJ at 10° of dorsal flexion to optimise force production by AbH (see section 2.3.2) may overcome the sensitivity of the technique to changes in joint-angle configuration (Bampouras et al., 2006). Similarly, the positioning of the foot at 35° of ankle plantar flexion minimised the contribution to the MVC force from the flexor hallucis longus and plantar-flexor muscles (Goldmann & Brüggemann, 2012). Additionally, the cathode electrode placement was optimised to AbH's motor point location (see section 2.2.1) to ensure the targeted stimulation of this muscle. This, in turn, ensured that the force corresponding to the interpolated twitch stimulus originated from AbH, even if the MVC force had the inevitable synergistic contribution from the flexor hallucis brevis. Lastly, if one assumes that VAR ~1 (i. e. ~100%) represents full activation capacity, the implementation of the twitch interpolation technique as presented in Chapter 5 represents a robust method to quantify insufficiencies in AbH activation.

Finally, testing the efficacy in strengthening AbH by long-term exposure to the NMES paradigm presented in this thesis was not possible in light of the COVID19 pandemic. Future work should investigate the effectiveness of a long-term period of AbH training with NMES using 22s-trains of 1ms pulses delivered at 20-100-20Hz with an intensity of 200% MT and a 1:4 duty cycle.

The proposed NMES paradigm has a potential clinical utility to prevent or tackle the progression of common foot-related pathologies and to ensure an efficient daily life and athletic locomotion. For example, Hallux Valgus is one of the most prevalent foot pathologies requiring clinical specialist assessment and treatment (Stewart et al., 2013). Specifically, it affects 23% of adults (18-65 years old), 36% of the elderly (>65 years old) population and 8% of those aged <18 (Stewart et al., 2013). In this condition, the AbH's integrity deteriorates progressively reaching up to ~20% atrophy as the severity of the

deformation increases with age (Stewart et al., 2013; Aiyer et al., 2015). Given the location of AbH, NMES represents an ideal candidate to target this muscle and combat the progression of Hallux Valgus, especially at the onset or early stages of the deformity. This is an important consideration as the application of NMES at a later stage of the condition may not be beneficial given the irreversible structural changes that occur at the 1MPJ as a result of the deformity. When considering the healthy and athletic population, the benefits of strengthening AbH via NMES may include an efficient push-off during walking and running (Farris et al., 2019). Additionally, stronger feet due to a strengthened AbH may also prove beneficial in sports that require greater toe-flexion strength or frequent change of direction of movement whilst running such as dancing (Matsumoto & Yamamoto, 2022) or American football (Yuasa et al., 2018), respectively.

In practice, the effectiveness of the targeted training of AbH with NMES will be determined by the adherence of the patients/athletes to its application. In order to facilitate its accessibility, the proposed training paradigm should be delivered using a portable device to transfer its application from a laboratory environment to the patients/athletes' own home or training ground. Previous work in our laboratory, in collaboration with the Department of Engineering and Design at LSBU, produced a working prototype device that can deliver NMES to AbH. However, the development of this prototype is still in its infancy and it is not currently programmed to deliver the paradigm proposed in this thesis. In addition, this device delivers direct currents at a constant voltage (and variable current intensity) which is different from other commercial stimulators that deliver them at a constant current intensity. Although these specifications mean that the stimulator can be programmed to deliver an alternating-frequency train, the current intensity and the effectiveness of evoking a sustained contraction may vary. These technical limitations as well as identifying the optimal time to intervene in the progression of Hallux Valgus or NMES application as part of sport-specific training programmes should also be addressed in future research.

7.3 Conclusion

This thesis identified a relatively high prevalence of an inability in the healthy people tested to fully activate AbH voluntarily. It was further demonstrated that NMES has the potential to overcome this inability by evoking force from AbH comparable to individuals who are able to fully activate the muscle. NMES therefore could perhaps be used as a strengthening modality not only for the pathological but also asymptomatic feet. The overarching feature of the optimised NMES paradigm developed in this thesis is that it has been built on the use of wide duration pulses (1ms), which keeps the intensity low; yet to a sufficient level where muscle strengthening can be anticipated (200% MT). In doing so, it overcomes the discomfort associated with high-intensity protocols, thus promoting its tolerability and adherence. Combined with an alternating frequency pattern and long train durations, this paradigm can potentially promote higher and longer-lasting force production because the force evoked by stimulation at 100Hz is sustained for longer when interspersed with pulses delivered at 20Hz as opposed to shorter constant frequency trains. The increased capacity of this stimulation pattern to evoke force, as assessed by $T2_{100Hz}$, is likely underpinned by PTP. The force produced during these NMES trains can be further preserved by implementing a 1:4 duty-cycle with long rest intervals that permit the replenishment of metabolites required for contraction. Lastly, this thesis has shown that the joint moment–angle relationship of AbH can be constructed using dynamometry and NMES. Cumulatively, the findings from this series of studies present an optimised and tolerable NMES paradigm for a targeted strengthening intervention of AbH, and an approach to quantify the resulting strength gains achieved.

Practical implications

- NMES overcomes the prevalent inability to voluntary activate AbH and can be used as a strengthening modality not only for the pathological but also asymptomatic feet

- Chapters 3, 4, 5 and 6 have collectively optimised an NMES paradigm that promotes force production while reducing discomfort of AbH. This optimised paradigm delivers NMES to the motor point of AbH using 22s-trains of 1ms pulses delivered at 20-100-20Hz with an intensity of 200% MT and a 1:4 duty cycle.

-An approach that can be used for assessing strengthening gains via the construction of the joint moment-angle relationship has been presented in Chapter 2 and can be used to assess the effectiveness of the developed NMES paradigm.

- NMES can be applied to the intrinsic foot musculature for strengthening purposes and may provide the basis of complementary treatment of foot pathologies including Hallux Valgus.

References

Adams, G. R., Harris, R. T., Woodard, D., & Dudley, G. A. (1993). Mapping of electrical muscle stimulation using MRI. *Journal of Applied Physiology*, *74*(2), 532–537. https://doi.org/10.1152/jappl.1993.74.2.532

Aeles, J., Kelly, L. A., Yoshitake, Y., & Cresswell, A. G. (2020). Fine-wire recordings of flexor hallucis brevis motor units up to maximal voluntary contraction reveal a flexible, nonrigid mechanism for force control. Journal of Neurophysiology, 123(5), 1766-1774.

Agawany, A. E., & Meguid, E. A. (2010). Mode of insertion of the abductor hallucis muscle in human feet and its arterial supply. *Folia Morphologica*, *69*(1), 54–61.

Aiyer, A., Stewart, S., & Rome, K. (2015). The effect of age on muscle characteristics of the abductor hallucis in people with hallux valgus: a cross-sectional observational study. *Journal of Foot and Ankle Research*, *8*(1), 19. https://doi.org/10.1186/s13047-015-0078-5

Alcazar, J., Csapo, R., Ara, I., & Alegre, L. M. (2019). On the shape of the force-velocity relationship in skeletal muscles: The linear, the hyperbolic, and the double-hyperbolic. Frontiers in physiology, 769.

Allen, D. G., Lamb, G. D., & Westerblad, H. (2008). Skeletal Muscle Fatigue: Cellular Mechanisms. *Physiological Reviews*, *88*(1), 287–332. https://doi.org/10.1152/physrev.00015.2007

Allen, G. M., Gandevia, S. C., & McKenzie, D. K. (1995). Reliability of measurements of muscle strength and voluntary activation using twitch interpolation. *Muscle & Nerve*, *18*(6), 593–600. https://doi.org/10.1002/mus.880180605

Alon, G., & Smith, G. V. (2005). Tolerance and conditioning to neuro-muscular electrical stimulation within and between sessions and gender. *Journal of Sports Science and*

Medicine, *4*(4), 395–405.

Angin, S., Crofts, G., Mickle, K. J., & Nester, C. J. (2014). Ultrasound evaluation of foot muscles and plantar fascia in pes planus. Gait & posture, 40(1), 48-52.

Arampatzis, A., Morey-Klapsing, G., Karamanidis, K., DeMonte, G., Stafilidis, S., & Brüggemann, G. P. (2005). Differences between measured and resultant joint moments during isometric contractions at the ankle joint. Journal of biomechanics, 38(4), 885-892.

Arampatzis, A., Karamanidis, K., De Monte, G., Stafilidis, S., Morey-Klapsing, G., & Brüggemann, G. P. (2004). Differences between measured and resultant joint moments during voluntary and artificially elicited isometric knee extension contractions. Clinical biomechanics, 19(3), 277-283.

Arinci İncel, N., Genç, H., Erdem, H. R., & Yorgancioglu, Z. R. (2003). Muscle Imbalance in Hallux Valgus. American Journal of Physical Medicine & Rehabilitation, 82(5), 345–349. https://doi.org/10.1097/01.PHM.0000064718.24109.26

Bakker, A. J., Cully, T. R., Wingate, C. D., Barclay, C. J., & Launikonis, B. S. (2017). Doublet stimulation increases Ca2+ binding to troponin C to ensure rapid force development in skeletal muscle. Journal of General Physiology, 149(3), 323-334.

Baldwin, E. R., Klakowicz, P. M., & Collins, D. F. (2006). Wide-pulse-width, high-frequency neuromuscular stimulation: implications for functional electrical stimulation. Journal of Applied Physiology, 101(1), 228-240.

Bampouras, T. M., Reeves, N. D., Baltzopoulos, V., & Maganaris, C. N. (2006). Muscle activation assessment: effects of method, stimulus number, and joint angle. Muscle & Nerve: Official Journal of the American Association of Electrodiagnostic Medicine, 34(6), 740-746.

Barss, T. S., Ainsley, E. N., Claveria-Gonzalez, F. C., Luu, M. J., Miller, D. J., Wiest, M.

J., & Collins, D. F. (2018). Utilizing Physiological Principles of Motor Unit Recruitment to Reduce Fatigability of Electrically-Evoked Contractions: A Narrative Review. Archives of Physical Medicine and Rehabilitation, 99(4), 779–791. https://doi.org/10.1016/j.apmr.2017.08.478

Baudry, S., Klass, M., & Duchateau, J. (2005). Postactivation potentiation influences differently the nonlinear summation of contractions in young and elderly adults. Journal of Applied Physiology, 98(4), 1243-1250.

Belanger, A. Y., & McComas, A. J. (1981). Extent of motor unit activation during effort. Journal of Applied Physiology, 51(5), 1131–1135. https://doi.org/10.1152/jappl.1981.51.5.1131

Bergquist, A. J., Clair, J. M., & Collins, D. F. (2011a). Motor unit recruitment when neuromuscular electrical stimulation is applied over a nerve trunk compared with a muscle belly: triceps surae. Journal of Applied Physiology, 110(3), 627–637. https://doi.org/10.1152/japplphysiol.01103.2010

Bergquist, A. J., Clair, J. M., Lagerquist, O., Mang, C. S., Okuma, Y., & Collins, D. F. (2011b). Neuromuscular electrical stimulation: implications of the electrically evoked sensory volley. European Journal of Applied Physiology, 111(10), 2409–2426. https://doi.org/10.1007/s00421-011-2087-9

Bergquist, A. J., Wiest, M. J., & Collins, D. F. (2012). Motor unit recruitment when neuromuscular electrical stimulation is applied over a nerve trunk compared with a muscle belly: quadriceps femoris. Journal of Applied Physiology, 113(1), 78–89. https://doi.org/10.1152/japplphysiol.00074.2011

Bickel, C. S., Gregory, C. M., & Dean, J. C. (2011). Motor unit recruitment during neuromuscular electrical stimulation: a critical appraisal. European Journal of Applied Physiology, 111(10), 2399–2407. https://doi.org/10.1007/s00421-011-

2128-4

Bigland-Ritchie, B., Jones, D. A., & Woods, J. J. (1979). Excitation frequency and muscle fatigue: electrical responses during human voluntary and stimulated contractions. Experimental neurology, 64(2), 414-427.

Binder-Macleod, S. A., & Guerin, T. (1990). Preservation of force output through progressive reduction of stimulation frequency in human quadriceps femoris muscle. Physical Therapy, 70(10), 619-625.

Heckman, C. J., & Binder, M. D. (1991). Computer simulation of the steady-state input-output function of the cat medial gastrocnemius motoneuron pool. Journal of neurophysiology, 65(4), 952-967.

Binder-Macleod, S., & Kesar, T. (2005). Catchlike property of skeletal muscle: recent findings and clinical implications. Muscle & Nerve: Official Journal of the American Association of Electrodiagnostic Medicine, 31(6), 681-693.

Binder-Macleod, S. A., & McDermond, L. R. (1992). Changes in the Force-Frequency Relationship of the Human Quadriceps Femoris Muscle Following Electrically and Voluntarily Induced Fatigue. Physical Therapy, 72(2), 95–104. https://doi.org/10.1093/ptj/72.2.95

Binder-Macleod, S. A., Halden, E. E., & Jungles, K. A. (1995). Effects of stimulation intensity on the physiological responses of human motor units. Medicine and science in sports and exercise, 27(4), 556-565.

Binder-Macleod, S. A., Lee, S. C., Fritz, A. D., & Kucharski, L. J. (1998). New look at force-frequency relationship of human skeletal muscle: effects of fatigue. Journal of neurophysiology, 79(4), 1858-1868.

Bojsen-Møller, F., & Lamoreux, L. (1979). Significance of free dorsiflexion of the toes in walking. Acta Orthopaedica Scandinavica, 50(4), 471-479.

Boom, H. B. K., Mulder, A. J., & Veltink, P. H. (1993). Fatigue during functional neuromuscular stimulation. Progress in Brain Research, 97(C), 409–418. https://doi.org/10.1016/S0079-6123(08)62300-6

Boon, A. J., & Harper, C. M. (2003). Needle EMG of abductor hallucis and peroneus tertius in normal subjects. Muscle & Nerve, 27(6), 752–756. https://doi.org/10.1002/mus.10356

Bostock, H., Cikurel, K., & Burke, D. (1998). Threshold tracking techniques in the study of human peripheral nerve. Muscle & Nerve, 21(2), 137–158. https://doi.org/10.1002/(SICI)1097-4598(199802)21:2<137::AID-MUS1>3.0.CO;2-C

Bouguetoch, A., Martin, A., & Grosprêtre, S. (2021). Insights into the combination of neuromuscular electrical stimulation and motor imagery in a training-based approach. European Journal of Applied Physiology, 121(3), 941-955.

Brenner, E. (1999). Insertion of the abductor hallucis muscle in feet with and without Hallux valgus. The Anatomical Record, 254(3), 429–434. https://doi.org/10.1002/(SICI)1097-0185(19990301)254:3<429::AID-AR14>3.0.CO;2-5

Bruening, D. A., Ridge, S. T., Jacobs, J. L., Olsen, M. T., Griffin, D. W., Ferguson, D. H., ... & Johnson, A. W. (2019). Functional assessments of foot strength: a comparative and repeatability study. BMC musculoskeletal disorders, 20(1), 1-9.

Burke, D., Mogyoros, I., Vagg, R., & Kiernan, M. C. (1999). Temperature dependence of excitability indices of human cutaneous afferents. Muscle & nerve, 22(1), 51-60.

Burke, D., Kiernan, M. C., & Bostock, H. (2001). Excitability of human axons. Clinical Neurophysiology, 112(9), 1575–1585. https://doi.org/10.1016/S1388-2457(01)00595-8

Burke, D. (2016). Clinical uses of H reflexes of upper and lower limb muscles. Clinical neurophysiology practice, 1, 9-17.

Cheng, A. J., Place, N., Bruton, J. D., Holmberg, H. C., & Westerblad, H. (2013). Doublet discharge stimulation increases sarcoplasmic reticulum Ca2+ release and improves performance during fatiguing contractions in mouse muscle fibres. The Journal of physiology, 591(15), 3739-3748.

Cheng, A. J., Neyroud, D., Kayser, B., Westerblad, H., & Place, N. (2017). Intramuscular Contributions to Low-Frequency Force Potentiation Induced by a High-Frequency Conditioning Stimulation. Frontiers in Physiology, 8(SEP), 1–10. https://doi.org/10.3389/fphys.2017.00712

Choi, A., Kwon, N. Y., Kim, K., Kim, Y., Oh, J., Oh, H. M., & Park, J. H. (2017). Anatomical Localization of Motor Points of the Abductor Hallucis Muscle: A Cadaveric Study. Annals of Rehabilitation Medicine, 41(4), 589. https://doi.org/10.5535/arm.2017.41.4.589

Chung, K. A., Lee, E., & Lee, S. (2016). The effect of intrinsic foot muscle training on medial longitudinal arch and ankle stability in patients with chronic ankle sprain accompanied by foot pronation. Physical Therapy Rehabilitation Science, 5(2), 78–83. https://doi.org/10.14474/ptrs.2016.5.2.78

Clausen, T. (2003). Na + -K + Pump Regulation and Skeletal Muscle Contractility. Physiological Reviews, 83(4), 1269–1324. https://doi.org/10.1152/physrev.00011.2003

Collins, D. F., Burke, D., & Gandevia, S. C. (2001). Large Involuntary Forces Consistent with Plateau-Like Behavior of Human Motoneurons. The Journal of Neuroscience, 21(11), 4059–4065. https://doi.org/10.1523/JNEUROSCI.21-11-04059.2001

Collins, D. F., Burke, D., & Gandevia, S. C. (2002). Sustained contractions produced by

plateau-like behaviour in human motoneurones. The Journal of Physiology, 538(1), 289–301. https://doi.org/10.1113/jphysiol.2001.012825

Collins, David F. (2007). Central Contributions to Contractions Evoked by Tetanic Neuromuscular Electrical Stimulation. Exercise and Sport Sciences Reviews, 35(3), 102–109. https://doi.org/10.1097/jes.0b013e3180a0321b

Colson, S., Martin, A., & Van Hoecke, J. (2000). Re-examination of training effects by electrostimulation in the human elbow musculoskeletal system. International journal of sports medicine, 21(04), 281-288.

Colson, S. S., Martin, A., & Van Hoecke, J. (2009). Effects of electromyostimulation versus voluntary isometric training on elbow flexor muscle strength. Journal of Electromyography and Kinesiology, 19(5), e311-e319.

Conwit, R. ., Stashuk, D., Tracy, B., McHugh, M., Brown, W. ., & Metter, E. . (1999). The relationship of motor unit size, firing rate and force. Clinical Neurophysiology, 110(7), 1270–1275. https://doi.org/10.1016/S1388-2457(99)00054-1

Cutsem, M. V., Feiereisen, P., Duchateau, J., & Hainaut, K. (1997). Mechanical properties and behaviour of motor units in the tibialis anterior during voluntary contractions. Canadian journal of applied physiology, 22(6), 585-597.

Regina Dias Da Silva, S., Neyroud, D., Maffiuletti, N. A., Gondin, J., & Place, N. (2015). Twitch potentiation induced by two different modalities of neuromuscular electrical stimulation: Implications for motor unit recruitment. Muscle & nerve, 51(3), 412-418.

Dahmane, R., Djordjevič, S., Šimunič, B., & Valenčič, V. (2005). Spatial fiber type distribution in normal human muscle: histochemical and tensiomyographical evaluation. Journal of biomechanics, 38(12), 2451-2459.

De Haan, A., Gerrits, K. H. L., & De Ruiter, C. J. (2009). Counterpoint: the interpolated twitch does not provide a valid measure of the voluntary activation of muscle.

Journal of Applied Physiology.

De Luca, C. J. (1997). The use of surface electromyography in biomechanics. Journal of applied biomechanics, 13(2), 135-163.

De Monte, G., & Arampatzis, A. (2009). In vivo moment generation and architecture of the human plantar flexors after different shortening–stretch cycles velocities. Journal of Electromyography and Kinesiology, 19(2), 322-330.

Dean, J. C., Yates, L. M., & Collins, D. F. (2007). Turning on the central contribution to contractions evoked by neuromuscular electrical stimulation. Journal of Applied Physiology, 103(1), 170–176. https://doi.org/10.1152/japplphysiol.01361.2006

Dean, Jesse C., Clair-Auger, J. M., Lagerquist, O., & Collins, D. F. (2014). Asynchronous recruitment of low-threshold motor units during repetitive, low-current stimulation of the human tibial nerve. Frontiers in Human Neuroscience, 8(DEC), 1–12. https://doi.org/10.3389/fnhum.2014.01002

Del Toro, D. R., & Park, T. A. (1996). Abductor hallucis false motor points: electrophysiologic mapping and cadaveric dissection. Muscle & Nerve: Official Journal of the American Association of Electrodiagnostic Medicine, 19(9), 1138-1143.

Del Vecchio, A., Negro, F., Holobar, A., Casolo, A., Folland, J. P., Felici, F., & Farina, D. (2019). You are as fast as your motor neurons: speed of recruitment and maximal discharge of motor neurons determine the maximal rate of force development in humans. The Journal of physiology, 597(9), 2445-2456.

Delitto, A., Strube, M. J., Shulman, A. D., & Minor, S. D. (1992). A Study of Discomfort with Electrical Stimulation. Physical Therapy, 72(6), 410–421. https://doi.org/10.1093/ptj/72.6.410

Di Filippo, E. S., Mancinelli, R., Marrone, M., Doria, C., Verratti, V., Toniolo, L., …

Pietrangelo, T. (2017). Neuromuscular electrical stimulation improves skeletal muscle regeneration through satellite cell fusion with myofibers in healthy elderly subjects. Journal of Applied Physiology, 123(3), 501–512. https://doi.org/10.1152/japplphysiol.00855.2016

Dideriksen, J. L., Muceli, S., Dosen, S., Laine, C. M., & Farina, D. (2015). Physiological recruitment of motor units by high-frequency electrical stimulation of afferent pathways. Journal of Applied Physiology, 118(3), 365–376. https://doi.org/10.1152/japplphysiol.00327.2014

Dirks, M. L., Wall, B. T., Snijders, T., Ottenbros, C. L. P., Verdijk, L. B., & van Loon, L. J. C. (2014). Neuromuscular electrical stimulation prevents muscle disuse atrophy during leg immobilization in humans. Acta Physiologica, 210(3), 628–641. https://doi.org/10.1111/apha.12200

Donnelly, C., Stegmüller, J., Blazevich, A. J., von Roten, F. C., Kayser, B., Neyroud, D., & Place, N. (2021). Modulation of torque evoked by wide-pulse, high-frequency neuromuscular electrical stimulation and the potential implications for rehabilitation and training. Scientific Reports, 11(1), 1-13.

Donoghue, D., & Stokes, E. K. (2009). How much change is true change? The minimum detectable change of the Berg Balance Scale in elderly people. Journal of Rehabilitation Medicine, 41(5), 343-346.

Doucet, B. M., Lam, A., & Griffin, L. (2012). Neuromuscular electrical stimulation for skeletal muscle function. The Yale Journal of Biology and Medicine, 85(2), 201–215. Retrieved from http://www.ncbi.nlm.nih.gov/pubmed/22737049

Dreibati, B., Lavet, C., Pinti, A., & Poumarat, G. (2010). Influence of electrical stimulation frequency on skeletal muscle force and fatigue. Annals of physical and rehabilitation medicine, 53(4), 266-277.

Duchateau, J., & Enoka, R. M. (2011). Human motor unit recordings: origins and insight into the integrated motor system. Brain research, 1409, 42-61.

Duchateau, J., & Hainaut, K. (1986). Nonlinear summation of contractions in striated muscle. I. Twitch potentiation in human muscle. Journal of Muscle Research & Cell Motility, 7(1), 11-17.

Duchateau, J., Semmler, J. G., & Enoka, R. M. (2006). Neural Changes Associated with Training Training adaptations in the behavior of human motor units. J Appl Physiol, 101(60), 1766–1775. https://doi.org/10.1152/japplphysiol.00543.2006.

Duchateau, J., Stragier, S., Baudry, S., & Carpentier, A. (2021). Strength Training: In Search of Optimal Strategies to Maximize Neuromuscular Performance. Exercise and Sport Sciences Reviews, 49(1), 2–14. https://doi.org/10.1249/JES.0000000000000234

Edwards, R. H. T., Young, A., Hosking, G. P., & Jones, D. A. (1977). Human Skeletal Muscle Function: Description of Tests and Normal Values. Clinical Science, 52(3), 283–290. https://doi.org/10.1042/cs0520283

Ellrich, J., Steffens, H., Treede, R. D., & Schomburg, E. D. (1998). The Hoffmann reflex of human plantar foot muscles. Muscle & Nerve: Official Journal of the American Association of Electrodiagnostic Medicine, 21(6), 732-738.

Enoka, R. M., Amiridis, I. G., & Duchateau, J. (2020). Electrical stimulation of muscle: electrophysiology and rehabilitation. Physiology.

Espeit, L., Rozand, V., Millet, G. Y., Gondin, J., Maffiuletti, N. A., & Lapole, T. (2021). Influence of wide-pulse neuromuscular electrical stimulation frequency and superimposed tendon vibration on occurrence and magnitude of extra torque. Journal of Applied Physiology.

Falla, D., & Farina, D. (2008). Non-uniform adaptation of motor unit discharge rates

during sustained static contraction of the upper trapezius muscle. Experimental Brain Research, 191(3), 363–370. https://doi.org/10.1007/s00221-008-1530-6

Farina, D., Merletti, R., & Enoka, R. M. (2004). The extraction of neural strategies from the surface EMG. Journal of applied physiology, 96(4), 1486-1495.

Farris, D. J., Kelly, L. A., Cresswell, A. G., & Lichtwark, G. A. (2019). The functional importance of human foot muscles for bipedal locomotion. Proceedings of the National Academy of Sciences of the United States of America, 116(5), 1645–1650. https://doi.org/10.1073/pnas.1812820116

Filipovic, A., Kleinöder, H., Dörmann, U., & Mester, J. (2011). Electromyostimulation—a systematic review of the influence of training regimens and stimulation parameters on effectiveness in electromyostimulation training of selected strength parameters. The Journal of Strength & Conditioning Research, 25(11), 3218-3238.

Filipovic, A., Kleinöder, H., Dörmann, U., & Mester, J. (2012). Electromyostimulation—a systematic review of the effects of different electromyostimulation methods on selected strength parameters in trained and elite athletes. The Journal of Strength & Conditioning Research, 26(9), 2600-2614.

Fiolkowski, P., Brunt, D., Bishop, M., Woo, R., & Horodyski, M. (2003). Intrinsic pedal musculature support of the medial longitudinal arch: an electromyography study. The Journal of Foot and Ankle Surgery, 42(6), 327–333. https://doi.org/10.1053/j.jfas.2003.10.003

Fitts, R. H. (1994). Cellular mechanisms of muscle fatigue. Physiological Reviews, 74(1), 49–94. https://doi.org/10.1152/physrev.1994.74.1.49

Fleshman, J. W., Munson, J. B., Sypert, G. W., & Friedman, W. A. (1981). Rheobase, input resistance, and motor-unit type in medial gastrocnemius motoneurons in the cat. Journal of Neurophysiology, 46(6), 1326-1338.

Folland, J. P., Irish, C. S., Roberts, J. C., Tarr, J. E., & Jones, D. A. (2002). Fatigue is not a necessary stimulus for strength gains during resistance training. British journal of sports medicine, 36(5), 370-373.

Fouré, A., Nosaka, K., Wegrzyk, J., Duhamel, G., Le Troter, A., Boudinet, H., ... & Gondin, J. (2014). Time course of central and peripheral alterations after isometric neuromuscular electrical stimulation-induced muscle damage. PLoS One, 9(9), e107298.

Franchi, M. V., Reeves, N. D., & Narici, M. V. (2017). Skeletal muscle remodeling in response to eccentric vs. concentric loading: morphological, molecular, and metabolic adaptations. Frontiers in physiology, 8, 447.

Frigon, A., Thompson, C. K., Johnson, M. D., Manuel, M., Hornby, T. G., & Heckman, C. J. (2011). Extra Forces Evoked during Electrical Stimulation of the Muscle or Its Nerve Are Generated and Modulated by a Length-Dependent Intrinsic Property of Muscle in Humans and Cats. Journal of Neuroscience, 31(15), 5579–5588. https://doi.org/10.1523/JNEUROSCI.6641-10.2011

Frimenko, R. E., Lievers, B., Coughlin, M. J., Anderson, R. B., Crandall, J. R., & Kent, R. W. (2012). Etiology and biomechanics of first metatarsophalangeal joint sprains (turf toe) in athletes. Critical Reviews™ in Biomedical Engineering, 40(1).

Fuglevand, A. J., & Keen, D. A. (2003). Re-Evaluation of Muscle Wisdom in the Human Adductor Pollicis using Physiological Rates of Stimulation. The Journal of Physiology, 549(3), 865–875. https://doi.org/10.1113/jphysiol.2003.038836

Galea, V. (2001). Electrical characteristics of human ankle dorsi-and plantar-flexor muscles. Comparative responses during fatiguing stimulation and recovery. European journal of applied physiology, 85(1), 130-140.

Gandevia, S. C., & McKenzie, D. K. (1988). Activation of human muscles at short muscle

lengths during maximal static efforts. The Journal of physiology, 407(1), 599-613.

Gandevia, S. C., Allen, G. M., Butler, J. E., & Taylor, J. L. (1996). Supraspinal factors in human muscle fatigue: evidence for suboptimal output from the motor cortex. The Journal of physiology, 490(2), 529-536.

Gandevia, S. C. (2001). Spinal and supraspinal factors in human muscle fatigue. Physiological reviews.

Gans, C. (1982). Fiber architecture and muscle function. Exercise and sport sciences reviews, 10(1), 160-207.

Gardiner, P. F. (2006). Changes in α-motoneuron properties with altered physical activity levels. Exercise and sport sciences reviews, 34(2), 54-58.

Gardiner, P., Dai, Y., & Heckman, C. J. (2006). Effects of exercise training on α-motoneurons. Journal of applied physiology, 101(4), 1228-1236.

Gazula, V. R., Roberts, M., Luzzio, C., Jawad, A. F., & Kalb, R. G. (2004). Effects of limb exercise after spinal cord injury on motor neuron dendrite structure. Journal of Comparative Neurology, 476(2), 130-145.

Geddes, L. A. (2004). Accuracy limitations of chronaxie values. IEEE Transactions on Biomedical Engineering, 51(1), 176-181.

Gillies, A. R., & Lieber, R. L. (2011). Structure and function of the skeletal muscle extracellular matrix. Muscle & nerve, 44(3), 318-331.

Glaviano, N. R., & Saliba, S. (2016). Can the use of neuromuscular electrical stimulation be improved to optimize quadriceps strengthening?. Sports Health, 8(1), 79-85.

Gobbo, M., Gaffurini, P., Bissolotti, L., Esposito, F., & Orizio, C. (2011). Transcutaneous neuromuscular electrical stimulation: influence of electrode positioning and stimulus amplitude settings on muscle response. European journal of applied physiology,

111(10), 2451-2459.

Gobbo, M., Maffiuletti, N. A., Orizio, C., & Minetto, M. A. (2014). Muscle motor point identification is essential for optimizing neuromuscular electrical stimulation use. Journal of neuroengineering and rehabilitation, 11(1), 1-6.

Goldmann, J. P., & Brüggemann, G. P. (2012). The potential of human toe flexor muscles to produce force. Journal of Anatomy, 221(2), 187-194.

Gomes, G. K., Franco, C. M., Nunes, P. R. P., & Orsatti, F. L. (2019). High-frequency resistance training is not more effective than low-frequency resistance training in increasing muscle mass and strength in well-trained men. The Journal of Strength & Conditioning Research, 33, S130-S139.

Gómez-Pinilla, F., Ying, Z., Roy, R. R., Molteni, R., & Edgerton, V. R. (2002). Voluntary exercise induces a BDNF-mediated mechanism that promotes neuroplasticity. Journal of neurophysiology, 88(5), 2187-2195.

Gondin, J., Brocca, L., Bellinzona, E., d'Antona, G., Maffiuletti, N. A., Miotti, D., ... & Bottinelli, R. (2011). Neuromuscular electrical stimulation training induces atypical adaptations of the human skeletal muscle phenotype: a functional and proteomic analysis. Journal of applied physiology, 110(2), 433-450.

Gondin, J., Duclay, J., & Martin, A. (2006). Soleus- and Gastrocnemii-Evoked V-Wave Responses Increase After Neuromuscular Electrical Stimulation Training. Journal of Neurophysiology, 95(6), 3328–3335. https://doi.org/10.1152/jn.01002.2005

Gondin, J., Guette, M., Ballay, Y., & Martin, A. (2005). Electromyostimulation training effects on neural drive and muscle architecture. Medicine & Science in Sports & Exercise, 37(8), 1291–1299. https://doi.org/10.1249/01.mss.0000175090.49048.41

Gondin, J., Giannesini, B., Vilmen, C., Dalmasso, C., Le Fur, Y., Cozzone, P. J., & Bendahan, D. (2010). Effects of stimulation frequency and pulse duration on fatigue

and metabolic cost during a single bout of neuromuscular electrical stimulation. Muscle & Nerve: Official Journal of the American Association of Electrodiagnostic Medicine, 41(5), 667-678.

Goo, Y. M., Kim, T. H., & Lim, J. Y. (2016). The effects of gluteus maximus and abductor hallucis strengthening exercises for four weeks on navicular drop and lower extremity muscle activity during gait with flatfoot. Journal of physical therapy science, 28(3), 911-915.

Gooding, T. M., Feger, M. A., Hart, J. M., & Hertel, J. (2016). Intrinsic foot muscle activation during specific exercises: a T2 time magnetic resonance imaging study. Journal of athletic training, 51(8), 644-650.

Gordon, D. A., Enoka, R. M., & Stuart, D. G. (1990). Motor-unit force potentiation in adult cats during a standard fatigue test. The Journal of physiology, 421(1), 569-582.

Gorgey, A. S., Mahoney, E., Kendall, T., & Dudley, G. A. (2006). Effects of neuromuscular electrical stimulation parameters on specific tension. European journal of applied physiology, 97(6), 737-744.

Gorgey, A. S., & Dudley, G. A. (2008). The role of pulse duration and stimulation duration in maximizing the normalized torque during neuromuscular electrical stimulation. journal of orthopaedic & sports physical therapy, 38(8), 508-516.

Gorgey, A. S., Black, C. D., Elder, C. P., & Dudley, G. A. (2009). Effects of electrical stimulation parameters on fatigue in skeletal muscle. journal of orthopaedic & sports physical therapy, 39(9), 684-692.

Gregory, C. M., & Bickel, C. S. (2005). Recruitment Patterns in Human Skeletal Muscle During Electrical Stimulation. Physical Therapy, 85(4), 358–364. https://doi.org/10.1093/ptj/85.4.358

Gregory, C. M., Dixon, W., & Bickel, C. S. (2007). Impact of varying pulse frequency and

duration on muscle torque production and fatigue. Muscle & Nerve, 35(4), 504–509. https://doi.org/10.1002/mus.20710

Grosprêtre, S., Gueugneau, N., Martin, A., & Lepers, R. (2017). Central Contribution to Electrically Induced Fatigue depends on Stimulation Frequency. Medicine and Science in Sports and Exercise, 49(8), 1530–1540. https://doi.org/10.1249/MSS.0000000000001270

Grosprêtre, S., Gueugneau, N., Martin, A., & Lepers, R. (2018). Presynaptic inhibition mechanisms may subserve the spinal excitability modulation induced by neuromuscular electrical stimulation. Journal of Electromyography and Kinesiology, 40(April), 95–101. https://doi.org/10.1016/j.jelekin.2018.04.012

Grosset, J.-F., Canon, F., Pérot, C., & Lambertz, D. (2014). Changes in contractile and elastic properties of the triceps surae muscle induced by neuromuscular electrical stimulation training. European Journal of Applied Physiology, 114(7), 1403–1411. https://doi.org/10.1007/s00421-014-2871-4

Gueugneau, N., Grosprêtre, S., Stapley, P., & Lepers, R. (2017). High-frequency neuromuscular electrical stimulation modulates interhemispheric inhibition in healthy humans. Journal of Neurophysiology, 117(1), 467–475. https://doi.org/10.1152/jn.00355.2016

Hainaut, K., & Duchateau, J. (1992). Neuromuscular Electrical Stimulation and Voluntary Exercise. Sports Medicine, 14(2), 100–113. https://doi.org/10.2165/00007256-199214020-00003

Headlee, D. L., Leonard, J. L., Hart, J. M., Ingersoll, C. D., & Hertel, J. (2008). Fatigue of the plantar intrinsic foot muscles increases navicular drop. Journal of Electromyography and Kinesiology, 18(3), 420–425. https://doi.org/10.1016/j.jelekin.2006.11.004

Heckman, C. J., & Binder, M. D. (1991). Computer simulation of the steady-state input-output function of the cat medial gastrocnemius motoneuron pool. Journal of neurophysiology, 65(4), 952-967.

Heckman, C. J., & Enoka, R. M. (2012). Motor Unit. In Comprehensive Physiology (Vol. 2, pp. 2629–2682). Hoboken, NJ, USA: John Wiley & Sons, Inc. https://doi.org/10.1002/cphy.c100087

Heo, H. J., Koo, Y. M., & Yoo, W. G. (2011). Comparison of selective activation of the abductor hallucis during various exercises. Journal of physical therapy science, 23(6), 915-918.

Herbert, R. D., & Gandevia, S. C. (1999). Twitch interpolation in human muscles: Mechanisms and implications for measurement of voluntary activation. Journal of Neurophysiology, 82(5), 2271–2283. https://doi.org/10.1152/jn.1999.82.5.2271

Herbert, R. D., & Gandevia, S. C. (1996). Muscle activation in unilateral and bilateral efforts assessed by motor nerve and cortical stimulation. Journal of Applied Physiology, 80(4), 1351-1356.

Herrero, J. A., Izquierdo, M., Maffiuletti, N. A., & Garcia-Lopez, J. (2006). Electromyostimulation and plyometric training effects on jumping and sprint time. International journal of sports medicine, 27(07), 533-539.

Herzig, D., Maffiuletti, N. A., & Eser, P. (2015). The Application of Neuromuscular Electrical Stimulation Training in Various Non-neurologic Patient Populations: A Narrative Review. PM & R: The Journal of Injury, Function, and Rehabilitation, 7(11), 1167–1178. https://doi.org/10.1016/j.pmrj.2015.03.022

Herzog, W. (2018). The multiple roles of titin in muscle contraction and force production. Biophysical Reviews, 10(4), 1187-1199.

Hill, A. V. (1938). The heat of shortening and the dynamic constants of muscle.

Proceedings of the Royal Society of London. Series B-Biological Sciences, 126(843), 136-195.

Holcomb, W. R. (2006). Combating force decline across repetitions when using NMES. International Journal of Athletic Therapy and Training, 11(3), 20-22.

Holtermann, A., Roeleveld, K., Engstrøm, M., & Sand, T. (2007). Enhanced H-reflex with resistance training is related to increased rate of force development. European journal of applied physiology, 101(3), 301-312.

Howlett, O. A., Lannin, N. A., Ada, L., & McKinstry, C. (2015). Functional electrical stimulation improves activity after stroke: a systematic review with meta-analysis. Archives of physical medicine and rehabilitation, 96(5), 934-943.

Huxley, A. F. (1957). Muscle structure and theories of contraction. Prog. Biophys. Biophys. Chem, 7, 255-318.

Jacob, H. A. C. (2001). Forces acting in the forefoot during normal gait–an estimate. Clinical Biomechanics, 16(9), 783-792.

James, D. C., Chesters, T., Sumners, D. P., Cook, D. P., Green, D. A., & Mileva, K. N. (2013). Wide-Pulse Electrical Stimulation to an Intrinsic Foot Muscle Induces Acute Functional Changes in Forefoot–Rearfoot Coupling Behaviour during Walking. International journal of sports medicine, 34(05), 438-443.

James, D. C., Solan, M. C., & Mileva, K. N. (2018). Wide-pulse, high-frequency, low-intensity neuromuscular electrical stimulation has potential for targeted strengthening of an intrinsic foot muscle: a feasibility study. Journal of foot and ankle research, 11(1), 1-10.

Jang, S. H., & Seo, Y. S. (2018). Effect of neuromuscular electrical stimulation training on the finger extensor muscles for the contralateral corticospinal tract in normal subjects: a diffusion tensor tractography study. Frontiers in human neuroscience,

12, 432.

Johns, R. K., & Fuglevand, A. J. (2011). Number of motor units in human abductor hallucis. Muscle & Nerve, 43(6), 895–896. https://doi.org/10.1002/mus.22071

Johnson, M. I., Paley, C. A., Howe, T. E., & Sluka, K. A. (2015). Transcutaneous electrical nerve stimulation for acute pain. Cochrane Database of Systematic Reviews, (6).

Jones, D. A., Bigland-Ritchie, B., & Edwards, R. H. T. (1979). Excitation frequency and muscle fatigue: Mechanical responses during voluntary and stimulated contractions. Experimental Neurology, 64(2), 401–413. https://doi.org/10.1016/0014-4886(79)90279-6

Jones, S., Man, W. D. C., Gao, W., Higginson, I. J., Wilcock, A., & Maddocks, M. (2016). Neuromuscular electrical stimulation for muscle weakness in adults with advanced disease. Cochrane database of systematic reviews, (10).

Jones, D. A. (1996). High-and low-frequency fatigue revisited. Acta Physiologica Scandinavica, 156(3), 265-270.

Joseph, M. S., Tillakaratne, N. J., & de Leon, R. D. (2012). Treadmill training stimulates brain-derived neurotrophic factor mRNA expression in motor neurons of the lumbar spinal cord in spinally transected rats. Neuroscience, 224, 135-144.

Joseph, J. (1954). Range of movement of the great toe in men. The Journal of Bone and Joint Surgery. British volume, 36(3), 450-457.

Jubeau, M., Zory, R., Gondin, J., Martin, A., & Maffiuletti, N. A. (2006). Late neural adaptations to electrostimulation resistance training of the plantar flexor muscles. European journal of applied physiology, 98(2), 202-211.

Jung, D.-Y., Kim, M.-H., Koh, E.-K., Kwon, O.-Y., Cynn, H.-S., & Lee, W.-H. (2011). A

comparison in the muscle activity of the abductor hallucis and the medial longitudinal arch angle during toe curl and short foot exercises. Physical Therapy in Sport, 12(1), 30–35. https://doi.org/10.1016/j.ptsp.2010.08.001

Kadri, M. A., Noé, F., Nouar, M. B., & Paillard, T. (2017). Effects of training programs based on ipsilateral voluntary and stimulated contractions on muscle strength and monopedal postural control of the contralateral limb. European journal of applied physiology, 117(9), 1799-1806.

Karamanidis, K., & Arampatzis, A. (2005). Mechanical and morphological properties of different muscle–tendon units in the lower extremity and running mechanics: effect of aging and physical activity. Journal of Experimental Biology, 208(20), 3907-3923.

Karu, Z. Z., Durfee, W. K., & Barzilai, A. M. (1995). Reducing muscle fatigue in FES applications by stimulating with N-let pulse trains. IEEE Transactions on Biomedical Engineering, 42(8), 809-817.

Keeton, R. B., & Binder-Macleod, S. A. (2006). Low-frequency fatigue. Physical Therapy, 86(8), 1146–1150. Retrieved from http://www.ncbi.nlm.nih.gov/pubmed/16879048

Kelly, L. A., Cresswell, A. G., Racinais, S., Whiteley, R., & Lichtwark, G. (2014). Intrinsic foot muscles have the capacity to control deformation of the longitudinal arch. Journal of The Royal Society Interface, 11(93), 20131188.

Kelly, L. A., Kuitunen, S., Racinais, S., & Cresswell, A. G. (2012). Recruitment of the plantar intrinsic foot muscles with increasing postural demand. Clinical Biomechanics, 27(1), 46–51. https://doi.org/10.1016/j.clinbiomech.2011.07.013

Kelly, L. A., Lichtwark, G., & Cresswell, A. G. (2015). Active regulation of longitudinal arch compression and recoil during walking and running. Journal of The Royal Society Interface, 12(102), 20141076. https://doi.org/10.1098/rsif.2014.1076

Kelly, L. A., Racinais, S., & Cresswell, A. G. (2013). Discharge properties of abductor

hallucis before, during, and after an isometric fatigue task. Journal of Neurophysiology, 110(4), 891–898. https://doi.org/10.1152/jn.00944.2012

Kent-Braun, J. A., Fitts, R. H., & Christie, A. (2011). Skeletal muscle fatigue. Comprehensive Physiology, 2(2), 997-1044.

Kiernan, M. C., Lin, C. S. Y., & Burke, D. (2004). Differences in activity-dependent hyperpolarization in human sensory and motor axons. The Journal of physiology, 558(1), 341-349.

Kiernan, M. C., Cikurel, K., & Bostock, H. (2001). Effects of temperature on the excitability properties of human motor axons. Brain, 124(4), 816-825.

Kim, M.-H., Kwon, O.-Y., Kim, S.-H., & Jung, D.-Y. (2013). Comparison of muscle activities of abductor hallucis and adductor hallucis between the short foot and toe-spread-out exercises in subjects with mild hallux valgus. Journal of Back and Musculoskeletal Rehabilitation, 26(2), 163–168. https://doi.org/10.3233/BMR-2012-00363

Kim, M.-H., Yi, C.-H., Weon, J.-H., Cynn, H.-S., Jung, D.-Y., & Kwon, O.-Y. (2015). Effect of toe-spread-out exercise on hallux valgus angle and cross-sectional area of abductor hallucis muscle in subjects with hallux valgus. Journal of Physical Therapy Science, 27(4), 1019–1022. https://doi.org/10.1589/jpts.27.1019

Kirby, K. A. (2017). Longitudinal arch load-sharing system of the foot. Revista Española de Podología, 28(1), e18–e26. https://doi.org/10.1016/j.repod.2017.03.003

Klakowicz, P. M., Baldwin, E. R., & Collins, D. F. (2006). Contribution of M-waves and H-reflexes to contractions evoked by tetanic nerve stimulation in humans. Journal of neurophysiology, 96(3), 1293-1302.

Knellwolf, T. P., Burton, A. R., Hammam, E., & Macefield, V. G. (2019). Firing properties of muscle spindles supplying the intrinsic foot muscles of humans in unloaded and

freestanding conditions. Journal of Neurophysiology, 121(1), 74–84. https://doi.org/10.1152/jn.00539.2018

Knikou, M. (2008). The H-reflex as a probe: pathways and pitfalls. Journal of neuroscience methods, 171(1), 1-12.

Kouzaki, K., Nosaka, K., Ochi, E., & Nakazato, K. (2016). Increases in M-wave latency of biceps brachii after elbow flexor eccentric contractions in women. European journal of applied physiology, 116(5), 939-946.

Krutki, P., Mrówczyński, W., Bączyk, M., Łochyński, D., & Celichowski, J. (2017). Adaptations of motoneuron properties after weight-lifting training in rats. Journal of Applied Physiology, 123(3), 664-673.

Kura, H., Luo, Z.-P., Kitaoka, H. B., & An, K.-N. (1997). Quantitative analysis of the intrinsic muscles of the foot. The Anatomical Record, 249(1), 143–151. https://doi.org/10.1002/(SICI)1097-0185(199709)249:1<143::AID-AR17>3.0.CO;2-P

Kurihara, T., Yamauchi, J., Otsuka, M., Tottori, N., Hashimoto, T., & Isaka, T. (2014). Maximum toe flexor muscle strength and quantitative analysis of human plantar intrinsic and extrinsic muscles by a magnetic resonance imaging technique. Journal of foot and ankle research, 7(1), 1-6.

Lagerquist, O., Walsh, L. D., Blouin, J. S., Collins, D. F., & Gandevia, S. C. (2009). Effect of a peripheral nerve block on torque produced by repetitive electrical stimulation. Journal of Applied Physiology, 107(1), 161-167.

Lagerquist, O., & Collins, D. F. (2010). Influence of stimulus pulse width on M-waves, H-reflexes, and torque during tetanic low-intensity neuromuscular stimulation. Muscle & nerve, 42(6), 886-893.

Lake, D. A. (1992). Neuromuscular electrical stimulation. Sports medicine, 13(5), 320-

336.

Lakin, R. C., DeGnore, L. T., & Pienkowski, D. (2001). Contact mechanics of normal tarsometatarsal joints. JBJS, 83(4), 520.

Langeard, A., Bigot, L., Loggia, G., Bherer, L., Chastan, N., & Gauthier, A. (2021). Ankle dorsiflexors and plantarflexors neuromuscular electrical stimulation training impacts gait kinematics in older adults: A pilot study. Gait & Posture, 84, 335-339.

Latey, P. J., Burns, J., Nightingale, E. J., Clarke, J. L., & Hiller, C. E. (2018). Reliability and correlates of cross-sectional area of abductor hallucis and the medial belly of the flexor hallucis brevis measured by ultrasound. Journal of foot and ankle research, 11(1), 1-11.

Leardini, A., Stagni, R., & O'Connor, J. J. (2001). Mobility of the subtalar joint in the intact ankle complex. Journal of biomechanics, 34(6), 805-809.

Létocart, A., & Grosset, J. F. (2021). Achilles Tendon Adaptation to Neuromuscular Electrical Stimulation: Morphological and Mechanical Changes. International Journal of Sports Medicine, 42(07), 651-661.

Lieber, R. L., & Bodine-Fowler, S. C. (1993). Skeletal muscle mechanics: implications for rehabilitation. Physical therapy, 73(12), 844-856.

Luu, M. J., Jones, K. E., & Collins, D. F. (2021). Decreased excitability of motor axons contributes substantially to contraction fatigability during neuromuscular electrical stimulation. Applied Physiology, Nutrition, and Metabolism, 46(4), 346-355.

Lynn, S. K., Padilla, R. A., & Tsang, K. K. W. (2012). Differences in Static- and Dynamic-Balance Task Performance After 4 Weeks of Intrinsic-Foot-Muscle Training: The Short-Foot Exercise Versus the Towel-Curl Exercise. Journal of Sport Rehabilitation, 21(4), 327–333. https://doi.org/10.1123/jsr.21.4.327

MacIntosh, B. R., & Willis, J. C. (2000). Force-frequency relationship and potentiation in mammalian skeletal muscle. Journal of Applied Physiology, 88(6), 2088–2096. https://doi.org/10.1152/jappl.2000.88.6.2088

Macefield, V. G., Fuglevand, A. J., & Bigland-Ritchie, B. R. E. N. D. A. (1996). Contractile properties of single motor units in human toe extensors assessed by intraneural motor axon stimulation. Journal of neurophysiology, 75(6), 2509-2519.

Maddocks, M., Gao, W., Higginson, I. J., & Wilcock, A. (2013). Neuromuscular electrical stimulation for muscle weakness in adults with advanced disease. Cochrane Database of Systematic Reviews, (1).

Maddocks, M., Nolan, C. M., Man, W. D. C., Polkey, M. I., Hart, N., Gao, W., … Higginson, I. J. (2016). Neuromuscular electrical stimulation to improve exercise capacity in patients with severe COPD: a randomised double-blind, placebo-controlled trial. The Lancet Respiratory Medicine, 4(1), 27–36. https://doi.org/10.1016/S2213-2600(15)00503-2

Maffiuletti, N. A. (2010). Physiological and methodological considerations for the use of neuromuscular electrical stimulation. European journal of applied physiology, 110(2), 223-234.

Maffiuletti, N. A., & Martin, A. L. A. I. N. (2001). Progressive versus rapid rate of contraction during 7 wk of isometric resistance training. Medicine and science in sports and exercise, 33(7), 1220-1227.

Maffiuletti, N. A., Pensini, M., & Martin, A. (2002). Activation of human plantar flexor muscles increases after electromyostimulation training. Journal of applied physiology, 92(4), 1383-1392.

Maffiuletti, N. A., Minetto, M. A., Farina, D., & Bottinelli, R. (2011). Electrical stimulation for neuromuscular testing and training: state-of-the art and unresolved issues.

Maffiuletti, N. A., Roig, M., Karatzanos, E., & Nanas, S. (2013). Neuromuscular electrical stimulation for preventing skeletal-muscle weakness and wasting in critically ill patients: a systematic review. BMC medicine, 11(1), 1-10.

Maffiuletti, N. A., Gondin, J., Place, N., Stevens-Lapsley, J., Vivodtzev, I., & Minetto, M. A. (2018). Clinical use of neuromuscular electrical stimulation for neuromuscular rehabilitation: what are we overlooking?. Archives of physical medicine and rehabilitation, 99(4), 806-812.

Maffiuletti, N. A., Green, D. A., Vaz, M. A., & Dirks, M. L. (2019). Neuromuscular electrical stimulation as a potential countermeasure for skeletal muscle atrophy and weakness during human spaceflight. Frontiers in physiology, 10, 1031.

Maganaris, C. N. (2001). Force–length characteristics of in vivo human skeletal muscle. Acta Physiologica Scandinavica, 172(4), 279-285.

Mancinelli, R., Toniolo, L., Di Filippo, E. S., Doria, C., Marrone, M., Maroni, C. R., ... & Fulle, S. (2019). Neuromuscular electrical stimulation induces skeletal muscle fiber remodeling and specific gene expression profile in healthy elderly. Frontiers in physiology, 10, 1459.

Mandrile, F., Farina, D., Pozzo, M., & Merletti, R. (2003). Stimulation artifact in surface EMG signal: effect of the stimulation waveform, detection system, and current amplitude using hybrid stimulation technique. IEEE Transactions on neural systems and rehabilitation engineering, 11(4), 407-415.

Mang, C. S., Lagerquist, O., & Collins, D. F. (2010). Changes in corticospinal excitability evoked by common peroneal nerve stimulation depend on stimulation frequency. Experimental Brain Research, 203(1), 11–20. https://doi.org/10.1007/s00221-010-2202-x

Martin, A., Grosprêtre, S., Vilmen, C., Guye, M., Mattei, J. P., Bendahan, D., & Gondin,

J. (2016). The Etiology of Muscle Fatigue Differs between Two Electrical Stimulation Protocols. Medicine and science in sports and exercise, 48(8), 1474-1484.

Mason, J., Frazer, A. K., Avela, J., Pearce, A. J., Howatson, G., & Kidgell, D. J. (2020). Tracking the corticospinal responses to strength training. European journal of applied physiology, 1-16.

Matheson, G. O., Dunlop, R. J., McKenzie, D. C., Smith, C. F., & Allen, P. S. (1997). Force output and energy metabolism during neuromuscular electrical stimulation: a 31P-NMR study. Scandinavian journal of rehabilitation medicine, 29(3), 175-180.

Matsumoto, M., & Yamamoto, K. (2022). Foot arch height, toe flexor strength, and dynamic balance ability in collegiate female dancers and non-dancers. Journal of Physical Therapy Science, 34(2), 135-139.

Matkowski, B., Lepers, R., & Martin, A. (2015). Torque decrease during submaximal evoked contractions of the quadriceps muscle is linked not only to muscle fatigue. Journal of Applied Physiology, 118(9), 1136-1144.

McKeon, P. O., Hertel, J., Bramble, D., & Davis, I. (2015). The foot core system: a new paradigm for understanding intrinsic foot muscle function. British Journal of Sports Medicine, 49(5), 290–290. https://doi.org/10.1136/bjsports-2013-092690

McNeil, C. J., Butler, J. E., Taylor, J. L., & Gandevia, S. C. (2013). Testing the excitability of human motoneurones. Frontiers in Human Neuroscience, 7(APR 2013), 1–9. https://doi.org/10.3389/fnhum.2013.00152

Merletti, R., Knaflitz, M., & De Luca, C. J. (1990). Myoelectric manifestations of fatigue in voluntary and electrically elicited contractions. Journal of applied physiology, 69(5), 1810-1820.

Merrill, D. R., Bikson, M., & Jefferys, J. G. (2005). Electrical stimulation of excitable tissue: design of efficacious and safe protocols. Journal of neuroscience methods,

141(2), 171-198.

Merton, P. A. (1954). Voluntary strength and fatigue. The Journal of Physiology, 123(3), 553–564. https://doi.org/10.1113/jphysiol.1954.sp005070

Mesin, L., Merlo, E., Merletti, R., & Orizio, C. (2010). Investigation of motor unit recruitment during stimulated contractions of tibialis anterior muscle. Journal of Electromyography and Kinesiology, 20(4), 580-589.

Mettler, J. A., & Griffin, L. (2010). What are the stimulation parameters that affect the extent of twitch force potentiation in the adductor pollicis muscle?. European journal of applied physiology, 110(6), 1235-1242.

Mettler, J. A., Magee, D. M., & Doucet, B. M. (2018). High-frequency neuromuscular electrical stimulation increases anabolic signaling. Medicine and science in sports and exercise, 50(8), 1540-1548.

Mickle, K. J., Nester, C. J., Crofts, G., & Steele, J. R. (2013). Reliability of ultrasound to measure morphology of the toe flexor muscles. Journal of Foot and Ankle Research, 6(1), 12. https://doi.org/10.1186/1757-1146-6-12

Mickle, K. J., & Nester, C. J. (2018). Morphology of the toe flexor muscles in older adults with toe deformities. Arthritis care & research, 70(6), 902-907.

Mignardot, J. B., Deschamps, T., Le Goff, C. G., Roumier, F. X., Duclay, J., Martin, A., ... & Cornu, C. (2015). Neuromuscular electrical stimulation leads to physiological gains enhancing postural balance in the pre-frail elderly. Physiological reports, 3(7), e12471.

Minetto, M. A., Holobar, A., Botter, A., & Farina, D. (2009). Discharge Properties of Motor Units of the Abductor Hallucis Muscle During Cramp Contractions. Journal of Neurophysiology, 102(3), 1890–1901. https://doi.org/10.1152/jn.00309.2009

Minetto, M., Botter, A., Bottinelli, O., Miotti, D., Bottinelli, R., & D'Antona, G. (2013). Variability in Muscle Adaptation to Electrical Stimulation. International Journal of Sports Medicine, 34(06), 544–553. https://doi.org/10.1055/s-0032-1321799

Miyazaki, S., & Yamamoto, S. (1993). Moment acting at the metatarsophalangeal joints during normal barefoot level walking. Gait & Posture, 1(3), 133–140. https://doi.org/10.1016/0966-6362(93)90054-5

Mogyoros, I., Kiernan, M. C., & Burke, D. (1996). Strength-duration properties of human peripheral nerve. Brain, 119(2), 439–447. https://doi.org/10.1093/brain/119.2.439

Moran, U., Gottlieb, U., Gam, A., & Springer, S. (2019). Functional electrical stimulation following anterior cruciate ligament reconstruction: a randomized controlled pilot study. Journal of neuroengineering and rehabilitation, 16(1), 1-9.

Mortimer, J. T., & Bhadra, N. (2009). Fundamentals of electrical stimulation. In Neuromodulation (pp. 109-121). Academic Press.

Mortka, K., Wiertel-Krawczuk, A., & Lisiński, P. (2020). Muscle Activity Detectors—Surface Electromyography in the Evaluation of Abductor Hallucis Muscle. Sensors, 20(8), 2162.

Mulligan, E. P., & Cook, P. G. (2013). Effect of plantar intrinsic muscle training on medial longitudinal arch morphology and dynamic function. Manual Therapy, 18(5), 425–430. https://doi.org/10.1016/j.math.2013.02.007

Muscolino, J. E. (2016). The muscular system manual-E-Book: the skeletal muscles of the human body. Elsevier Health Sciences.

Nakagawa, K., Bergquist, A. J., Yamashita, T., Yoshida, T., & Masani, K. (2020). Motor point stimulation primarily activates motor nerve. Neuroscience Letters, 736, 135246.

Narici, Marco, Franchi, M., & Maganaris, C. (2016). Muscle structural assembly and functional consequences. The Journal of Experimental Biology, 219(Pt 2), 276–284. https://doi.org/10.1242/jeb.128017

Natsume, T., Ozaki, H., Saito, A., Abe, T., & Naito, H. (2015). Effects of electrostimulation with blood flow restriction on muscle size and strength. Medicine and science in sports and exercise, 47(12), 2621-2627.

Natsume, T., Ozaki, H., Kakigi, R., Kobayashi, H., & Naito, H. (2018). Effects of training intensity in electromyostimulation on human skeletal muscle. European Journal of Applied Physiology, 118(7), 1339–1347. https://doi.org/10.1007/s00421-018-3866-3

Nester, C., Bowker, P., & Bowden, P. (2002). Kinematics of the midtarsal joint during standing leg rotation. Journal of the American Podiatric Medical Association, 92(2), 77-81.

Nester, C. J., Jarvis, H. L., Jones, R. K., Bowden, P. D., & Liu, A. (2014). Movement of the human foot in 100 pain free individuals aged 18–45: implications for understanding normal foot function. Journal of foot and ankle research, 7(1), 1-10.

Newsham, K. R. (2010). Strengthening the Intrinsic Foot Muscles. Athletic Therapy Today, 15(1), 32–35. https://doi.org/10.1123/att.15.1.32

Neyroud, D., Dodd, D., Gondin, J., Maffiuletti, N. A., Kayser, B., & Place, N. (2014). Wide-pulse-high-frequency neuromuscular stimulation of triceps surae induces greater muscle fatigue compared with conventional stimulation. Journal of Applied Physiology, 116(10), 1281–1289. https://doi.org/10.1152/japplphysiol.01015.2013

Neyroud, D., Gonzalez, M., Mueller, S., Agostino, D., Grosprêtre, S., Maffiuletti, N. A., ... & Place, N. (2019). Neuromuscular adaptations to wide-pulse high-frequency neuromuscular electrical stimulation training. European journal of applied

physiology, 119(5), 1105-1116.

Neyroud, D., Cheng, A. J., Bourdillon, N., Kayser, B., Place, N., & Westerblad, H. (2016). Muscle fatigue affects the interpolated twitch technique when assessed using electrically-induced contractions in human and rat muscles. Frontiers in physiology, 7, 252.

Neyroud, D., Grosprêtre, S., Gondin, J., Kayser, B., & Place, N. (2018). Test–retest reliability of wide-pulse high-frequency neuromuscular electrical stimulation evoked force. Muscle & nerve, 57(1), E70-E77.

Nix, S., Smith, M., & Vicenzino, B. (2010). Prevalence of hallux valgus in the general population: a systematic review and meta-analysis. Journal of foot and ankle research, 3(1), 1-9.

O'Leary, D. D., Hope, K., & Sale, D. G. (1997). Posttetanic potentiation of human dorsiflexors. Journal of Applied Physiology, 83(6), 2131-2138.

Okuma, Y., Bergquist, A. J., Hong, M., Chan, K. M., & Collins, D. F. (2013). Electrical stimulation site influences the spatial distribution of motor units recruited in tibialis anterior. Clinical Neurophysiology, 124(11), 2257-2263.

Oskouei, M. A. E., Van Mazijk, B. C. F., Schuiling, M. H. C., & Herzog, W. (2003). Variability in the interpolated twitch torque for maximal and submaximal voluntary contractions. Journal of Applied Physiology, 95(4), 1648–1655. https://doi.org/10.1152/japplphysiol.01189.2002

Packman-Braun, R. (1988). Relationship Between Functional Electrical Stimulation Duty Cycle and Fatigue in Wrist Extensor Muscles of Patients with Hemiparesis. Physical Therapy, 68(1), 51–56. https://doi.org/10.1093/ptj/68.1.51

Palmieri, R. M., Ingersoll, C. D., & Hoffman, M. A. (2004). The Hoffmann reflex: Methodologic considerations and applications for use in sports medicine and

athletic training research. Journal of Athletic Training, 39(3), 268–277.

Papaiordanidou, M., Varray, A., Fattal, C., & Guiraud, D. (2014). Neural and muscular mechanisms of electrically induced fatigue in patients with spinal cord injury. Spinal Cord, 52(3), 246–250. https://doi.org/10.1038/sc.2013.172

Papaiordanidou, Maria, Billot, M., Varray, A., & Martin, A. (2014). Neuromuscular Fatigue Is Not Different between Constant and Variable Frequency Stimulation. PLoS ONE, 9(1), e84740. https://doi.org/10.1371/journal.pone.0084740

Park, H., & Poo, M. M. (2013). Neurotrophin regulation of neural circuit development and function. Nature Reviews Neuroscience, 14(1), 7-23.

Paton, M. E., & Brown, J. M. M. (1994). An electromyographic analysis of functional differentiation in human pectoralis major muscle. Journal of Electromyography and Kinesiology, 4(3), 161–169. https://doi.org/10.1016/1050-6411(94)90017-5

Pierrot-Deseilligny, E., Bussel, B., Held, J. P., & Katz, R. (1976). Excitability of human motoneurones after discharge in a conditioning reflex. Electroencephalography and clinical neurophysiology, 40(3), 279-287.

Place, N., Yamada, T., Bruton, J. D., & Westerblad, H. (2010). Muscle fatigue: from observations in humans to underlying mechanisms studied in intact single muscle fibres. European Journal of Applied Physiology, 110(1), 1–15. https://doi.org/10.1007/s00421-010-1480-0

Quittan, M., Wiesinger, G. F., Sturm, B., Puig, S., Mayr, W., Sochor, A., … Fialka-Moser, V. (2001). Improvement of Thigh Muscles by Neuromuscular Electrical Stimulation in Patients with Refractory Heart Failure. American Journal of Physical Medicine & Rehabilitation, 80(3), 206–214. https://doi.org/10.1097/00002060-200103000-00011

Rampichini, S., Cè, E., Limonta, E., & Esposito, F. (2014). Effects of fatigue on the

electromechanical delay components in gastrocnemius medialis muscle. European Journal of Applied Physiology, 114(3), 639–651. https://doi.org/10.1007/s00421-013-2790-9

Rankin, R. R., & Stokes, M. J. (1992). Fatigue effects of rest intervals during electrical stimulation of the human quadriceps muscle. Clinical Rehabilitation, 6(3), 195–201. https://doi.org/10.1177/026921559200600303

Rassier, D. E., MacIntosh, B. R., & Herzog, W. (1999). Length dependence of active force production in skeletal muscle. Journal of applied physiology, 86(5), 1445-1457.

Ratkevičius, A., Mizuno, M., Povilonis, E., & Quistorff, B. (1998). Energy metabolism of the gastrocnemius and soleus muscles during isometric voluntary and electrically induced contractions in man. The Journal of physiology, 507(Pt 2), 593.

Reeves, N. D., & Narici, M. V. (2003). Behavior of human muscle fascicles during shortening and lengthening contractions in vivo. Journal of applied physiology, 95(3), 1090-1096.

Rich, C., & Cafarelli, E. (2000). Submaximal motor unit firing rates after 8 wk of isometric resistance training. Medicine and science in sports and exercise, 32(1), 190-196.

Ridge, S. T., Myrer, J. W., Olsen, M. T., Jurgensmeier, K., & Johnson, A. W. (2017). Reliability of doming and toe flexion testing to quantify foot muscle strength. Journal of Foot and Ankle Research, 10(1), 55. https://doi.org/10.1186/s13047-017-0237-y

Rolian, C., Lieberman, D. E., Hamill, J., Scott, J. W., & Werbel, W. (2009). Walking, running and the evolution of short toes in humans. Journal of Experimental Biology, 212(5), 713–721. https://doi.org/10.1242/jeb.019885

Russ, D. W., & Binder-Macleod, S. A. (1999). Variable-frequency trains offset low-frequency fatigue in human skeletal muscle. Muscle & Nerve: Official Journal of the

American Association of Electrodiagnostic Medicine, 22(7), 874-882.

Sale, D. G. (2002). Postactivation potentiation: role in human performance. Exercise and sport sciences reviews, 30(3), 138-143.

Scaglioni, G., Ferri, A., Minetti, A. E., Martin, A., Van Hoecke, J., Capodaglio, P., … Narici, M. V. (2002). Plantar flexor activation capacity and H reflex in older adults: Adaptations to strength training. Journal of Applied Physiology, 92(6), 2292–2302. https://doi.org/10.1152/japplphysiol.00367.2001

Schmidt, R., Schmelz, M., Weidner, C., Handwerker, H. O., & Torebjork, H. E. (2002). Innervation territories of mechano-insensitive C nociceptors in human skin. Journal of neurophysiology, 88(4), 1859-1866.

Schmidt, R., Schmelz, M., Ringkamp, M., Handwerker, H. O., & Torebjörk, H. E. (1997). Innervation territories of mechanically activated C nociceptor units in human skin. Journal of neurophysiology, 78(5), 2641-2648.

Shield, A., & Zhou, S. (2004). Assessing voluntary muscle activation with the twitch interpolation technique. Sports Medicine, 34(4), 253-267.

Shimoura, K., Nishida, Y., Abiko, S., Suzuki, Y., Zeidan, H., Kajiwara, Y., ... & Aoyama, T. (2020). Immediate effect of neuromuscular electrical stimulation on the abductor hallucis muscle: A randomized controlled trial. Electromagnetic Biology and Medicine, 39(4), 257-261.

Siddique, U., Rahman, S., Frazer, A. K., Pearce, A. J., Howatson, G., & Kidgell, D. J. (2020). Determining the Sites of Neural Adaptations to Resistance Training: A Systematic Review and Meta-analysis. Sports Medicine, 50(6), 1107–1128. https://doi.org/10.1007/s40279-020-01258-z

Širca, A., Eržen, I., & Pečak, F. (1990). Histochemistry of Abductor Hallucis Muscle in Children with Idiopathic Clubfoot and in Controls. Journal of Pediatric Orthopaedics,

10(4), 477–482. https://doi.org/10.1097/01241398-199010040-00009

Smith, M. F., Collins, N., & Vicenzino, B. (2019). Intrinsic foot muscle atrophy in individuals with chronic plantar heel pain: a cross-sectional investigation using ultrasound imaging. Journal of Science and Medicine in Sport, 22, S17.

Soysa, A., Hiller, C., Refshauge, K., & Burns, J. (2012). Importance and challenges of measuring intrinsic foot muscle strength. Journal of Foot and Ankle Research, 5(1), 29. https://doi.org/10.1186/1757-1146-5-29

Stevens, J. E., Mizner, R. L., & Snyder-Mackler, L. (2004). Neuromuscular electrical stimulation for quadriceps muscle strengthening after bilateral total knee arthroplasty: a case series. Journal of Orthopaedic & Sports Physical Therapy, 34(1), 21-29.

Stevens-Lapsley, J. E., Balter, J. E., Wolfe, P., Eckhoff, D. G., & Kohrt, W. M. (2012a). Early neuromuscular electrical stimulation to improve quadriceps muscle strength after total knee arthroplasty: a randomized controlled trial. Physical therapy, 92(2), 210-226

.Stevens-Lapsley, J. E., Balter, J. E., Wolfe, P., Eckhoff, D. G., Schwartz, R. S., Schenkman, M., & Kohrt, W. M. (2012b). Relationship between intensity of quadriceps muscle neuromuscular electrical stimulation and strength recovery after total knee arthroplasty. Physical therapy, 92(9), 1187-1196.

Stewart, S., Ellis, R., Heath, M., & Rome, K. (2013). Ultrasonic evaluation of the abductor hallucis muscle in hallux valgus: A cross-sectional observational study. BMC Musculoskeletal Disorders, 14(1), 45. https://doi.org/10.1186/1471-2474-14-45

Serra, F. T., Carvalho, A. D., Araujo, B. H. S., Torres, L. B., dos Santos Cardoso, F., Henrique, J. S., ... & da Silva, S. G. (2019). Early exercise induces long-lasting morphological changes in cortical and hippocampal neurons throughout of a

sedentary period of rats. Scientific reports, 9(1), 1-11.

Taylor, M. J., Fornusek, C., & Ruys, A. J. (2018). Reporting for Duty: The duty cycle in Functional Electrical Stimulation research. Part I: Critical commentaries of the literature. European journal of translational myology, 28(4).

Tosovic, D., Ghebremedhin, E., Glen, C., Gorelick, M., & Brown, J. M. (2012). The architecture and contraction time of intrinsic foot muscles. Journal of Electromyography and Kinesiology, 22(6), 930-938.

Vanderthommen, M., & Duchateau, J. (2007). Electrical stimulation as a modality to improve performance of the neuromuscular system. Exercise and Sport Sciences Reviews, 35(4), 180–185. https://doi.org/10.1097/jes.0b013e318156e785

Vanderthommen, M., Duteil, S., Wary, C., Raynaud, J. S., Leroy-Willig, A., Crielaard, J. M., & Carlier, P. G. (2003). A comparison of voluntary and electrically induced contractions by interleaved 1H-and 31P-NMRS in humans. Journal of Applied Physiology, 94(3), 1012-1024.

Veale, J. L., Mark, R. F., & Rees, S. (1973). Differential sensitivity of motor and sensory fibres in human ulnar nerve. Journal of Neurology, Neurosurgery & Psychiatry, 36(1), 75-86.

Verges, S., Maffiuletti, N. A., Kerherve, H., Decorte, N., Wuyam, B., & Millet, G. Y. (2009). Comparison of electrical and magnetic stimulations to assess quadriceps muscle function. Journal of Applied Physiology, 106(2), 701–710. https://doi.org/10.1152/japplphysiol.01051.2007

Versino, M., Candeloro, E., Tavazzi, E., Moglia, A., Sandrini, G., & Alfonsi, E. (2007). The H reflex from the abductor brevis hallucis muscle in healthy subjects. Muscle & Nerve: Official Journal of the American Association of Electrodiagnostic Medicine, 36(1), 39-46.

Vitry, F., Martin, A., & Papaiordanidou, M. (2019). Torque gains and neural adaptations following low-intensity motor nerve electrical stimulation training. Journal of Applied Physiology, 127(5), 1469-1477.

Wegrzyk, J., Fouré, A., Le Fur, Y., Maffiuletti, N. A., Vilmen, C., Guye, M., ... & Gondin, J. (2015a). Responders to wide-pulse, high-frequency neuromuscular electrical stimulation show reduced metabolic demand: a 31P-MRS study in humans. PLoS One, 10(11), e0143972.

Wegrzyk, J., Fouré, A., Vilmen, C., Ghattas, B., Maffiuletti, N. A., Mattei, J. P., ... & Gondin, J. (2015b). Extra Forces induced by wide-pulse, high-frequency electrical stimulation: Occurrence, magnitude, variability and underlying mechanisms. Clinical Neurophysiology, 126(7), 1400-1412.

Weier, A. T., Pearce, A. J., & Kidgell, D. J. (2012). Strength training reduces intracortical inhibition. Acta physiologica, 206(2), 109-119.

Weir, J. P. (2005). Quantifying test-retest reliability using the intraclass correlation coefficient and the SEM. The Journal of Strength & Conditioning Research, 19(1), 231-240.

Westerblad, H., Lännergren, J., & Allen, D. G. (1997). Slowed relaxation in fatigued skeletal muscle fibers of Xenopus and mouse: contribution of [Ca2+] i and cross-bridges. The Journal of general physiology, 109(3), 385-399.

Wong, Y. S. (2007). Influence of the Abductor Hallucis Muscle on the Medial Arch of the Foot: A Kinematic and Anatomical Cadaver Study. Foot & Ankle International, 28(5), 617–620. https://doi.org/10.3113/FAI.2007.0617

Yamauchi, J., & Koyama, K. (2019a). Force-generating capacity of the toe flexor muscles and dynamic function of the foot arch in upright standing. Journal of Anatomy, 234(4), 515–522. https://doi.org/10.1111/joa.12937

Yamauchi, J., & Koyama, K. (2019b). Relation between the ankle joint angle and the maximum isometric force of the toe flexor muscles. Journal of Biomechanics, 85, 1–5. https://doi.org/10.1016/j.jbiomech.2018.12.010

Yan, S., Gauthier, A. P., Similowski, T., Faltus, R., Macklem, P. T., & Bellemare, F. (1993). Force-frequency relationships of in vivo human and in vitro rat diaphragm using paired stimuli. European Respiratory Journal, 6(2), 211-218.

Yuasa, Y., Kurihara, T., & Isaka, T. (2018). Relationship between toe muscular strength and the ability to change direction in athletes. Journal of human kinetics, 64, 47.

Zhang, X., Pauel, R., Deschamps, K., Jonkers, I., & Vanwanseele, B. (2019). Differences in foot muscle morphology and foot kinematics between symptomatic and asymptomatic pronated feet. Scandinavian journal of medicine & science in sports, 29(11), 1766-1773.

Zucker, R. S., & Regehr, W. G. (2002). Short-term synaptic plasticity. Annual review of physiology, 64(1), 355-405.

Appendix 1

2.4.5 Between-day repeatability analysis of PNS stimulation parameters

The repeatability of the parameters derived via PNS was quantified through the calculation of intraclass correlation coefficients (ICC). However, though informative, ICC values do not quantify absolute changes (Donoghue et al., 2009). Calculating the standard error of measurement (SEm), based on the SD, indicates the spread of measurement errors when estimating an examinee's true score from the observed score and in the corresponding units of measurements. Importantly, the SEm enables the determination of the Minimal Detectable Change (MDC) to infer, with 95% confidence, a meaningful change and exclude error in the measurement (Donoghue et al., 2009). Therefore, the calculation of MDC provides an objective reference to indicate meaningful adaptations following a longitudinal NMES intervention targeting AbH.

Aim

The purpose of this study was twofold: (1) to assess the between-day repeatability of the measures of muscle excitability (M_{max130}) and contractility (twitch force) derived from PNS, and (2) to determine the MDC for each parameter in order to infer meaningful or significant neuromuscular changes. Further, the repeatability of the procedures for EMG sensor positioning and identification of medial plantar nerve location between-days are also reported in this section.

Methods

This investigation consisted of 3 experiments. In the first, 4 participants were tested to assess the between-day repeatability of the performance parameters derived from PNS and the location of the medial plantar nerve (4M, 22.8±2.6 years, 78.3±18.2kg, 1.7±0.0m). For the second study, 8 participants were recruited to test the MDC of the study parameters (7M/1F, mean ± SD: 21.5±2.4 years, 75.6±13.5 kg, 1.7± 0.1 m). All

participants visited the laboratory on five different days at the same time of day. In the 3rd study, the tests were repeated on three different days and completed by a cohort of fifteen participants (12M/3F, 24.3±5.7 years, 76.3±14.9kg, 1.7±0.1m) in order to assess the repeatability of the $F_{paired10/100}$ and $T2_{100Hz}$ obtained from paired stimuli.

Optimisation procedures were undertaken at the commencement of each daily session for PNS of MPN, which included: EMG electrode positioning, Medial plantar nerve site location and construction of the recruitment curve (see section 2.4.2; Fig. 2.7A) to reveal the supramaximal intensity (M_{max130}). Then, five x M_{max130} were delivered to the MPN, while participants were seated with their hallux suspended from a uni-axial force transducer (see section 2.3).

Assessment of the between-day repeatability of the latency (ms), amplitude (mV), and area of the last positive (terminal) phase (TP; mV•ms) derived from the M_{max130} (*n*=8; Fig. 2.7B) was carried out. The between-day repeatability of the peak twitch amplitude (pTw; N) and half-relaxation time (HRT; ms) from the corresponding twitch force (*n*=8; Fig. 2.7C) was assessed. The between-day repeatability of $F_{paired10/100}$ (arbitrary units) and $T2_{100Hz}$ (N) was also assessed (*n*=15; Fig. 2.7D).

In addition, cross-correlation analysis (*n*=4) was performed in Spike 2 software (v7.12; CED Ltd., UK) to assess the similarity of the M_{max130} and twitch force waveforms between-days (Fig. 2.9). M_{max130} waveform similarity between days serves as an indication of the accuracy of EMG sensor placement over the muscle belly of AbH. The first M_{max130} and corresponding twitch force recorded in each of the five sessions were cross-correlated to assess for between-day similarity analysis. For this, the cross-correlation was set to have a maximum shift (absolute width of the x-axis) of 10ms and an offset (positive and negative temporal interval from and to zero) of 5ms for the M_{max130}, and a maximum shift of 100ms and an offset of 50ms for the twitch force. The phase-shift (lag) between the compared profiles and the Pearson's correlation coefficient (r) at zero time-shift are

indicators of the similarity of the profiles to assess the accuracy for EMG sensor placement and by proxy the repeatability of the responses between-days.

The accuracy of medial plantar nerve location (*n*=4) was assessed using a 3-dimensional motion capture system of three optical cameras, sampling at 30Hz and analysed in the proprietary software (see 2.2.3). Specifically, medial plantar nerve location was assessed by the vector joining 2 x 4mm passive skin-mounted reflective markers positioned on the medial plantar nerve and mid-portion of the Hallux toenail.

Descriptive statistics were first derived for all performance parameters (not cross-correlations). The SD of each measurement was then used to calculate the CoV. ICCs were calculated for single $ICC_{[3,1]}$ and mean of multiple $ICC_{[3,k]}$ measurements for each parameter to assess the degree of between-day repeatability (see 2.2.3). Using the SD and ICC values, the SEm ($\boldsymbol{SEm = Average\ SD \times \sqrt{(1 - ICC)}}$) was calculated to determine the MDC ($\boldsymbol{MDC = SEm \times \sqrt{n} \times 1.96}$; where *n* represents the number of measurements, (i.e. *n*=5) for each parameter (Weir, 2005; Donoghue et al., 2009).

Results

The between-day repeatability of medial plantar nerve identification (*n*=4), based on the distance between medial plantar nerve and the Hallux toenail markers location, was excellent ($ICC_{[3,1]}$=0.99) ranging between 0.4-1.3%.

The between-day repeatability of individual M_{max130} latencies (ms) was excellent ($ICC_{[3,k]}$=0.91) ranging between 4.5-13.8% (Table 2.6). MDC of 0.8ms was established for M_{max130} latency based on the between-day measurements.

The between-day repeatability of individual M_{max130} peak-to-peak amplitudes (mV) was excellent ($ICC_{[3,k]}$= 0.96) and ranged between 13.0-53.2%. The MDC for M_{max130} peak-to-peak amplitude is 1.6mV.

The between-day repeatability of individual M_{max130} terminal phase areas (TP; mV•ms) was excellent ($ICC_{[3,k]}$ =0.98) with a variability ranging between 11.5-44.3%. The MDC for TP is 1.3mV•ms.

The between-day repeatability of single pulse twitch force peak amplitudes (pTw; N) was excellent ($ICC_{[3,k]}$=0.91) with a variability ranging between 15.0-46.7%, and an MDC of 1.5N.

The between-day repeatability of single pulse half relaxation times (HRT; ms) was good ($ICC_{[3,k]}$=0.80) with a variability ranging between 3.9-28.9%. The MDC for HRT is 18.7N.

The between-day repeatability of the fatigue index ($F_{paired10/100}$) was good ($ICC_{[3,k]}$=0.81) with a variability ranging between 0.9-14.6%. The MDC for $F_{paired10/100}$ is 0.07.

The between-day repeatability of the potentiated twitch ($T2_{100Hz}$) was good ($ICC_{[3,k]}$=0.80) with a variability ranging between 6.9-40.2%. The MDC for $T2_{100Hz}$ is 2.6N.

Table 2.6. Population average (mean ± SD) values and CoV (%) for the parameters extracted from the M_{max130}, twitch force (*n*=8) and the force evoked by paired stimuli (*n*=15). $ICC_{[3,k]}$ demonstrates the reliability in the measurements between testing sessions, and MDC indicates the magnitude of change needed to be detected to infer anything other than variability in the measurement. TP: M_{max130} terminal phase area; pTw: peak twitch force; HRT: half relaxation time; $F_{paired10/100}$: low-to-high frequency fatigue index; $T2_{100Hz}$: potentiated twitch force in response to the second pulse of the paired

stimuli.

	Excitability (M_{max130})			Contractility (twitch force)			
	Latency (ms)	Amplitude (mV)	TP (mV•ms)	pTw (N)	HRT (ms)	$F_{paired10/100}$	$T2_{100Hz}$ (N)
Mean	6.6 (0.9)	9.1 (6.9)	8.6 (5.7)	4.0 (1.8)	73.9 (11.5)	0.80 (0.1)	8.1 (2.5)
CoV	8.3 (3.2)	26.4 (13.2)	26.2 (11.2)	31.0 (10.1)	12.4 (7.6)	6.2 (3.9)	21.1 (9.7)
$ICC_{[3,k]}$	0.91	0.96	0.98	0.91	0.80	0.81	0.80
SEm	0.2	0.4	0.3	0.4	4.3	0.02	0.8
MDC	0.8	1.6	1.3	1.5	18.7	0.07	2.6

The cross-correlations assessing the between-day similarity of the M_{max130} waveforms (Fig. 2.9A&B) were indicative of variation in the EMG sensor placement, particularly for 2 participants, where the correlation coefficient at zero phase-shift ranged between r=-0.57 and 0.93 in one, and between r=0.02 and 0.99 in the other (Table 2.7). This variation seems not to be of physiological origin, since between-day waveform correlations for the corresponding twitch force responses (Fig. 2.9C&D) were generally excellent throughout in all participants (Table 2.8). Although the same force output can be generated by the activation of different fibres to different extents, a supramaximal intensity was used to minimise this.

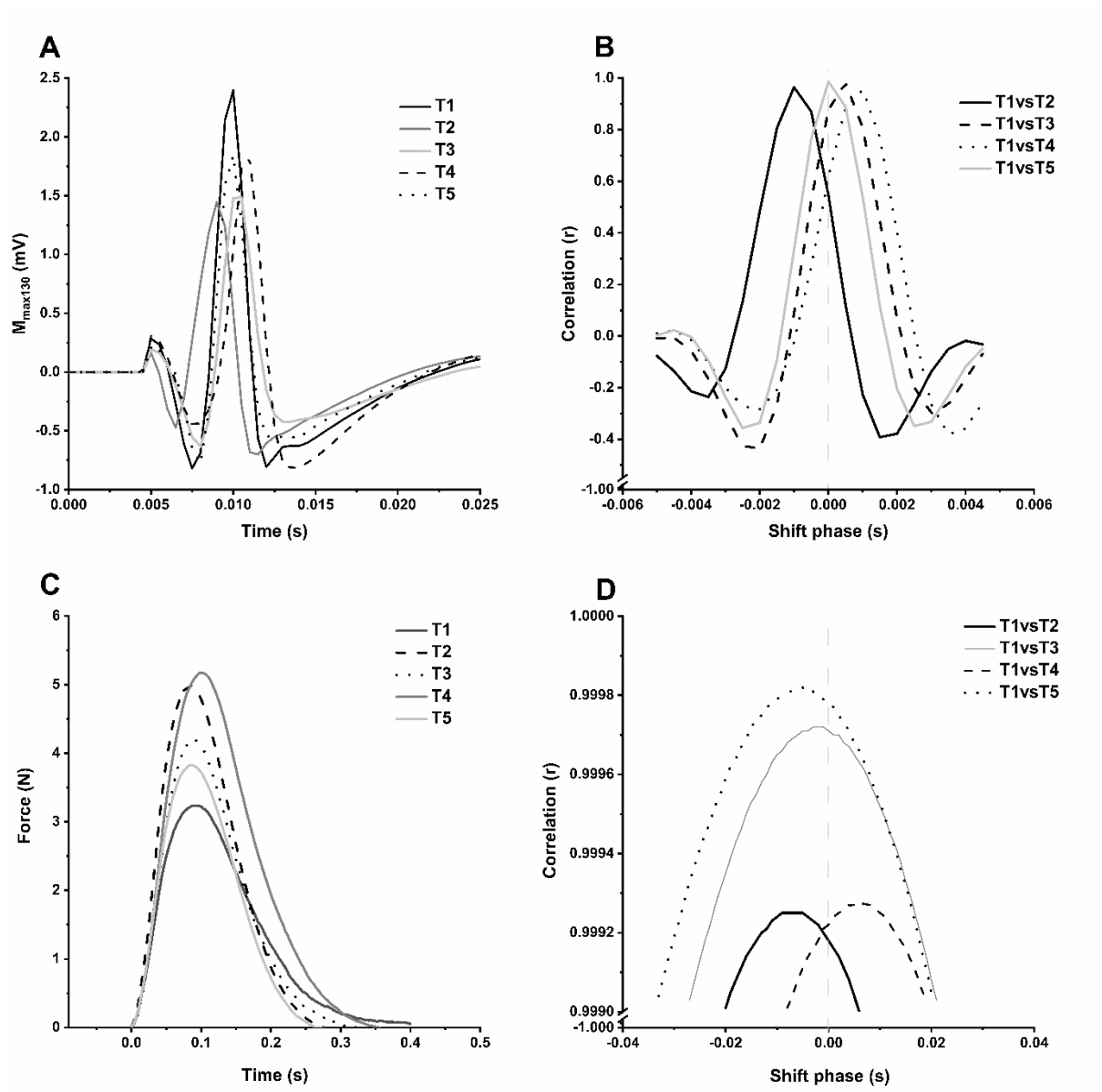

Figure 2.9. Exemplar between-day M_{max130} (**A**) and corresponding twitch force (**C**) profiles acquired from the five trials (T1-5) conducted by one participant. Also illustrated is the strength and variation of the between-day M_{max130} (**B**) and force (**D**) waveform correlations. Zero phase shift (grey line) represents absolute agreement between trials.

Table 2.7. Between-day cross correlations of M_{max130} responses, where *r* is the correlation coefficient at zero time shift (max=10ms, offset=5ms), $lag^{(r@lag)}$ indicates the phase shift and correlation between waveforms at that time. Furthermore, p indicates whether waveforms are significantly repeatable. Participant 2 and 4 demonstrate variation in the EMG sensor placement, for whom *r* ranged between -0.57 and 0.93, and between 0.02 and 0.99, respectively.

	Participant 1			Participant 2			Participant 3			Participant 4		
	r	**$lag^{(r@lag)}$**	**p value**	**r**	**$lag^{(r@lag)}$**	**p value**	**r**	**$lag^{(r@lag)}$**	**p value**	**r**	**$lag^{(r@lag)}$**	**p value**
T1 vs T2	0.83	$-0.0005^{(0.90)}$	<0.001	0.45	$-0.001^{(0.96)}$	<0.01	0.86	$0^{(0.86)}$	<0.001	0.55	$-0.001^{(0.96)}$	<0.001
T1 vs T3	0.92	$0^{(0.92)}$	<0.001	0.93	$0^{(0.93)}$	<0.001	0.88	$0^{(0.88)}$	<0.001	0.88	$0.0005^{(0.98)}$	<0.001
T1 vs T4	0.74	$-0.0005^{(0.88)}$	<0.001	-0.57	$-0.0025^{(0.79)}$	<0.001	0.46	$-0.001^{(0.82)}$	<0.01	0.62	$0.001^{(0.95)}$	<0.001
T1 vs T5	0.86	$0^{(0.86)}$	<0.001	-0.52	$-0.003^{(0.88)}$	<0.001	0.77	$-0.0005^{(0.96)}$	<0.001	0.99	$0^{(0.99)}$	<0.001
T2 vs T3	0.96	$0^{(0.96)}$	<0.001	0.66	$0.001^{(0.96)}$	<0.001	0.99	$0^{(0.99)}$	<0.001	0.16	$0.0015^{(0.95)}$	0.308
T2 vs T4	0.98	$0^{(0.98)}$	<0.001	0.17	$-0.001^{(0.76)}$	0.287	0.71	$-0.0005^{(0.95)}$	<0.001	0.02	$0.002^{(0.96)}$	0.914
T2 vs T5	0.97	$0^{(0.97)}$	<0.001	-0.45	$-0.002^{(0.86)}$	<0.01	0.85	$-0.0005^{(0.94)}$	<0.001	0.44	$0.001^{(0.95)}$	<0.01
T3 vs T4	0.89	$-0.0005^{(0.91)}$	<0.001	-0.37	$-0.002^{(0.80)}$	<0.05	0.65	$-0.0005^{(0.93)}$	<0.001	0.88	$0.0005^{(0.96)}$	<0.001
T3 vs T5	0.98	$0^{(0.98)}$	<0.001	-0.47	$-0.003^{(0.83)}$	<0.01	0.82	$-0.0005^{(0.95)}$	<0.001	0.91	$-0.0005^{(0.96)}$	<0.001
T4 vs T5	0.90	$0.0005^{(0.91)}$	<0.001	0.68	$-0.001^{(0.92)}$	<0.001	0.85	$0.0005^{(0.85)}$	<0.001	0.68	$-0.001^{(0.92)}$	<0.001

Table 2.8. Between-day cross correlations of twitch force responses, where *r* is the correlation coefficient at zero time shift (max=100ms, offset=50ms), lag$^{(r@lag)}$ indicate the phase shift and correlation between waveforms at that time, and p value indicates whether waveforms are significantly repeatable. The twitch force waveform from all participants (*n*=4) demonstrates excellent correlation between days.

	Participant 1			Participant 2			Participant 3			Participant 4		
	r	lag$^{(r@lag)}$	p-value	r	lag$^{(r@lag)}$	p-value	r	lag$^{(r@lag)}$	p-value	r	lag$^{(r@lag)}$	p-value
T1 vs T2	0.91	-0.014$^{(0.96)}$	<0.001	0.90	-0.016$^{(0.97)}$	<0.001	0.94	-0.015$^{(0.99)}$	<0.001	0.98	-0.007$^{(0.99)}$	<0.001
T1 vs T3	1.00	-0.001$^{(1.00)}$	<0.001	0.99	0.001$^{(0.99)}$	<0.001	1.00	-0.001$^{(1.00)}$	<0.001	0.99	-0.002$^{(0.99)}$	<0.001
T1 vs T4	0.99	0$^{(0.99)}$	<0.001	0.95	-0.014$^{(0.99)}$	<0.001	0.97	-0.011$^{(0.99)}$	<0.001	0.99	0.006$^{(1.00)}$	<0.001
T1 vs T5	0.99	-0.005$^{(1.00)}$	<0.001	0.98	0.002$^{(0.98)}$	<0.001	0.96	-0.012$^{(0.99)}$	<0.001	0.99	-0.006$^{(0.99)}$	<0.001
T2 vs T3	0.92	0.014$^{(0.96)}$	<0.001	0.88	0.018$^{(0.96)}$	<0.001	0.95	0.014$^{(0.99)}$	<0.001	1.00	0.005$^{(1.00)}$	<0.001
T2 vs T4	0.89	0.014$^{(0.93)}$	<0.001	0.96	0.003$^{(0.97)}$	<0.001	0.99	0.003$^{(0.99)}$	<0.001	0.96	0.013$^{(0.99)}$	<0.001
T2 vs T5	0.95	0.009$^{(0.97)}$	<0.001	0.87	0.019$^{(0.95)}$	<0.001	0.99	0.002$^{(0.99)}$	<0.001	1.00	0.002$^{(1.00)}$	<0.001
T3 vs T4	0.99	0.001$^{(0.99)}$	<0.001	0.94	-0.015$^{(0.99)}$	<0.001	0.97	-0.01$^{(0.99)}$	<0.001	0.98	0.008$^{(0.99)}$	<0.001
T3 vs T5	0.99	-0.004$^{(1.00)}$	<0.001	1.00	0.001$^{(1.00)}$	<0.001	0.96	-0.011$^{(0.99)}$	<0.001	1.00	-0.003$^{(1.00)}$	<0.001
T4 vs T5	0.98	-0.004$^{(0.99)}$	<0.001	0.94	0.016$^{(0.99)}$	<0.001	1.00	-0.001$^{(1.00)}$	<0.001	0.97	-0.012$^{(0.99)}$	<0.001

Interpretation

The results reported here show that: i) identifying medial plantar nerve location is repeatable between days; and ii) despite the between-day variability of the M_{max130} waveform, which most likely was due to imperfect replication of EMG sensor positioning, its parameters and those of the corresponding twitch force are by-in-large repeatable. These findings suggest that the parameters derived from PNS to evaluate muscle excitability and contractility are repeatable when assessed between-days. Their corresponding MDC values permit to infer, with 95% confidence, meaningful changes that are not the result of variability of measurement error in the assessment of an NMES intervention in AbH.

The assessment of the supramaximal compound muscle action potential (M_{max130}) is subject to the accuracy of EMG sensor positioning over the muscle belly of AbH, and it has been shown here that this is not completely repeatable. This is not due to physiological variation, since the corresponding twitch force was completely repeatable (Table 2.8; Fig. 2.9C&D). Whilst this variation is true for half of the participants (2 out of *n*=4) tested here, the present results do suggest that the variability in the M_{max130} waveform does not translate on the discrete time-amplitude parameters of the potential, as they showed excellent repeatability (Table 2.6).

This study demonstrated that the properties of the AbH M_{max130}, and its corresponding twitch force, are stable when evoked with supramaximal (M_{max130}) electrical stimulation of the medial plantar nerve on different days. Consequently, for the majority of the characteristic parameters, only relatively small changes (MDC values) are required to infer meaningful adaptations to a long-term NMES intervention (Table 2.6).